PERFORMANCE EVALUATION OF IDAHO HMA MIXES USING GYRATORY STABILITY

FINAL REPORT
May 1, 2007

NIATT Project No. KLK 482
ITD Project No. SPR-0004(022) RP 175

Prepared for

Idaho Transportation Department
Mr. Michael Santi, PE
Assistant Material Engineer

Prepared by

National Institute for Advanced Transportation Technology
University of Idaho

Fouad Bayomy, Ph.D., P.E. (PI)
Ahmad Abu Abdo, Graduate Research Assistant

ABSTRACT

The primary goal of this project was to evaluate the validity of the Contact Energy Index (CEI), a concept that was developed in a previous ITD project, to the Hveem mixes in Idaho. And to establish threshold design values for the CEI that can be used for the HMA mix design in Idaho. During the research, the CEI concept was extended and redefined to determine the mix Gyratory Stability. The Gyratory Stability, which is an energy based indicator, reflects the mix resistance to deformation. A secondary objective was to develop and evaluate a mix design parameter that can be used as an indicator to the mix resistance to fatigue and fracture. A new test was developed and fracture resistance parameter, referred to as (J_c), was developed. The fracture resistance parameter, is measured by the semi-circular notched bending fracture (SCBNF) test. Hence, the research experimental program was designed to evaluate Gyratory Stability (GS) and Fracture resistance parameter (*Jc*) along with other mix properties such as the Asphalt Pavement Analyzer (APA) rutting test and Aggregate IMaging System (AIMS) for various HMA mixes in the state of Idaho.

The experimental program of this research included more than fifty field mixes procured from projects around the state of Idaho. Forty seven of these mixes were designed based on Hveem design method, which was, at the time of the project initial stages, the current method at the Idaho Transportation Department (ITD). More lab mixes were made by altering some of the field mixes properties to address specific research issues during the experimental phase. Results of tests conducted on all mixes were analyzed in terms of the Gyratory Stability, Fracture resistance *Jc*, APA rut values, and aggregate shape and texture properties using imaging methods by (AIMS). Two additional mixes were designed using the Superpave mix design method. The two Superpave mixes were used in new projects, and were added to the research project at a later stage. The dynamic modulus (E*) and flow number tests were conducted on the two Superpave mix as a

pilot study. Further, a Visual Basic Software and an Excel macro were developed to facilitate the calculations of Gyratory Stability.

Results of Hveem mixes showed that Gyratory Stability correlated well with the Hveem Stability of Hveem designed mixes. It was observed that mixes had varies Gyratory Stability values for the same Hveem Stability. This may indicate that the GS is more sensitive to changes in mix design parameters than Hveem Stability. It was also found the GS is sensitive to aggregate gradation and binder contents. A three tier GS limits of 5, 12 and 15 are suggested to classify Hveem designed HMA mixtures based on their GS stability.

Results of the APA rut testing did not correlate well with the GS of these mixes. It is believed that the main reason is that the testing temperature of the APA varies based on the high temperature of the asphalt binder, where the GS is determined at the standard compaction temperature of (149 °C). A better correlation between GS and permanent deformation in APA was obtained for mixes that have the same PG grade and tested at the same temperature in the APA.

Aggregate Imaging System (AIMS) analysis indicated that aggregate texture correlated with the GS. There was no clear relationship between angularity and sphericity with GS for the range of aggregates used in this study.

Results of the fracture resistance (J_c) showed that the J_c was found to be sensitive to changes in the mix aggregate gradations and to the aggregate shape and surface texture properties as measured by the AIMS. Mix with finer aggregate gradations showed higher resistance to fracture compared to the mix with coarser aggregate gradations. Mixes with rougher aggregate texture and more angular particles showed higher J_c values. Mixes that had high percentages of flattened and elongated aggregates showed lower J_c values. The J_c was found to be sensitive to the variation in the asphalt binder content and grade.

For the two Superpave mixes tested in this research, it was observed that the test results followed the same trend as the Hveem designed mixes. GS values of these mixes changed with the asphalt content. Results showed that GS determined at optimum asphalt content was the highest for both Mixes. GS correlated well with the APA test results. The J_c was found to be sensitive to the variation in the asphalt binder content. There is no clear relationship between the optimum asphalt content and J_c. Furthermore, the dynamic modulus test results on the two Superpave mixes showed that the rutting resistance parameter ($E^*/\sin\varphi$) at temperatures of 130 and 100 °F correlated well with the GS values of these mixes. In addition, GS correlated with the Flow Number test results. However, the correlation coefficient was relatively low (R^2 equal to 0.49). Results did not reveal direct correlation between the J_c and the fatigue resistance indicator ($E^*.\sin\varphi$) that is measured by the dynamic modulus test at both temperatures 70 and 40 °F when both mixes are compared. But with each mix both parameters followed the same trends.

Overall, the results indicate that the Gyratory Stability (GS) and the Fracture Toughness Parameter (J_c) are simple and practical test methods that can be used in conjunction with the current Superpave mix design procedure. These parameters are not aimed to replace performance tests, but can be used for screening and discriminate among mixes during the mix design stage before conducting more sophisticated and time consuming performance tests.

ACKNOWLEDGEMENTS

This project was funded by the Idaho Transportation Department (ITD) under a contract with the National Institute for Advanced Transportation Technology (NIATT), project number KLK482. Many Individuals have contributed to the progress of this project.

From ITD, thanks are due to Mike Santi, Bob Smith, Muhammad Zubery, and Jeff Miles for their extreme help and support throughout all project phases. Thanks to Mr. Vince Spisak, materials engineer at District 2, for his great efforts to provide much needed help with field mixes. The rutting test using the APA and all Hveem stability testing were conducted at the ITD HQ lab in Boise. The efforts of Mr. Monte Tish and all lab team are greatly appreciated.

Dr. Eyad Masad of Texas Transportation Institute conducted the Image analysis of aggregates and prepared Chapter 4 of this report. Authors are grateful to his efforts.

The support of the NIATT administrative staff is also acknowledged. Ms. Judy LaLonde and Debbie Foster have provided close monitoring for the project progress reports and budget. Ms. Karen Faunce reviewed, and edited the manuscript of the final report. Authors are very thankful to all their efforts and support.

TABLE OF CONTENTS

LIST OF FIGURES

LIST OF TABLES

1. INTRODUCTION

1.1. BACKGROUND

This research project (KLK482) is the second of a series of projects that are conducted at the University of Idaho National Institute for Advanced Transportation technology (NIATT) to address the implementation of the new Superpave mix design system in the state of Idaho. A previous project (KLK464) addressed the development of a new deign parameter that can augment the Superpave mix design procedure.

The original Superpave mix design was based on volumetric criteria where the mix aggregate structure and optimum binder content was to satisfy certain volumetric criteria as established in the Superpave system. The procedures lacked a measurable parameter that can discriminate mixes based on their resistance to deformation or fracture. Thus, it lacked a mechanical test similar to the stability tests that used to be combined with the Marshall and Hveem methods. Initially the Superpave had three levels with level 1 being based only on volumetric analysis 9essentially for low volume roads) and level 3 that included advanced testing procedures that were developed specifically for high class roads. However, the final release included one level, which is the volumetric design procedure with no mechanical test attached to the design system. Hence, the Idaho Transportation Department (ITD) sought the development of more rigorous testing that can be augmented to the volumetric design procedure before full implementation of Superpave mix design system in Idaho. One of the thoughts that ITD considered was to use the Asphalt Pavement Analyzer (APA) to test for rutting resistance of the mixes. However, APA is also expensive to operate and is usually done after the mix design has been completed. ITD was looking for a test method or a design parameter that can be evaluated during the mix design phase.

The main outcome of the KLK464 project was the development of the Contact Energy Index (CEI). CEI is a mix parameter that can be determined from the energy released in the compaction of a mix sample in the Superpave Gyratory Compactor (SGC). CEI is calculated from compaction data that are obtained from the SGC during compaction of the mix sample. However, it required that the compactor be capable of providing the compaction forces applied to the sample at each number of gyrations.

Under KLK464, several mixes were considered from the NCHRP 9-16 project. Results revealed that CEI reflected mix design variability that included asphalt binder content, effect of presence of fine sands, aggregate angularity and texture. Furthermore, the results of dynamic modulus testing showed that CEI correlated well with the parameter $E^*/\sin\phi$ for filed mixes that were considered under the NCHRP 9-16 project. In addition, results of tests made on few mixes from the state of Idaho confirmed similar results of that for the NCHRP- 9-16 mixes. Since CEI reflected the ability of the mix to resist deformation, it can reflect the mix stability. Thus, CEI when calculated from compaction data to the number of gyrations equal to N-design was referred to as Gyratory Stability (GS). This led ITD to consider using CEI or GS as a mix design parameter to be augmented with the Superpave design procedures.

One of the main obstacles to implement the CEI concept directly was the fact that only three mixes from Idaho were considered under KLK464 project. So, there was no sufficient amount of data that can enable ITD to apply the newly developed concept. ITD needed to confirm the applicability of the CEI concept to the Hveem designed mixes, which ITD has long time experience with, before applying it to new Superpave mixes. ITD needed to determine a threshold design value for CEI so that it can be used for new designs. In addition, more fine tuning for CEI calculations were needed. And, the fact that ITD used old Troxeller compactor that was not equipped with force measuring devices made the determination of CEI with data from Troxeller compactor impossible. Therefore, there were several issues that need to be resolved and addressed before full application of the CEI or GS in the Superpave mix design in Idaho.

1.2. OBJECTIVES

The main goal of this project is to implement the new development of CEI and Gyratory Stability in the Idaho mix design practice and investigate its impacts on the long-term performance. The project objectives were later expanded and included development of fracture test to predict the mix resistance to fracture.

The specific objectives of the project are:

- Validate the development of CEI and GS on Hveem mixes from Idaho projects and establish design target values of Gyratory Stability for various Idaho mixes.
- Investigate the variability of GS or CEI with respect to the compaction methods and equipment used.
- Evaluation if there is a possible correlate the Gyratory stability to a performance measure, such as the rut depth measured by the APA or dynamic modulus test parameter ($E^*/\sin\phi$).
- Develop and evaluate a fracture parameter to asses mix resistance to fracture.
- Validate the development and evaluation of the GS, CEI and fracture parameters on Superpave mixes in Idaho.
- Develop software to facilitate the calculation procedures of CEI and Gyratory Stability.

1.3. SCOPE

The initial scope of the project was focused on determining the CEI and GS for mixes from projects in Idaho. There was a need to measure the Gyratory Stability of almost every mix designed and placed by ITD. Therefore, the scope of the project covers the mixes that are actually used in pavement projects. The extent of how many mixes to be tested as well as the time limit will be affected by how many projects are there and how soon these projects will be constructed. The project involves ITD mixes that are designed either by current Hveem or by the Superpave system. The research team worked closely with ITD to procure mixes and test samples from actual projects. Mixes shall be obtained from mix plants, as well as the raw materials (binder and aggregates) for further binder and aggregate evaluation. During the project, the scope was expanded to include dynamic modulus testing (using the new AASHTO T62-03 procedures) for limited number of Idaho Superpave mixes.

1.4. PROJECT TASKS

The following set of tasks were planned to achieve the stated objectives within the scope of the project.

Task 1: Mixes' Selection and Material Procurement:
Under this task, field mixes were selected to evaluate their Gyratory Stability. The selected mixes covered wide range of binders and aggregate gradations that are used in the state. ITD assisted in identifying the projects, facilitate contacts and material procurement. In addition, all Hveem stability testing was done by ITD.

Task 2: Binder Evaluation:
Binder properties were obtained from the asphalt suppliers. Properties included temperature succeptibility curves (Viscosity vs Temp) and Superpave binder evaluation by Dynamic Shear Rhyeometer (DSR).

Task 3: Aggregate Evaluation:
This task is limited only to determine the aggregate parameters pertaining to Superpave mix design system. This may include angularity, shape and gradation. The task was expanded to determine the aggregate texture and shape properties using Aggregate

Imaging System (AIMS). This task was subcontracted with Texas Transportation Institute (TTI), where aggregates were sent for evaluation by AIMS.

Task 4: Mix Preparation and Measurement of Gyratory Stability:
For all the selected mixes, ready mixed materials were obtained from project sites in accordance to the standard procedures adopted by ITD. The mixes were compacted at the UI lab using the Servopac SGC to measure the Gyratory stability. Additional samples were prepared for APA testing at the ITD lab. To develop independent measurements for Gyratory Stability, several methods were considered. These included in addition to the Servopac compactor, the use of PDA with Troxeller at ITD and using Pine compactor.

Task 5: Performance Evaluation Using APA:
To correlate the Gyratory stability to a lab performance test, several were tested in the APA (at ITD HQ lab) to investigate the correlations for APA results with Gyratory Stability values.

In addition to above tasks that were stated in the project proposal, additional work was planned to test Superpave mixes in Dynamic modulus testing to determine the relationship of the developed Gyratory Stability (GS) and the mix dynamic properties as measured in the E* test as established by the NCHRP projects 9-19 and 9-29.

1.5. REPORT ORGANIZATION

The report includes nine chapters as listed in the table of contents and three appendices. The appendices are provided only on CD due to their large sizes. Appendix A includes all Job Mix Formula (JMF) and properties of the selected mixes. Appendix B includes all the electronic files of the Gyratory compaction data for all compactors considered in this project. Also summary of all results are tabulated in Appendix B. the developed software for calculation of CEI and GS are provided on the CD as Appendix C.

2. GYRATORY STABILITY CONCEPT AND VARIOUS METHODS OF GYRATORY STABILITY MEASUREMENTS

2.1. INTRODUCTION

Significant research has been conducted, since the introduction of the Superpave asphalt mix design system, in order to supplement this design methodology with performance tests (Witczak, et al. 2002). These performance tests have proven to be extremely important in allowing design engineers to evaluate Hot Mix Asphalt (HMA) during the mix design stage. In addition to these performance tests, there has been interest in using the Superpave Gyratory Compaction (SGC) data to distinguish among mixes, based on the resistance of the aggregate structure to applied loads (Mallick 1999, DeSombre, et al. 2000; Bayomy, et al. 2002; Anderson, et al. 2002; Bahia, et al. 2003; and Dessouky, et al. 2004).

A number of studies have related the compaction curve characteristics, such as the slope of the compaction curve, to mix stability (Cominsky, et al. 1994 and Rand 1997). Bahia, et al. (2003) stated that the compaction curve consists of two different parts. The first part has a high rate of change in percent air voids and is related to densification during construction, using rollers at high temperatures. The second part has a very small rate of change in percent air voids and the aggregate structure experiences high shear forces. The compaction characteristics of the second part have been related to HMA performance at ambient temperature.

Several approaches have also been proposed to develop experimental tools and analysis methods to measure the shear stress during compaction, and to relate them to stability. McRea (1962 and 1965) proposed an equation to determine the shear stress in HMA during compaction in the gyratory testing machine. This equation was developed based on equilibrium analysis of HMA and the compaction mold. Subsequently, it was used to predict the mix stability and performance by several researchers (e.g. Kumar, et al. 1974; Mallick 1999; Sigurjonsson and Ruth 1990; and Ruth, et al. 1991). Butcher (1998) used the same equation with data from the Australian SGC (Servopac) and showed that the calculated shear stress is sensitive to changes in binder type.

A recent study by De Sombre, et al. (1998) estimated the shear stress and the compaction energy in asphalt mixes by using the Finland Gyratory Compactor. Guler, et al. (2000) instrumented the Superpave Gyratory Compactor with a load cell assembly referred to as the Pressure Distribution Analyzer, or PDA, to measure the forces applied at the bottom of a specimen during compaction. These forces were used in an equation to calculate the shear stress in the mix.

The research conducted under NCHRP 9-16 (2002) has proposed the use of the number of gyrations at maximum stress ratio in order to group laboratory mixes with good, fair, and poor expected rutting resistance. The parameter is directly obtainable from SGCs capable of measuring shear stress during compaction; or the Gyratory Load Cell Plate Assembly developed at the University of Wisconsin (Guler, et al. 2000 and Stackson, et al. 2002) can be used to obtain this parameter.

Bayomy, et al. (2002) and Dessouky, et al. (2004) have developed another approach to estimate the shear stress developed in the asphalt mix due to compaction in a Superpave Gyratory Compactor (SGC) equipped with force measuring cells. Using the response of the mix to the applied forces in the SGC and the mix deformation during compaction, the energy utilized to develop contacts between aggregates was quantified using the Contact Energy Index, or CEI. The CEI reflects the stability of the mix, which is related to the frictional forces among its aggregate particles. A spread sheet was developed to facilitate the calculation of CEI directly from the compaction data file, once the sample was compacted. Previous studies showed that CEI is sensitive to variation of mix constituents, such as aggregate characteristics, gradation, and binder content.

This approach is not intended to replace performance tests, but rather to identify mixes with weak aggregate structures prior to more involved performance testing. In addition, this approach can be used in the field to rapidly detect any changes in the mix that would adversely affect the aggregate structure and mix performance.

2.2. THE CONTACT ENERGY INDEX (CEI)

Bayomy, et al. (2004) has presented a detailed analysis and derivation of the shear stress using a free body diagram as shown in Figure 2.1. He developed a series of equations (Equations 2.1 to 2.3) to calculate the shear force applied at the mid-point of the HMA sample.

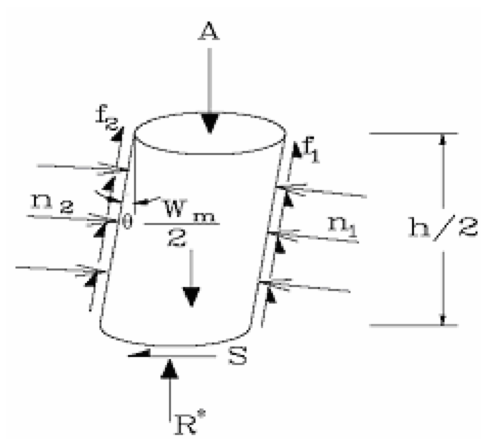

Figure 2.1 Normal and Shear Forces and Stresses Acting on the Sample

$$S_\theta = (N_2 - N_1)\cos\theta + \frac{1}{2}.(\Sigma P - W_d).\tan\theta \tag{2.1}$$

$$N_2 - N_1 = \frac{\left(F_v + \frac{W_m}{2}\right)\left(x_\theta - \frac{h}{2}\tan\theta\right) - \frac{1}{2}(\Sigma P - W_d)\left(x_\theta - \frac{r}{\mu}\tan\theta\right)}{\frac{h}{4\cos\theta} + \mu.r.\cos\theta - \frac{r\sin^2\theta}{\mu.\cos\theta}} \tag{2.2}$$

$$\Sigma P = \frac{Area.h.\tau}{2.L} \tag{2.3}$$

where,

S_θ: Shear force at mid height of sample, Newton.

F_v: Resultant force of the applied pressure, which is typically 600 kPa, Newton.

W_m: Weight of the asphalt sample, kg.

W_d: Weight of the mold, kg.

θ: Angle of gyrations, degrees.

h: Height of sample at any gyration.

r: Sample radius, 75 mm for standard Superpave 150 mm diameter sample.

N_1 & N_2: Normal forces acting on the half sample surface due to friction.

x_θ: The distance from the center to the point where the resulting force is acting. The maximum value of x_θ is r/3, and is zero when θ is zero. For a 150 mm diameter sample, where θ = 1.25°, by interpolation x_θ =10.417 mm.

μ: Friction coefficient, which is assumed constant and equals to 0.28.

ΣP: Average force on the three actuators, Newton.

τ: Shear Stress given by the Servopac Gyratory Compactor, kPa.

L: Radial distance to the point of application of the actuator load, which is equal to 165 mm.

The conservation of energy principle, or the first law of thermodynamics, states that: the total rate of work done on the system by all external forces must be equal to the rate of increase of the total energy of the system. The conservation of energy can be written in the following form:

$$\rho.\frac{du}{dt} = \sigma_{ij}.D_{ji} + \rho.r - q_{i,j} \qquad (2.4)$$

where,

ρ is the material density,

du/dt is the rate of change of the internal energy per unit volume,

σ_{ij} is the stress tensor,

D_{ji} is the deformation rate tensor,

$\rho.r$ is the heat supplied by the internal disturbance sources, and

q_{ii} is the heat provided by the flow of thermal energy through the boundary into the system or continuous body.

If the deformation is assumed to occur under isothermal conditions, the equation of energy conservation becomes:

$$\rho.\frac{du}{dt} = \sigma_{ij} . D_{ji} \tag{2.5}$$

The term σ_{ij} D_{ji} represents the mechanical work done by the external forces not converted into kinetic energy. The conservation of energy principle can be applied to the gyratory compaction. The time increment used in the above equation is taken as the time needed to complete one gyration. If the deformation induced within each gyration is considered to be all plastic deformation, then the change in the internal energy in each gyration (*du*) is equivalent to the dissipated energy, due to volumetric and shear strains as follows:

$$du = dv + ds \tag{2.6}$$

where,

dv is the change in the internal energy due to volumetric deformation, and

ds is the change in the internal energy due to shear deformation.

A typical compaction curve from the gyratory process is shown in Figure 2.2.

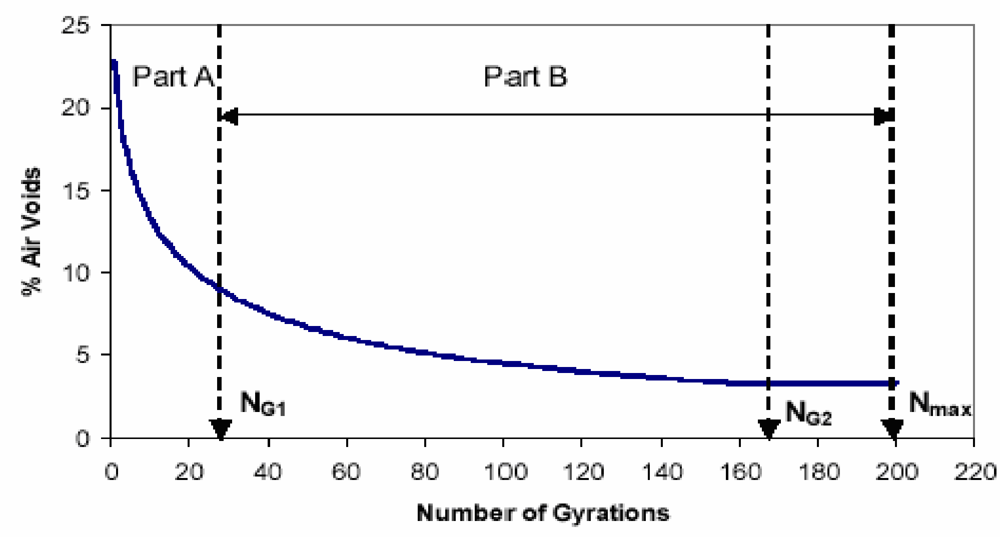

Figure 2.2 Typical Compaction Curve (Bayomy, et al. 2002)

The compaction curve can be divided into two parts: the first one (part A) has a steep change in percent air voids with an increase in number of gyrations. In part A, most of the applied energy is consumed in the volumetric change of the mix. That is, the reduction in percent air voids is essentially due to volumetric change by compaction. In this part, the aggregates don't experience a significant amount of shearing force. In the second part (part B) the compaction energy is consumed in adjusting the particle orientation and increasing the aggregates' contacts, which results in an increase in mix shear strength. This process is associated with a decrease in air void, but with a lower rate than in part A.

When the mix reaches its maximum stability, any excess in induced compaction energy is dissipated in particle sliding without an increase in particle interlocks. Consequently, no more shear strength is developed. This state is manifested by no change in mix air voids, a state known as "refusal" in mix compaction, which means that the mix cannot be compacted anymore. Therefore, increasing the number of gyrations after N_{G2} has no effect on the mix compaction, and the energy consumed in the mix from N_{G2} to N_{max} is dissipated. Therefore, the energy calculations for assessing the mix stability should be focused only on part B of the compaction curve.

A stability index, termed the Contact Energy Index (CEI), was presented in ITD-NIATT Project KLK464 Report (2002). It is calculated by the multiplication of vertical deformation and the shear force developed in the mix, which is the manifestation of all forces acting on the sample (Eq. 2.7.) The term CEI is an index that reflects the stability of the mix due to, for the most part, the contacts among its aggregate particles.

$$CEI = \sum_{N_{G1}}^{N_{G2}} S_{\theta}\, d_e \tag{2.7}$$

Thus, d_e is the change in height (mm) at each number of gyrations in part B of Figure 2.2 from N_{G1} to N_{G2} or N_{max}. Note that there is no change in height ($d_e = 0$), from N_{G2} and N_{max}, so that the Gyratory Stability value will not change, whether the summation is carried out to N_{G2} or to N_{max}.

The number of Gyrations $N_{G1,}$ that defines the beginning of part B, is where the rate of change of air voids is almost constant. That is, the change in the slope of the compaction curve is constant. Mathematically, this means that the third derivative of the compaction curve function should be zero. For practical purposes, it is considered that N_{G1} is where the difference in the change in the slope of the compaction curve is less than 0.001 (i.e., where the rate of change of the slope is zero).

Mechanistically, the shear strength development in the mix is related to particle contacts and the properties of the mastic around coarse particles. At the initial number of gyrations, mix deforms rapidly, and a change in sample height is mainly due to volumetric change. Starting from N_{G1}, mix starts to develop shear resistance and it continues to increase until it reaches its maximum value at N_{G2}. The shear strength stays unchanged to N-max. However, if the compaction continues beyond this point, a possibility of damage to the sample may occur, and the sample may lose its shear strength due to micro-fracturing at particle contacts.

2.3. THE GYRATORY STABILITY (GS)

For production samples where compaction stops at N-design, N_{G2} is then considered equal to N-design. Since N-design is smaller than N-max, and the sample height keeps changing after N-design, the calculated CEI to N_{G2} equal to N-design is smaller than that calculated to N-max. Therefore, standardization is needed to identify the selected N_{G2}. Since production samples are typically produced with the number of gyrations equal to N-design, the value of CEI for the energy product summed between N_{G1} and N-design is referred to as Gyratory Stability (GS). Therefore, GS is determined as:

$$GS = \sum_{N_{G1}}^{N_{design}} S_{\theta} d_e \tag{2.8}$$

2.4. SENSITIVITY OF GS TO THE METHOD OF MEASURING COMPACTION FORCES

2.4.1. Servopac SGC and PDA

As discussed earlier, GS calculations require the measurements of the forces acting on the sample during compaction. The Servopac compactor (Model 02-0744) provides measurements of shear stresses, from which the required forces S_{θ} can be back-calculated, as discussed in detail in references Bayomy, et al. (2002) and Dessouky, et al. (2004). For other types of Superpave Gyratory Compactors, forces applied on the sample during compaction can be measured by using the Pressure Distribution Analyzer (PDA).

Guler, et al. (2000) has suggested that the shear stress could be calculated as per Equation 2.9:

$$S = \frac{R.e}{A.h} \tag{2.9}$$

where,

R is the resultant ram force,

e is the average eccentricity for a given gyration cycle,

A is the sample cross section, and

h is the sample height at any gyration cycle.

The average eccentricity e can be measured using the PDA (Guler, et al. 2000 and Bahia, et al. 2003). The main components of the PDA are three 9-kN (2,000-lbf) load cells, two hardened steel plates that can snugly fit into the compaction mold, and a computer that is used for data acquisition from both the PDA and SGC devices. The load cells are placed on the upper plate of the assembly at a common radial distance 120. Each is attached by three screws so that the load pins of each load cell have a small contact point on the lower plate, which is in contact with the hot mixture during the compaction.

On the basis of the readings from the load cells, the two components of eccentricity of the total load, relative to the center of the plate, can be calculated for each of the 50 points collected during each gyration. The calculations are simply done using general moment equilibrium equations along two perpendicular axes passing through the center of one of the load cells, as shown in Figure 2.3 and Equations 2.10 – 2.12.

$$\Sigma M_x = 0 \Rightarrow e_x \tag{2.10}$$

$$\Sigma M_y = 0 \Rightarrow e_y \tag{2.11}$$

$$e = \sqrt{e_x^2 + (r_y - e_y)^2} \qquad (2.12)$$

where,

M_x is the moment around x-axis,

M_y is the moment around y-axis,

e_x, e_y are x and y components of eccentricity e respectively, and

r_y is the location of plate center point with respect to coordinate axis.

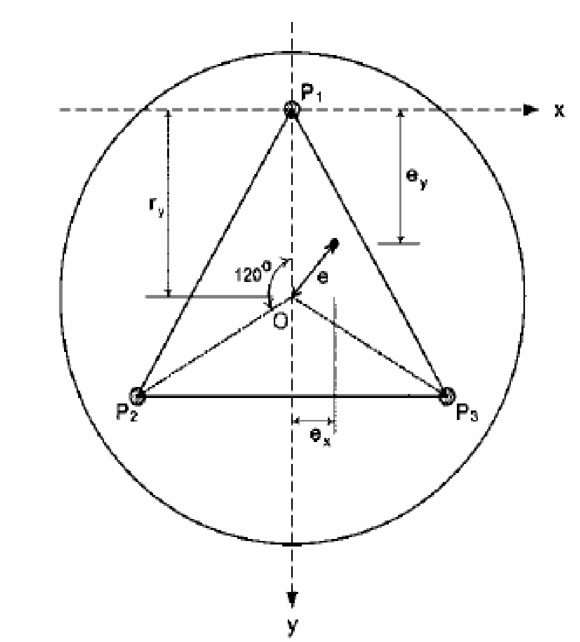

Figure 2.3 Free Body Diagram to Determine e_x and e_y

The PDA can be placed in the Servopac compactor, and the forces obtained directly from Servopac, and from the PDA, can be used to calculate GS. As shown in Figure 2.4, the GS values, whether determined from the Servopac data or by the PDA, are almost identical.

2.4.2. Troxler SGC and PDA

In order to examine the influence of the compactor type on GS results, twelve of the mixes were compacted using the Troxler (Model 4140) Superpave Gyratory Compactor, equipped with the PDA plate. All samples per mix have yielded approximately the same GS values, as shown in Figure 2.5, irrespective of the compactor type. The minor discrepancy of results can be attributed to the random variability in the mix batches and in the laboratory operations, since the samples compacted with the Troxler compactor were done at the ITD Central Laboratory, while those compacted by the Servopac were prepared at the University of Idaho. The results indicate that the PDA can be used to obtain the compaction forces and calculate GS.

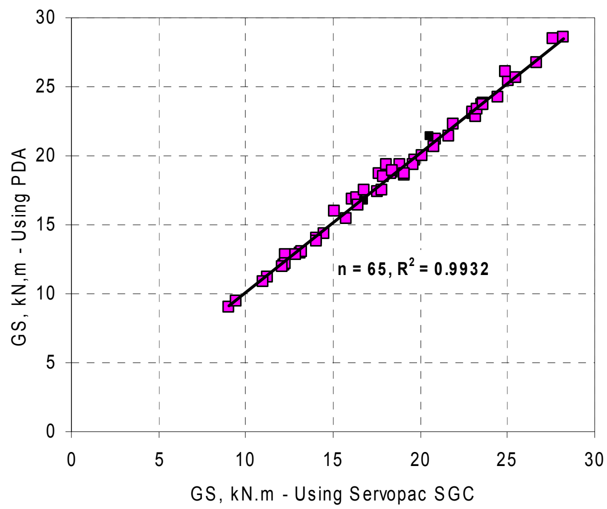

Figure 2.4 Comparison between GS Values Calculated Using Servopac and PDA

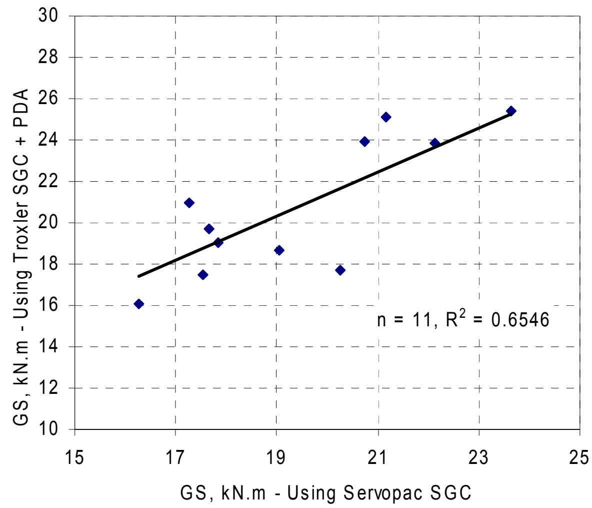

Figure 2.5 Comparison between GS Values Calculated Using Servopac and Troxler Compactors

2.4.3. Pine SGC

The Pine Instrument AFG1A SGC is designed to compact prepared HMA specimens at a constant consolidation pressure, a constant angle of gyration, and at a fixed speed of gyration (Dalton 2004). The Pine AFG1 compactor is equipped with a shear measurement system, which records the shear stress in terms of a unitless Gyratory Shear Ratio once per gyration. The Gyratory Shear Ratio is automatically recorded each time an HMA specimen is compacted, and the shear data can be recovered from the data file generated by the Pine AFG1A SGC. No special setting is required.

During the compaction process in the Pine AFG1A SGC, the compactor's ram applies a force (R) to the bottom plate as shown in Figure 2.6. This ram force is opposed by an equal but opposite force at the fixed top plate. Given the cross-sectional area of the mold (A), the ram pressure (P) can be computed as follows:

$$P = \frac{R}{A} \tag{2.13}$$

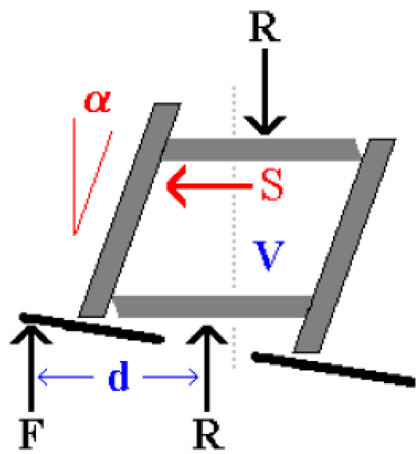

Figure 2.6 Simple Shear Diagram (Dalton 2004)

Further, to achieve the gyration angle during compaction, a vertical force (*F*) is applied. The force would vary based on the lever arm distance (*d*), the mix stiffness, the specimen volume (*V*), and the ram pressure. The Shear Stress may be determined by Equation 2.14 (Dalton 2004).

$$S = \frac{F.d}{V} \tag{2.14}$$

The Pine AFG1A SGC computes and reports the Gyratory Shear Ratio (σ) in its output, in addition to the changes in height, vertical pressure, and the gyration angle.

$$\sigma = \frac{S}{P} \tag{2.15}$$

These parameters are essential in calculating GS; therefore, the Pine AFG1A SGC has a high potential to be used for this purpose. Unfortunately, the Pine technical center was not able to provide the research team with the location of the force sensors in the Pine AFG1A SGC or the value of the level arm (*d*), which are essential to back-calculate the actual shear force generated in the HMA specimen during compaction, excluding the machine losses.

Therefore, it was decided to adopt a practical approach, by studying the forces diagram in the Pine SGC (Figure 2.6). It was found that it is very similar to the forces diagram in Servopac SGC used in determining GS (Figure 2.1). The only difference between the two compactors is how the gyration angle is applied (*F*). Pine SGC uses two pistons to apply the gyration angle, while the Servopac SGC uses three. If the shear stress computed using the Pine SGC could be correlated to the shear stress computed using the Servopac SGC, then there would be no need to revise the GS calculation procedure. Instead, the computed, correlated (modified) shear stress could be used directly.

The first step of this analysis was to determine if the forces applied on the specimen in the Pine AFG1A and the Servopac SGCs are the same, using the final air voids (AV %) as the criterion to compare the two compactors. It was found that the AV% for each mix, regardless of the SGC type, yielded approximately the same AV% (Figure 2.7). The minor discrepancy of results can be attributed to the random variability in the mix batches and in the laboratory operations. Thus, it can be assumed that the resultant applied forces are the same.

Then, the shear stresses computed by each compactor for the same mix were compared, and it was observed that these stresses follow the same trend (Figure 2.8), except that shear stresses computed by the Pine SGC are higher.

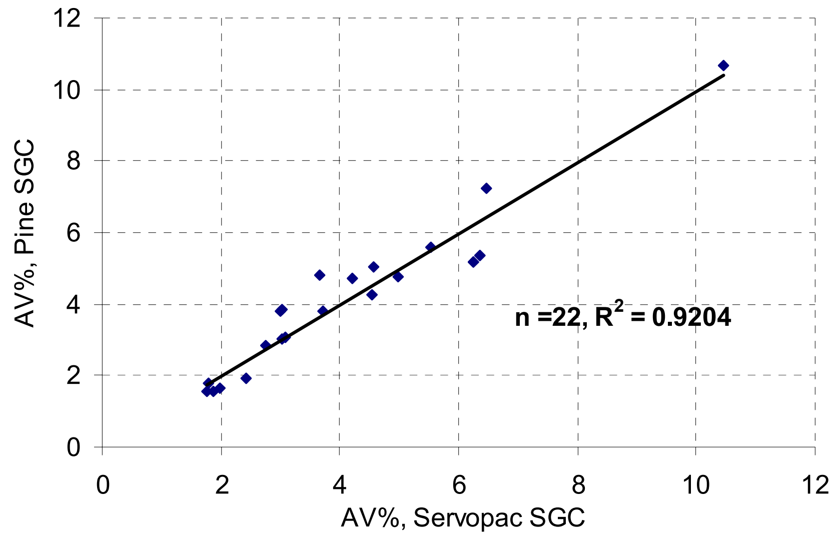

Figure 2.7 AV% Using Pine versus Servopac SGCs

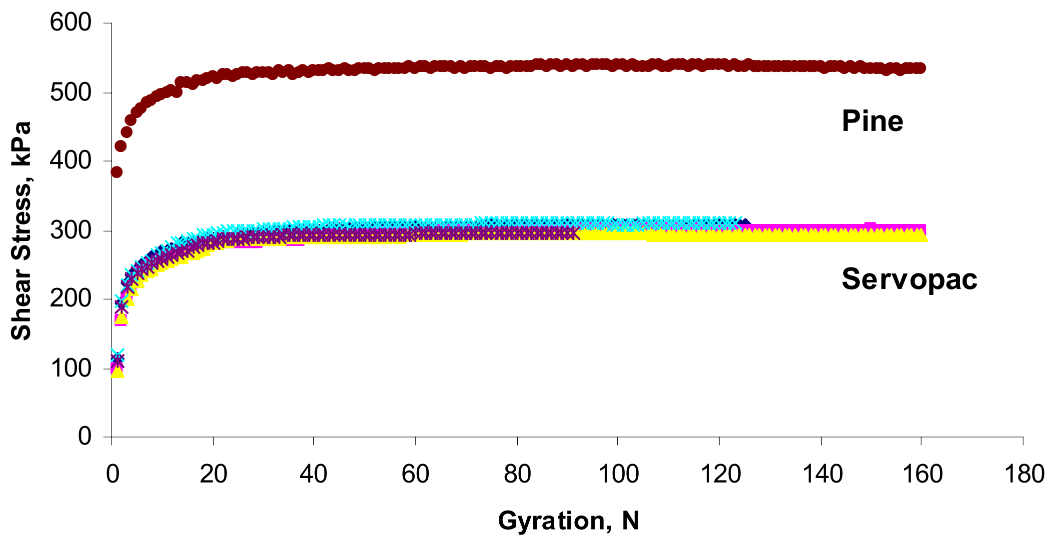

Figure 2.8 Comparison of Shear Stress Determined by Pine and Servopac SGCs

After a close examination, the shear stress computed by the Pine SGC seemed to correlate to the shear stresses computed by the Servopac. Thus, a numerical model was developed. It can be expressed as follows:

$$SS_{Servopac} = A.SS_{Pine} + B \tag{2.16}$$

where,

$SS_{Servopac}$ is the shear stress determined by Servopac SGC,

SS_{Pine} is the shear stress determined by Pine SGC, and

A and B are regression parameters and are equal to 0.82 and -52.14 respectively.

As a final step, using the modified shear stress computed by the Pine, the GS was calculated for all mixes, and compared to the GS values determined using the shear stress computed by the Servopac SGC. As shown in Figure 2.9, the GS values are approximately equal for the same mix. The minor differences are believed to be due to the variability in the mix batches and in the laboratory operations.

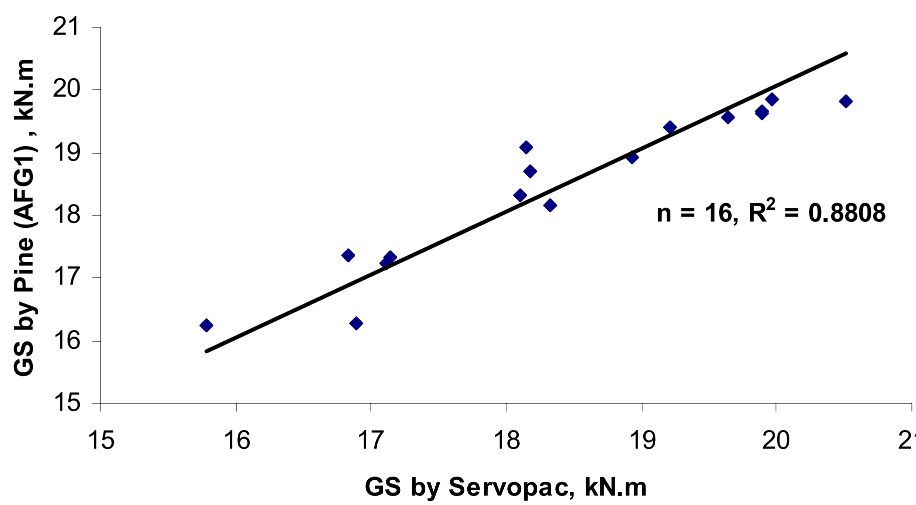

Figure 2.9 Gyratory Stability Calculated by Servopac and Pine SGC

2.5. SUMMARY

This research defines the Gyratory Stability (GS) as the same value as the Contac Energy Index (CEI), but measured between number of gyrations N_{G1} and N-design. The gyration number N_{G1} is determined based on an established criterion, which identifies the compaction point when the mix shear resistance starts to develop, and increases with more aggregate contacts. N-design is the number of gyrations defined by the Superpave system. For Hveem-designed mixes, N-design is considered to be the gyration at which the compacted mix reaches 4% air voids. Conclusions and observations on the evaluation of Gyratory Stability are the following:

The mix GS is a simple and quick parameter for measuring the mix stability. It is reproducible and independent of the compactor type.

GS can be determined using a shear-measurement-capable compactor with little modification. For an SGC with no shear measurement capacity, an external plate (i.e. PDA) can be used to determine the forces developed in the mix during compaction.

3. EXPERIMENTAL PROGRAMS USING IDAHO MIXES

3.1. INTRODUCTION

The experimental phase of this project involved two prgrams. First that involves Hveem designed mixes, and the second involves Superpave mixes. The overall objective of the Hveem mixes experimental program was to apply the Gyratory Stability concept on as many mixes as we could obtain, to represent the various mix conditions in the state of Idaho. At the beginning of the project, all Idaho mixes were designed in accordance with the Hveem design method. Near the end of the project period, however, ITD had begun construction of a few Superpave mixes in various parts of the state. Therefore, the mix evaluation process involved two groups of mixes: one group evaluated Hveem-designed and constructed mixes, and the second group evaluated Superpave mixes. These mixes were collected from the field sites at the time of construction. In order to not disturb the construction operation, mix samples were collected from the truck at the paver feeder in accordance with standard ITD sample collection methods. In this chapter, a description of the mixes used in this study, and their design parameters, are described for both mix groups.

3.2. HVEEM DESIGNED MIXES

In cooperation with the Idaho Transportation Department (ITD), fifty-two different mixes of HMA, designed and constructed in accordance to the Hveem method, were procured from various project sites located in Idaho. Figure 3.1 shows a map for the general geographical locations of the projects where these mixes were collected. Although these mixes were designed in accordance with the Hveem method, their binders were designed in accordance to the Superpave PG grading system. These mixes varied in their aggregate types, gradations (Mix Class I, II and III as per ITD general specifications (2004)), binder grade (PG 76-28, PG 70-28, PG 64-34, PG 64-28, PG 58-34, and PG 58-28), and binder content (3.3% - 6.1%). Mixes were selected to cover a wide range of Hveem stability values and various mix classes that are produced in Idaho. Most of the tests were performed on field batches as they were provided by the state engineer. Some of the mixes were duplicated in the laboratory and modified to test the effect of mix properties, such as asphalt content and binder grade, on Gyratory Stability (GS). Table 3.1, Table 3.2 and Table 3.3 describe the main characteristics of the selected mixes. Details about these mixes are documented in Appendix A "Mix design and Job Mix Formula (JMF) for all mixes."

Field batches for the mixes were tested to confirm their Hveem design parameters, and, using the SGC, samples were prepared in order to calculate GS values, as well as for Asphalt Pavement Analyzer (APA) and Fracture Toughness (J_c) testing. Samples were compacted, and the GS values for all mixes were calculated at the UI asphalt lab.

For the purpose of investigating whether GS correlated with Hveem stability, all specimens were compacted to a number of gyrations to produce samples with 4% air void (the design target for Hveem criteria). However, the maximum number of gyrations applied was limited to 250. In the case of coarser mixes, where 4% air void was not achievable, even at 250 gyrations, that sample was eliminated from the population used for Hveem stability correlation.

Details about these mixes are documented in Appendix A. Compaction data files are provided on the attached CD as Appendix B.

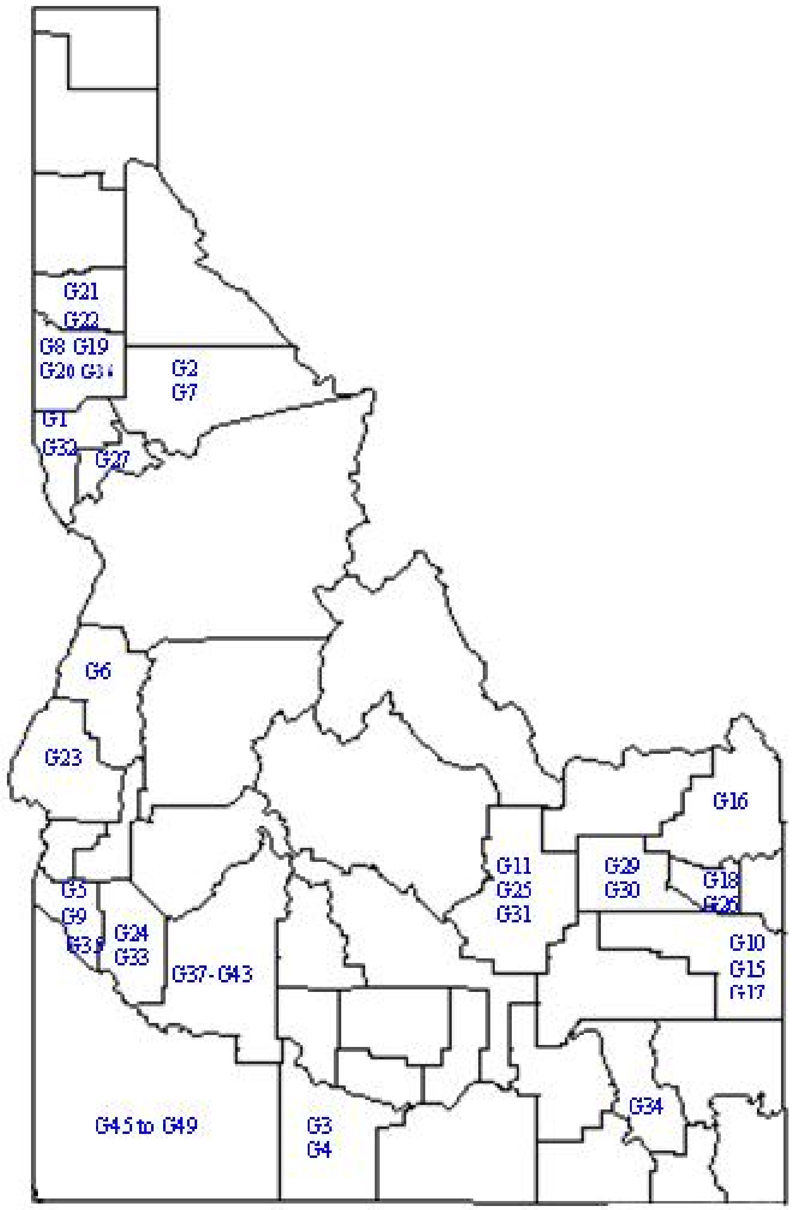

Figure 3.1 Idaho Counties and the Locations of Procured HMA Mixes

Table 3.1 Properties of Selected Field and Lab Modified Hveem Mixes (Class I)

Mix Class	Binder Grade	% AC	Mix Designation	J_c Testing	APA Testing
I	76-28	4.20	G24-L (-1% AC)	√	
		5.20	G24	√	√
			G24-L	√	√
		5.50	G08	√	
		5.55	G21	√	√
	70-28	4.80	G05	√	
		5.16	G01	√	
		5.30	G02	√	
			G03	√	
		5.5	G45-G48		
	64-34	3.90	G10	√	
	64-28	5.20	G18	√	
		5.20	G18-L	√	
		5.80	G26	√	√
		4.90	G03	√	
	58-34	5.30	G04	√	
			G06	√	
		5.30	G09	√	
		5.44	G22	√	√
		5.50	G49		
		5.70	G32	√	√
		5.30	G16	√	
	58-28	4.40	G44		
		4.90	G36		
		5.10	G37-G43		
		5.90	G11	√	

Table 3.2 Properties of Selected Field and Lab Modified Hveem Mixes (Class II)

Mix Class	Binder Grade	% AC	Mix Designation	J_c Testing	APA Testing
II	76-28	5.65	G20-L (76-28)	√	
	64-34	4.70	G34	√	
	64-28	5.00	G07	√	
		5.65	G20	√	√
			G20-L (64-28)	√	√
	58-34	3.30	G29-L (-1% AC)	√	
		4.20	G15	√	
		4.30	G25	√	√
			G29	√	√
			G29-L	√	√
			G30	√	
			G31	√	√
		5.30	G29-L (+1% AC)	√	
		5.65	G20-L (58-34)	√	
	58-28	4.80	G23	√	√
			G35	√	
		5.10	G17	√	
		5.65	G20-L (58-24)	√	

Table 3.3 Properties of Selected Field and Lab Modified Hveem Mixes (Class III)

Mix Class	Binder Grade	% AC	Mix designation	J_c testing	APA testing
III	64-34	4.30	G12	√	
			G13	√	
			G14	√	
	58-28	5.80	G27	√	√
			G27-L	√	√
		5.90	G19	√	
		6.10	G28	√	√

3.3. SUPERPAVE DESIGNED MIXES

The Idaho Transportation Department implemented the Superpave PG binder specifications several years ago, and recently utilized the Superpave mix design on a few projects in the state. In cooperation with ITD, raw materials from two different Superpave design mixes were obtained. These mixes were duplicated in the laboratory and were modified in order to study the effect of the mix properties, such as asphalt content and binder grade, on the performance of the mix.

Samples were compacted using the SGC in order to calculate their GS values. Then, samples were prepared for Asphalt Pavement Analyzer (APA), Fracture Toughness (Jc), Dynamic Modulus (E*), and Flow Number (Fn) testing. For the purpose of investigating whether GS correlated to Superpave specifications, samples at optimum conditions were compacted to N-design as specified by the Superpave mix design for Superpave mixes. However, for Hveem mixes, the samples were compacted to varied number of gyrations to produce specimens with 4% air voids, which is the design target for Superpave mix design. In any case, the number of Gyrations was limited to maximum of 250 if the 4% air voids was not achieved. Table 3.4 describes these mixes and the applied alterations.

Details about these mixes are documented in Appendix A. Compaction data files are provided on the attached CD in Appendix B.

Table 3.4 Properties of Selected Field and Lab Modified Superpave Mixes

Mix	Binder Grade	% AC	J_c Testing	APA Testing	E^* and *Fn* Testing
Mix 1	64-34	5.0 (-0.5 AC%)	√	√	√
		5.5 (opt. AC%)	√	√	√
		6.0 (+0.5 AC%)	√	√	√
		6.5 (+1.0 AC%)	√	√	√
Mix 2	64-28	5.0 (-1.0 AC%)	√		√
		5.9 (opt. AC%)	√	√	√
		7.0 (+1.0 AC%)	√	√	√
	64-22	5.9 (opt. AC%)	√	√	√
	64-34	5.9 (opt. AC%)	√	√	√

4. EVALUATION OF AGGREGATE TEXTURE AND SHAPE PROPERTIES USING IMAGE ANALYSIS

4.1. DEFINITION OF AGGREGATE SHAPE

Researchers have distinguished between the different aspects that constitute particle geometry. Particle geometry can be fully expressed in terms of three independent properties: form, angularity (or roundness), and surface texture. Figure 4.1 shows a schematic diagram that illustrates the differences between these properties. Form, the first order property, reflects variations in the proportions of a particle. Angularity, the second order property, reflects variations at the corners; that is, variations superimposed on shape. Surface texture is used to describe the surface irregularity at a scale that is too small to affect the overall shape. These three properties can be distinguished because of their different scales with respect to particle size, and this feature can also be used to order them. Any of these properties can vary widely without necessarily affecting the other two properties.

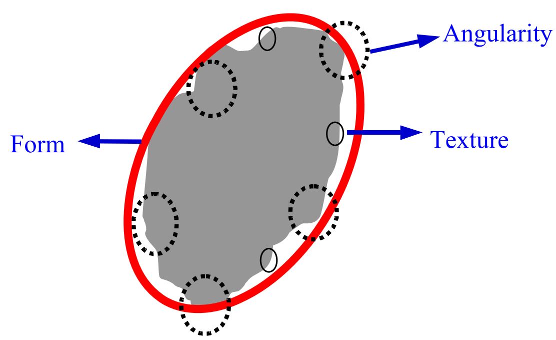

Figure 4.1 Components of an Aggregate Shape: Form, Angularity, and Texture

4.2. AIMS OPERATIONS

Details of the main components and design of the prototype Aggregate Imaging System (AIMS) have been reported by Masad (2003). Researchers developed AIMS to capture images and analyze the shape of a wide range of aggregate types and sizes, which represent those used in asphalt mixes, hydraulic cement concrete, and unbound aggregate layers of pavements. AIMS uses a simple setup that consists of one camera and two different types of lighting schemes to capture images of aggregates at different resolutions, from which aggregate shape properties are measured using image analysis techniques.

The system operates based on two modules. The first module is for the analysis of fine aggregates (smaller than 4.75 mm (#4)), where black and white images are captured. The second module is devoted to the analysis of coarse aggregates (larger than 4.75 mm (#4)). In the coarse module, gray images as well as black and white images are captured. Combining both the coarse and fine aggregate analysis into one system is considered advantageous, due to the reduced cost of developing the system. It also allows the use of the same analysis methods to quantify aggregate shapes, irrespective of their size, to facilitate relating aggregate shape to pavement performance.

Fine aggregates are analyzed for form and angularity using black and white images, which are captured using backlighting under the aggregate sample tray. This type of lighting creates a sharp contrast between the particle and the tray, thus giving a distinct outline of the particle. A study by Masad, et al. (2001) clearly shows that a high correlation exists between the angularity (measured on black and white images) and texture (measured on gray scale images) of fine aggregates. Therefore, only black and white images are used to analyze fine aggregates.

AIMS is designed to capture images for measuring fine aggregate angularity and form at a resolution such that a pixel size is less than 1 percent of the average aggregate diameter, and the field of view covers 6-10 aggregate particles (Masad, et al. 2000). In other words, the resolution of an image is a function of aggregate size. The image acquisition setup is configured to capture a typical image of 640 by 480 pixels at these resolutions in order to analyze various sizes of fine aggregates.

For coarse aggregates, researchers have found that there is a distinct difference between angularity and texture, and these properties have different effects on performance (Fletcher, et al. 2003). Consequently, AIMS analyzes coarse aggregates for shape and angularity using black and white images, and analyzes texture using gray images. A backlighting table is used to capture the black and white images, while a top lighting table captures gray images of particles surfaces. As for fine aggregates, the image acquisition setup captures images of 640 by 480 pixels. In the coarse aggregate module, only one particle is captured per image in order to facilitate the quantification of form, which is based on three-dimensional (3-D) measurements. As described later in this chapter, the use of the video microscope determines the depth of a particle, while the images of two-dimensional projections provide the other two dimensions to quantify form. Texture is determined by analyzing the gray images, using the wavelet method described later.

AIMS utilizes a closed-loop DC servo control unit of the x, y, and z axes for precise positioning and highly repeatable focusing. The x and y travel distance is 37.5 cm (15 inches); and the z travel distance is 10 cm (4 inches). The external controller is housed in a small 15 x 10 cm (6 x 4 inches) case.

The Optem Zoom 160 video microscope is also used in AIMS. The Zoom 160 has a range of X16, which means that an image can be magnified by 16 times. This magnification allows for the capture of a wide range of particle sizes without changing parts. AIMS is equipped with a Pulnix TM-9701 progressive scan video camera with a 16.9 mm (2/3 inch) CCD imager. It has an adjustable shutter speed from 1/60 s to

1/16000 s. The progressive scan video camera captures images at a higher speed than line scan cameras, and it is less affected by noise.

AIMS is equipped with both bottom lighting and top lighting, composed of a ring mounted on the video microscope (Figure 4.2). The ring light provides uniform illumination of the region directly in the view of the microscope.

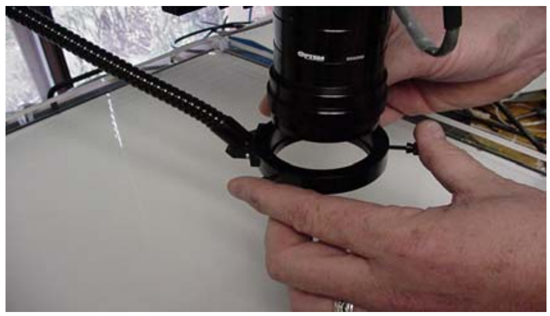

Figure 4.2 Top Lighting Used in AIMS

4.2.1. Fine Aggregate Module Operation Procedure

The analysis of fine aggregates starts by randomly placing an aggregate sample (ranging from a few grams for small fine aggregate sizes, up to a couple of hundred grams for the larger fine aggregate size) on the aggregate tray with the backlighting turned on. A camera lens of 0.5X objective is used to capture the images. The 0.5X objective lens will provide a field of view of 26.4 x 35.2 mm with a 1X Dovetail tube and a 2/3 foot camera format at a working distance of 181 mm. The camera and video microscope assembly moves incrementally in the x direction at a specified interval, capturing images at every increment. Once the x-axis range is complete, the aggregate tray moves in the y-direction for a specified distance, and the x-axis motion is repeated. This process continues until the whole area is scanned.

Depending on the size of aggregates to be analyzed, the z-location of the camera is specified in order to meet the resolution criteria in Table 4.1. These criteria are established such that the results are not influenced by size (Masad, et al. 2000). Aggregates that are not within the size for which the scan is conducted, and consequently do not meet the criteria in Table 4.1, are removed from the image.

Table 4.1 Resolutions and Field of View Used in Angularity Analysis of Fine Aggregates

Particle Size (mm)	Magnification	Field of View (mm)	Resolution (Pixel/mm)
4.725 – 2.36	2.00	13.2 x 17.6	36.36
2.36 – 1.18	4.125	6.4 x 8.5	75.29
1.18 – 0.6	8.25	3.2 x 4.3	148.84
0.6 – 0.30	16	1.65 x 2.2	290.91
0.30 – 0.15	16	1.65 x 2.2	290.91

4.2.2. Coarse Aggregate Module Operation Procedure

Coarse aggregate analysis starts by placing the aggregate sample on the tray with marked grid points. The camera lens used for capturing the coarse aggregate has a 0.25X objective lens. The maximum field of view achieved in the coarse aggregate module is 52.8 x 70.4 mm with a 1X Dovetail tube and a 2/3 inch camera format at a working distance of 370 mm. The camera and microscope move in the same manner as for fine aggregates, but with different distances and intervals. In this module, only one particle is captured in each image. Researchers use backlighting to capture the images for the analysis of angularity, and they use top lighting to capture images for texture analysis. Therefore, two scans are conducted for coarse aggregates.

Backlighting is used in order to capture black and white images. These images are analyzed later to determine angularity, and the major (longest) and minor (shortest) axes on these two-dimensional images. The analysis of coarse aggregate angularity starts by placing the aggregate particles in a grid pattern with a distance of 50 mm in the x-direction and 40 mm in the y-direction from center to center. The z-location of the camera is fixed for all aggregate sizes. Table 4.2 presents image resolutions used in the coarse aggregate angularity analysis.

Table 4.2 Resolutions and Field of View Used in Angularity Analysis of Coarse Aggregates

Particle Size (mm)	Magnification	Field of View (mm)	Resolution (pixel/mm)
9.5 – 4.725	1	52.8 X 70.4	9.12
12.7 – 9.5	1	52.8 X 70.4	9.12
19.0 – 12.7	1	52.8 X 70.4	9.12
25.4 – 19.0	1	52.8 X 70.4	9.12
> 25.4	1	52.8 X 70.4	9.12

Capturing images for the analysis of coarse aggregate texture is very similar to the angularity analysis except that top lighting is used instead of backlighting, in order to capture gray images. The texture scan starts by focusing the video microscope on a marked point on the lighting table while the backlighting is turned on. The location of the camera on the z-axis at this point is considered as a reference point (set to zero coordinate). Then an aggregate particle is placed over the calibration point. With the top light on, the video microscope moves up automatically on the z-axis in order to focus on the aggregate surface. The z-axis coordinate value on this new position is recorded. Since the video microscope has a fixed focal length, the difference between the z-axis coordinate at the new position and the reference position (zero) is equal to aggregate depth. This procedure is repeated for all particles. The particle depth is used, along with the dimensions measured on black and white images, to analyze particle shape or form as discussed later.

4.3. AIMS ANALYSIS METHODS

4.3.1. Texture Analysis Using Wavelets

Wavelet analysis is a powerful method for describing the decomposition of the different scales of texture in aggregate samples (Mallat 1989). In order to isolate fine variations in texture, very short-duration basis functions should be used. At the same time, very long-duration basis functions are suitable for capturing coarse details of texture. These measurements are accomplished in wavelet analysis by using short high-frequency basis functions and long low-frequency ones. The wavelet transform works by mapping an image onto a low-resolution image and a series of detailed images. The low-resolution image is obtained by iteratively blurring the original images, eliminating fine details in the image while retaining the coarse details. The remaining detailed images contain the information lost during this operation. The low-resolution image can be further decomposed into the next level of low resolution and detailed images.

Figure 4.3 illustrates the wavelet analysis. The texture information lies in the detail coefficients LH, HL, and HH. The LH coefficients pick up the high frequency content in the vertical direction, the HL coefficients pick up the high frequency content in the horizontal direction, and the HH coefficients pick up the high frequency content in the diagonal direction. Thus, depending upon the selected detail coefficient, directionally oriented texture information can be extracted. Since the directional orientation of the texture content is not emphasized in this project, texture contents in all the directions are given the same weight. Thus, a simple sum of the squares of the detail coefficients (the texture content) is computed as the texture index of the aggregate at that particular resolution. More importantly, detail coefficients have information at different scales, depending upon the level of decomposition. Multi-resolution (or scale) analysis is a very powerful tool that is not possible using a regular Fourier transform.

To describe the texture content at a given resolution or decomposition level, a parameter called the wavelet texture index is defined. The texture index at any given decomposition level is the arithmetic mean of the squared values of the detail coefficients at that level:

$$\textit{Texture Index}_n(\text{Wavelet Method}) = \frac{1}{3N}\sum_{i=1}^{3}\sum_{j=1}^{N}\left(D_{i,j}\left(x,y\right)\right)^2 \tag{4.1}$$

where,

n refers to the decomposition level,

N denotes the total number of coefficients in a detailed image of texture,

i takes values 1, 2, or 3, for the three detailed images of texture,

j is the wavelet coefficient index, and

(x, y) is the location of the coefficients in the transformed domain.

In this project, the texture is decomposed to six levels. However, only the results from level 6 are used since previous research has shown that level 6 is the least affected by color variations and the presence of dust particles on the surface (Masad 2003).

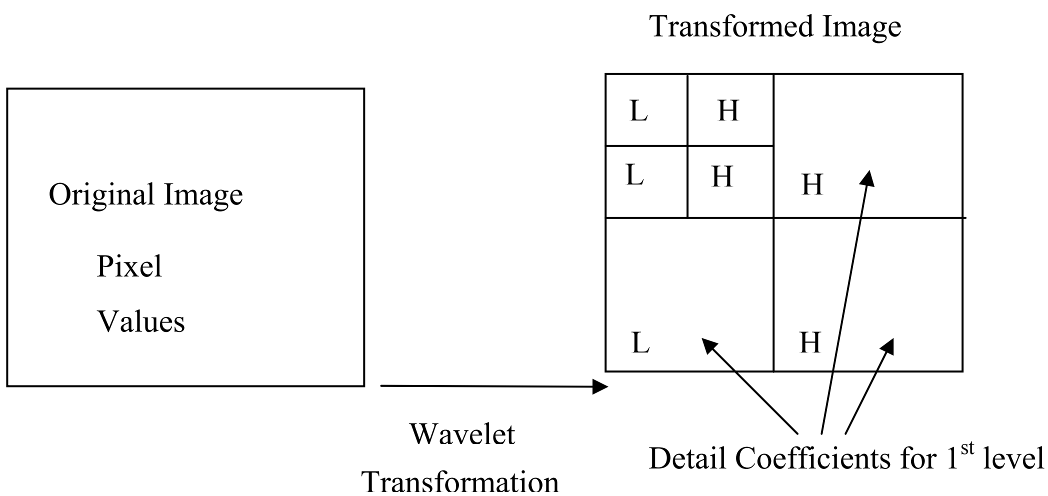

Figure 4.3 Two-level Wavelet Transformation

4.3.2. Angularity Analysis Using Gradient Method

In order to measure angularity, one needs a method that assigns a finite value of angularity to a highly angular particle with sharp angular corners, and simultaneously assigns near-zero angularity to a well-rounded particle. In addition, the method should be capable of distinguishing those particle shapes that have angularities between these two extremes, but which appear similar to the naked eye. The gradient method, described below, possesses both of these properties.

The gradient-based method for measuring angularity starts by calculating the gradient vectors at each edge-point using a Sobel mask, which operates at each point on the edge and its eight nearest neighbors. The gradient of an image $f(x, y)$ at location (x, y) is the vector:

$$\nabla f = \begin{bmatrix} G_x \\ G_y \end{bmatrix} = \begin{bmatrix} \dfrac{\partial f}{\partial x} \\ \dfrac{\partial f}{\partial y} \end{bmatrix} \qquad (4.2)$$

It is known from vector analysis that the gradient vector points in the direction of the maximum rate of change of f at (x, y). The magnitude of the vector is given by ∇f, where:

$$\nabla f = mag(\nabla f) = \left[G_x^2 + G_y^2\right]^{\frac{1}{2}} \tag{4.3}$$

The direction of the gradient vector can be represented by the angle $\theta(x, y)$ of the vector ∇f at (x, y):

$$\theta(x, y) = \tan^{-1}\left(\frac{G_x}{G_y}\right) \tag{4.4}$$

where the angle is measured with respect to the x axis.

It should be noted that computation of the gradient of an image is based on calculating the partial derivatives $\frac{\partial f}{\partial x}$ and $\frac{\partial f}{\partial y}$ at every pixel location. These derivatives are implemented in the discrete domain using the Sobel operator, which has the advantage of providing both a differentiating and a smoothing effect. The smoothing effect is particularly useful because the derivative operation has the effect of enhancing noise. At sharp corners of the edges of a particle image, the direction of the gradient vector changes rapidly. On the other hand, the direction of the gradient vector for rounded particles changes slowly for adjacent points on the edge.

For the angularity analysis of aggregates, researchers use the angle of orientation values (θ) of the edge-points, and the magnitude of the difference in these values $(\Delta\theta)$ for adjacent points on the edge, to describe how sharp (large $\Delta\theta$) or how rounded (small $\Delta\theta$) the corner is. Based on the orientation of the gradient-vectors at each edge-point, the angularity index is calculated for the aggregate particle. Angularity values for all boundary points are calculated, and their sum accumulated around the edge, to form the angularity index of the aggregate particle. The angularity index can be represented mathematically as:

$$\textit{Angularity Index}\text{ (Gradient Method)} = \sum_{i=1}^{N-3} \left| \theta_i - \theta_{i+3} \right| \qquad (4.5)$$

where,

the subscript i denotes the i^{th} point on the edge of the particle, and

N is the total number of points on the edge of the particle.

The step-size used in this project was 3. That is, the angle of orientation of every third point on the boundary of the aggregate was used to form the angularity index. This value was determined empirically to be optimum, given the resolution of the edge of the images used in the project.

4.3.3. Form Analysis Using Sphericity

Information about the three dimensions of a particle, namely the longest dimension, (dL), the intermediate dimension (dI), and the shortest dimension (ds) is essential for proper 3-D characterization of the aggregate form. Sphericity is defined in terms of these three dimensions as shown in Equation 4.6:

$$\text{Sphericity} = \sqrt[3]{\frac{\mathrm{d_s}.\mathrm{d_I}}{\mathrm{d_L^2}}} \qquad (4.6)$$

AIMS uses the auto focus microscope to measure the depth of a particle, while the two-dimensional projections are analyzed using eigenvector analysis to determine the principal axes. In this method, the binary image of the aggregate is treated as a two-dimensional population. Each pixel in the population is treated as a two-dimensional vector $x = (a, b)^T$, where a and b are the coordinate values of that pixel with respect to x and y axes. These vectors are used to compute the mean vector and covariance matrix of the population. The eigenvectors of the covariance matrix are computed, which are orthogonal to each other. The major and minor axes (or the longest and intermediate axes in this case) of the object (aggregate) are aligned along these eigenvectors. Since it is easy to find the centroid of the aggregate, the length of the axes is the same as the distance from the centroid of the aggregate to the edge along the two axes (eigenvectors). This method gives major and minor axes on the projection. These axes with the particle thickness are used to calculate the sphericity in Equation 4.6.

4.4. AGGREAGTE SHAPE CLASSIFICATION

A comprehensive methodology for classification of aggregates based on the distribution of their shape characteristics should exhibit the following features:

- It represents the three characteristics of aggregate shape (three dimensions of coarse aggregates, angularity, and texture).

- It unifies the methods used to measure the shape characteristics of fine and coarse aggregates.

- Similar to what is currently done for aggregate gradation, each of the shape characteristics is represented by a cumulative distribution function rather than an average value. Therefore, the methodology is capable of accommodating variations in shape within an aggregate sample, and better represents the effects of different processes such as blending and crushing on aggregate shape.

- It is developed based on statistical analysis of a wide range of aggregate types and sizes.

The classification methodology criteria, described above, arose from measuring the shape characteristics of aggregates from a wide range of sources and varying sizes using AIMS. The analysis generated a total of 195 tests on coarse aggregates and 75 tests on fine aggregates. On average, a coarse aggregate test involved 56 particles, while a fine aggregate test involved about 300 particles. All of this data was used in the development of the new classification system.

Researchers used cluster analysis to develop groups (or clusters) of aggregates based on the distribution of shape characteristics. Clustering is a widely used pattern recognition method for grouping data and variables. Grouping is done on the basis of similarities or differences. In many areas of engineering and science, it is important to group items into natural clusters. Basic references about clustering methods include most applied multivariate statistical texts (e.g., Johnson and Wichern, 2002; and Morrison, 2005). All clustering methods begin with a choice of a metric (a distance or closeness among objects) and a choice of a method for grouping objects.

The clustering method was applied to the analysis results of each shape property obtained from AIMS. The research team found that groups or clusters can be developed for each of the shape properties, irrespective of aggregate size. Figure 4.4 shows the developed classification limits. More details on the development of the classification methodology are available in Al-Rousan, et al. (2005).

The sphericity value gives a very good indication of the proportions of particle dimensions. However, one cannot determine whether an aggregate has flat, elongated, or flat and elongated particles using sphericity alone. To resolve this, the analysis shown in the chart in Figure 4.5 is included in the AIMS software to distinguish among flat, elongated, and flat and elongated particles. Superimposed on this chart are the 3:1 and 5:1 limits for the longest to shortest dimension ratio. The use of this chart is illustrated here, with the aid of the results from two aggregate samples denoted CA-2 and CA-4. Both aggregates CA-2 and CA-4 pass the 5:1 Superpave requirement (both had less than 10 percent content with a particle dimensional ratio of 5:1), but they had distinct distributions in terms of flat and elongated particles.

This type of analysis, shown in Figure 4.5, reveals valuable information about the distribution, which would not have been obtained if aggregates were classified based on the ratio of 5:1 only. Such details are needed to understand the influence of shape characteristics on asphalt mix performance. It is believed that some of the discrepancies in the literature with regard to the influence of shape on performance are attributed to the lack of such details; plus the reliance on indirect methods of measuring average indices to describe shape.

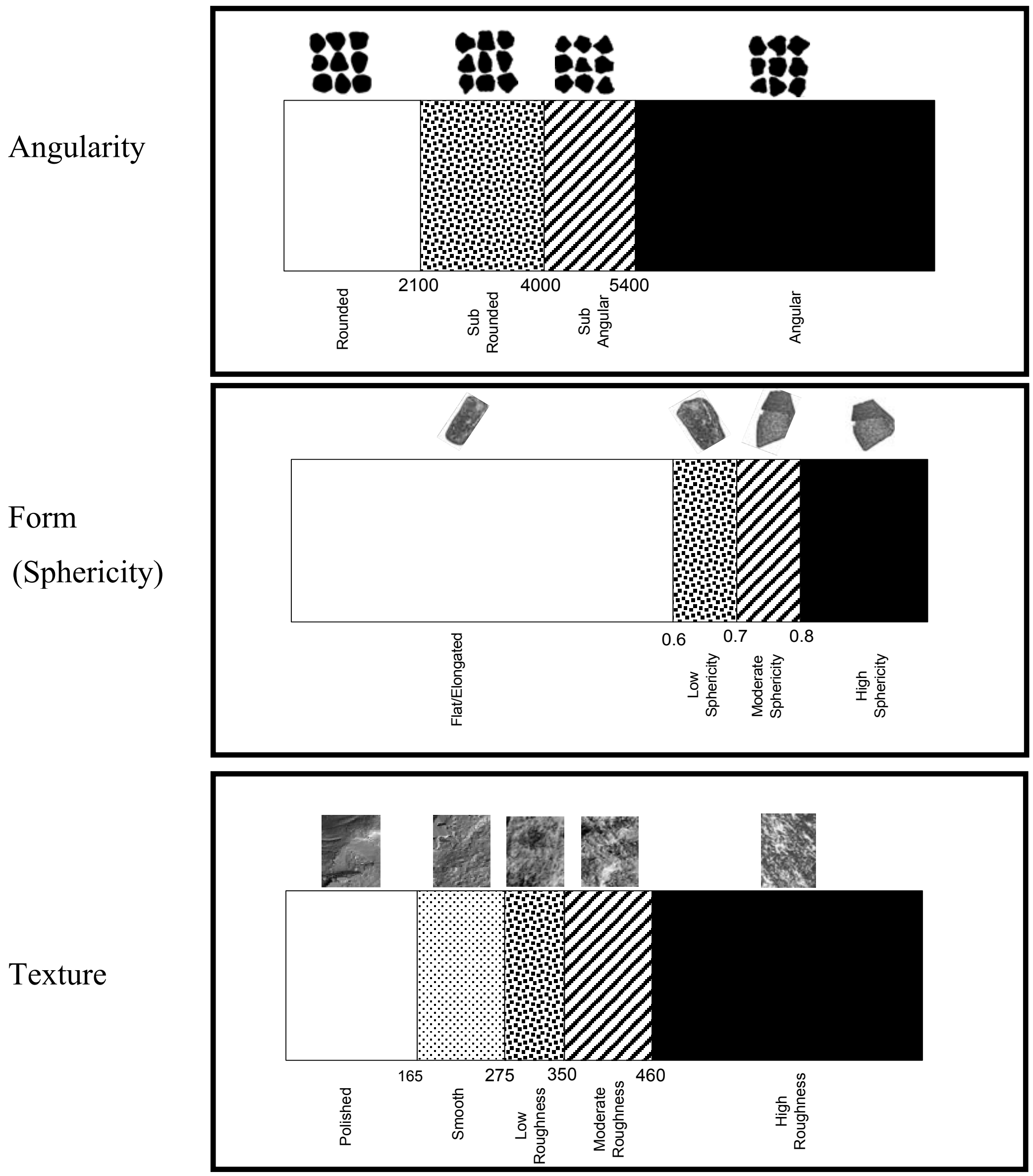

Figure 4.4 Aggregate Shape Classification Chart

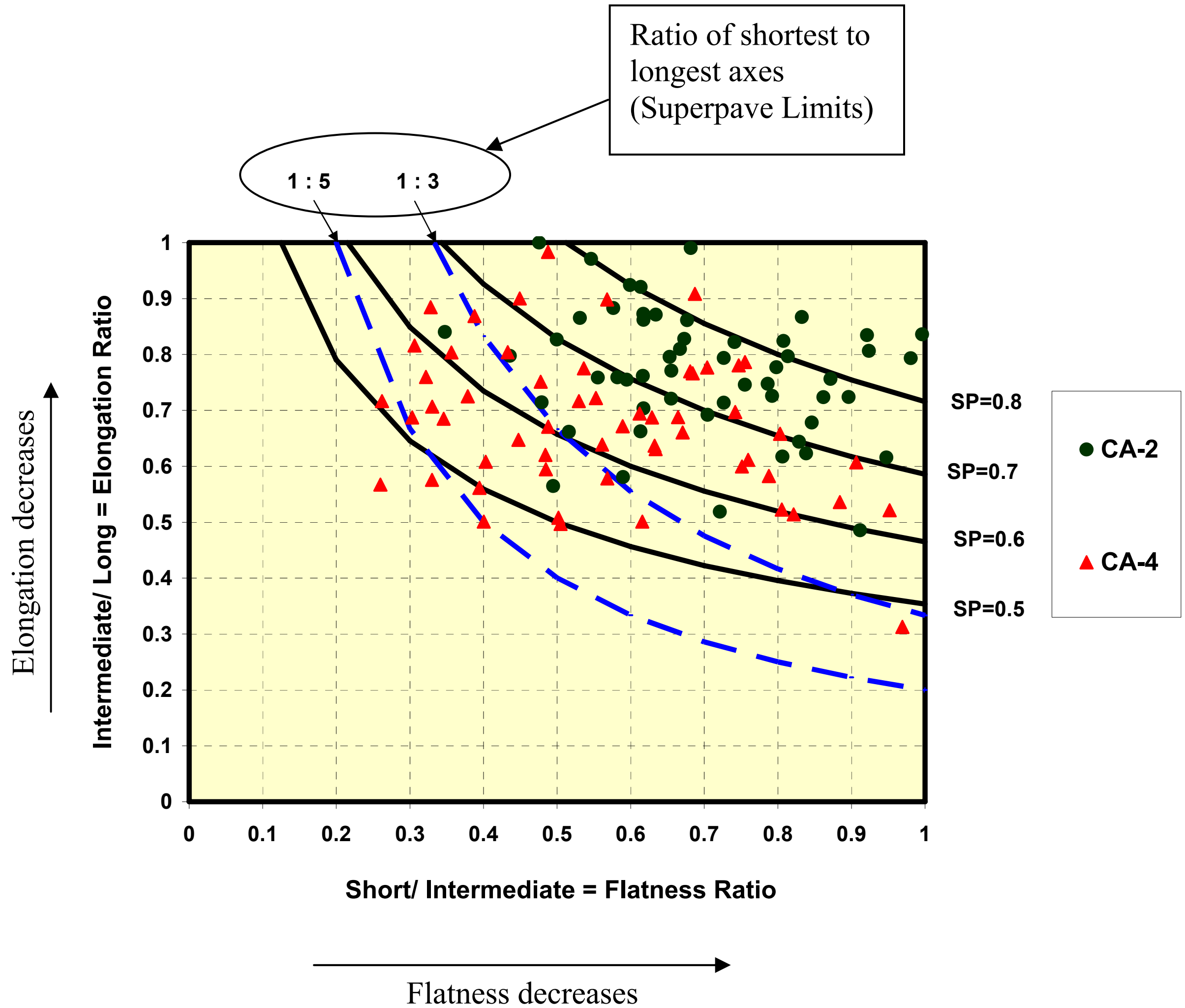

Figure 4.5 A Chart for Identifying Flat, Elongated, or Flat and Elongated Aggregates

4.5. ANALYSIS OF IDAHO AGGREGATES

Each coarse aggregate was sieved, and each coarse aggregate size with at least 56 particles was imaged and analyzed. The coarse aggregate analysis included texture, angularity and form. Statistical parameters (average and standard deviation) were also calculated for each of the aggregate sizes. The fine aggregates were also sieved and aggregates retained on sieves #8, #16, #30, and #60 were imaged and analyzed. The distributions of the shape characteristics for each aggregate size are given in the accompanying CD. The AIMS workbooks are programmed to facilitate the generation of graphical representations of the data and comparisons among different aggregates. For the sake of simplicity, the combined average and standard deviation for the different sizes from the fine and coarse fractions of each aggregate source were calculated. These values are shown in Tables 4.3 and 4.4 and Figures 4.6- 4.12. The following points summarize the main findings from these results:

- Coarse aggregates vary significantly in their texture. Mix 2 includes coarse aggregates with the highest texture compared with the other mixes (Figure 4.6).

- Mix 1 has coarse aggregates with the highest angularity (Figure 4.7). This high angularity can compensate for the relatively low texture of these aggregates.

- Mix 3 has the lowest angularity and texture. This mix can be susceptible to rutting, due to these unfavorable aggregate characteristics.

- Coarse aggregates of Mix 3 and aggregates from stockpile B of Mix 2 have the lowest sphericity values (Figure 4.8). These low sphericity values reflect the high percentage of particles with the longest to shortest dimension ratios, greater than 3:1 and greater than 5:1, as evident in the results shown in Figures 4.9 and 4.10. As would be expected from the definition of sphericity in Eq. 4.6, there is a very good correlation between sphericity and the percentage of particles with longest to shortest dimension ratios greater than 5:1 and 3:1 (Figure 4.11).

- There is wide variation in the angularity of fine aggregates. The sand used in Mix 2 has the lowest angularity (Figure 4.12)

Table 4.3 Summary of the Shape Characteristics of Coarse Aggregates

Aggregate Label	Texture		Angularity-Gradient		Sphericity		%Particles L/S>3	% Particles L/S>5
	Average	St. Dev	Average	St. Dev	Average	St. Dev		
G19-7650_Class_Mix_3	124.54	53.98	2829.98	1441.08	0.58	0.12	56.70	20.60
G20-8486_Class_Mix_2_Pile_A	205.96	47.56	3414.64	1449.06	0.65	0.11	34.50	5.50
G20-8486_Class_Mix_2_Pile_B	119.70	44.81	3504.20	1603.11	0.59	0.12	59.00	20.50
G20-8486_Class_Mix_2_Pile_C	108.77	33.04	2684.80	1286.58	0.65	0.10	36.60	2.70
G22-8327_Mix_Class_1_Pile_A	206.32	53.79	4062.62	1520.30	0.61	0.10	46.80	7.20
G22-8327_Mix_Class_1_Pile_B	147.86	45.67	3951.78	1418.58	0.60	0.11	23.40	5.40
G29-7068_Class_Mix_2	190.21	96.84	2950.84	1429.28	0.71	0.10	12.60	1.20

Table 4.4 Summary of the Angularity of Fine Aggregates

Aggregate Label	Angularity-Gradient	
	Average	St. Dev
G19-7650_Class_Mix_3	3724.82	1594.66
G20-8486_Class_Mix_2_Sand	3122.30	1439.88
G20-8486_Class_Mix_2_Pile_C	4209.80	1747.42
G22-8327_Mix_Class_1_Pile_C	4164.97	1677.99
G29-7068_Class_Mix_2	3442.01	1567.04

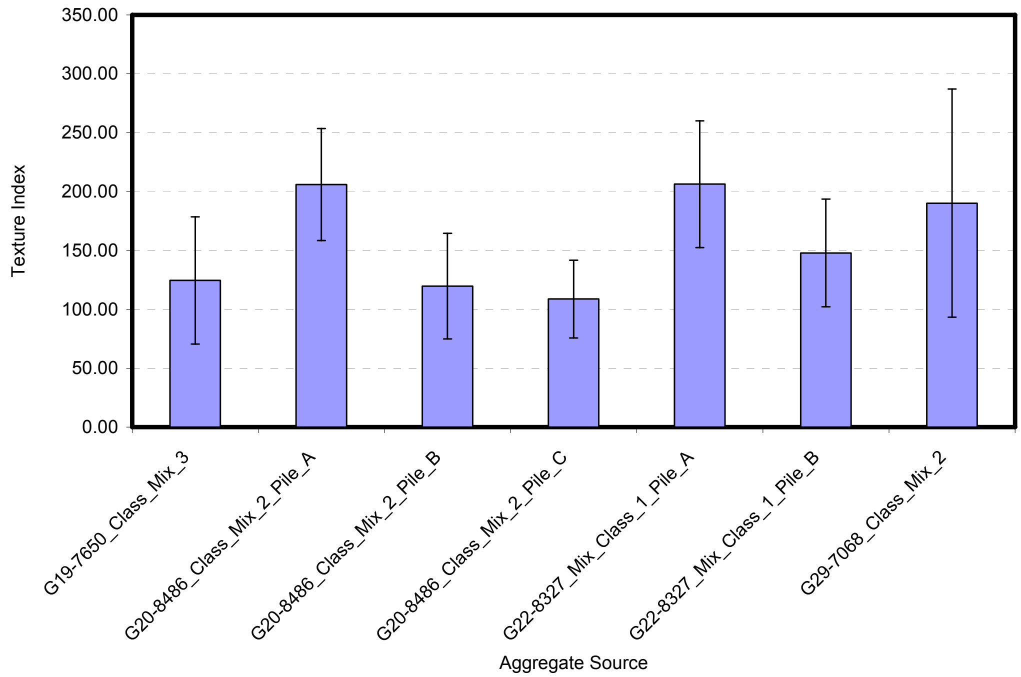

Figure 4.6 Texture of Coarse Aggregates

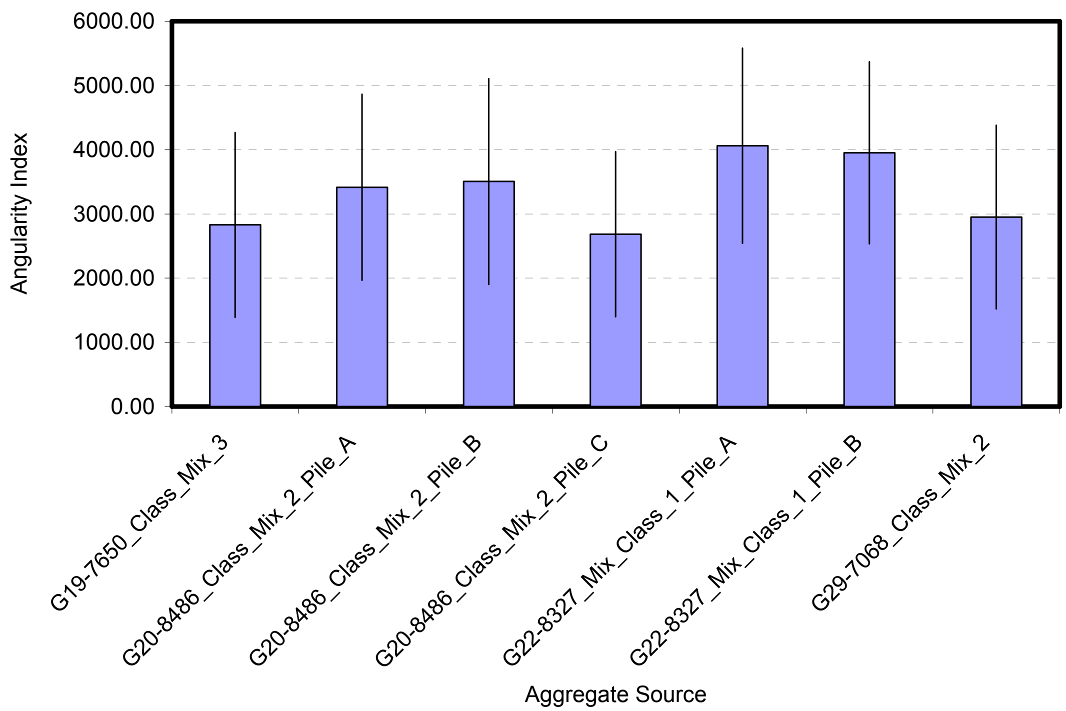

Figure 4.7 Angularity of Coarse Aggregates

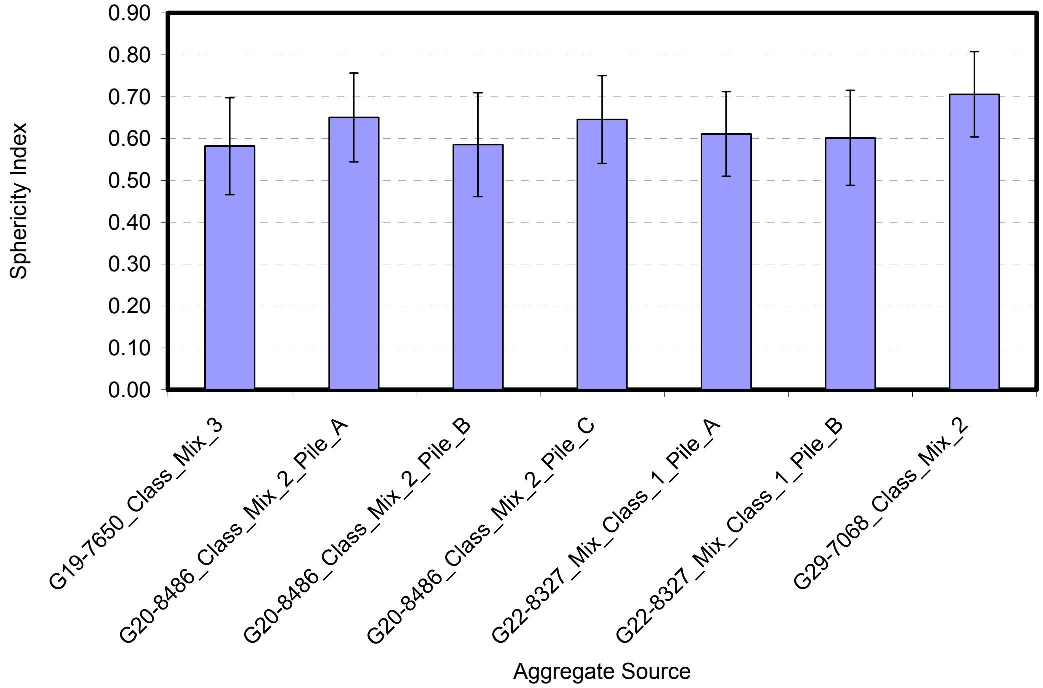

Figure 4.8 Sphericity of Coarse Aggregates

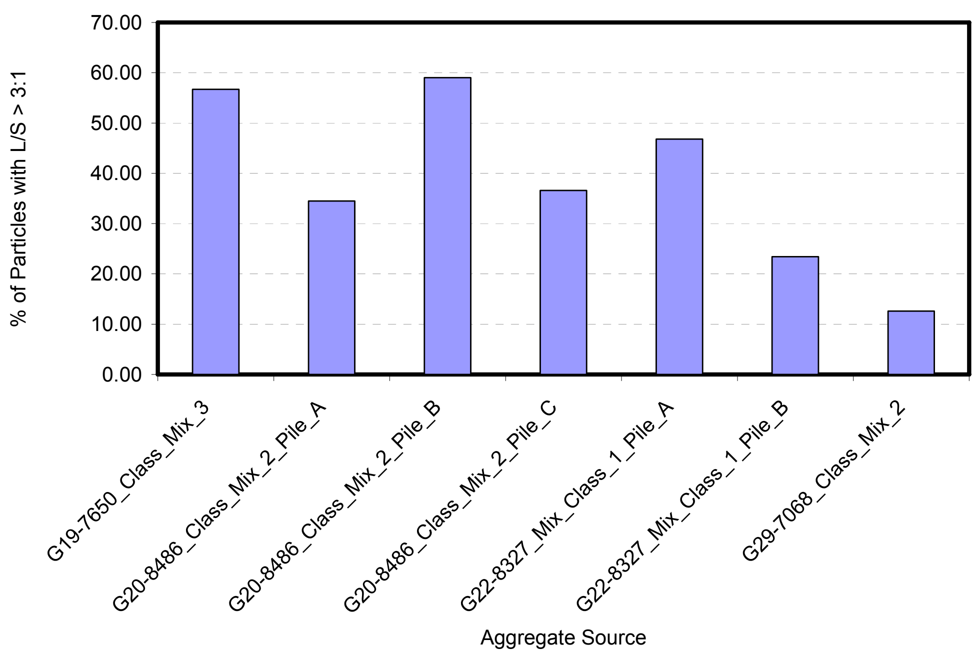

Figure 4.9 Percent of Particles with Longest to Shortest Dimensions Ratio Greater than 3:1

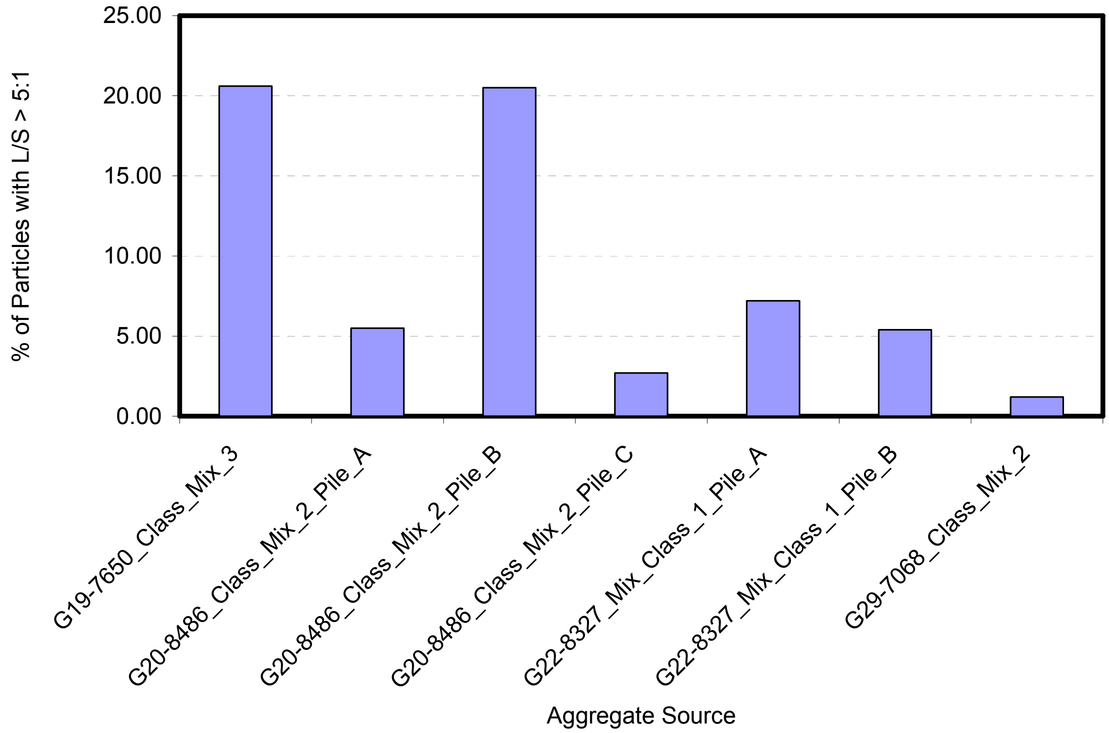

Figure 4.10 Percent of Particles with Longest to Shortest Dimensions Ratio Greater than 5:1

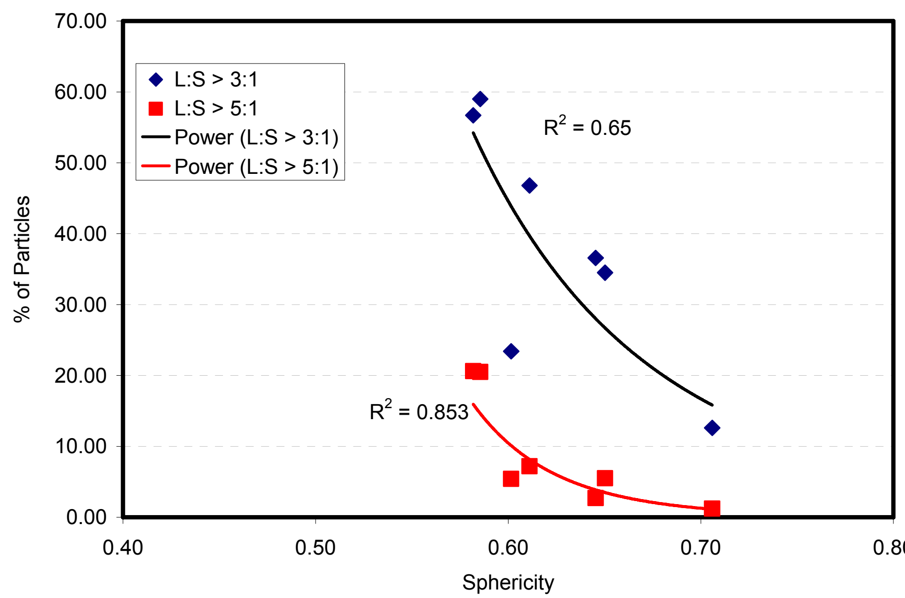

Figure 4.11 Correlations Between Sphericity Values and the Dimensions Ratio

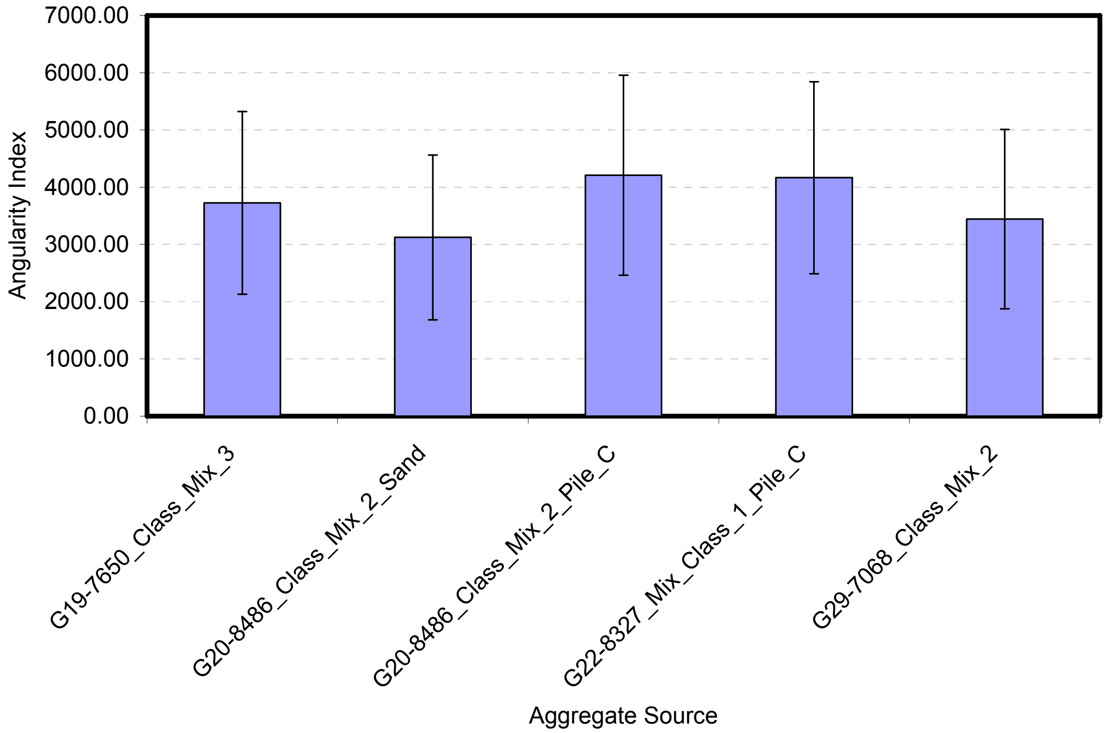

Figure 4.12 Angularity of Fine Aggregates

5. EVALUATION OF GYRATORY STABILITY

5.1. INTRODUCTION

The main goal of this study was to test the validity of Gyratory Stability (GS) as a mix indicator for familiar Hveem mixes used by ITD, and then use the results to develop bench mark values that can be applied to new Superpave mixes, in order to make a smooth transition from the Hveem design method to that for Superpave.

This study is focused on evaluating Hveem designed mixes that have been used in several projects across the state using the Superpave Gyratory Compactor (SGC). The purpose here is to assess the Gyratory Stability values of these mixes and compare them to the Hveem stability of these mixes. The mixes although designed by Hveem method, they all were made with Superpave PG graded asphalt binders.

5.2. EXPERIMENT MEASUREMENT AND ANALYSIS

5.2.1. Sample Preparations and Testing

Field batches for the mixes were tested to confirm their Hveem design parameters. The SGC was used to calculate the GS values and prepare samples for APA testing. Samples were compacted using the Servopac Gyratory Compactor, Troxler Compactor and Pine AFG1 Compactor.

For the purpose of investigating whether GS correlates with Hveem stability, all specimens were compacted to a number of gyrations to produce specimens with 4% air voids (the design target for Hveem criteria). This approach was used instead of N-design, since there is no defined N-design value for the considered Hveem mixes. However, the maximum number of gyrations applied was limited to 250. In the case of coarser mixes, where 4% voids were not achievable even at 250 Gyrations, samples were eliminated from the population used for the Hveem stability correlation.

5.2.2. Sensitivity of GS to Asphalt Binder Grade and Binder Content

The GS sensitivity to binder type (PG grade) was evaluated. This was achieved by compacting the same aggregate blends with different PG grades. An example of these results for Mix G20 is shown in Figure 5.1. Results showed that GS is not sensitive to the changes in binder grade. This is believed to be due to the fact that the compaction process occurs at a high temperature, where various binder types achieve the same viscosity, irrespective of their grade. At these temperatures, asphalt binder is in a liquid state and the difference in grade does not influence the resistance of the mix to applied forces.

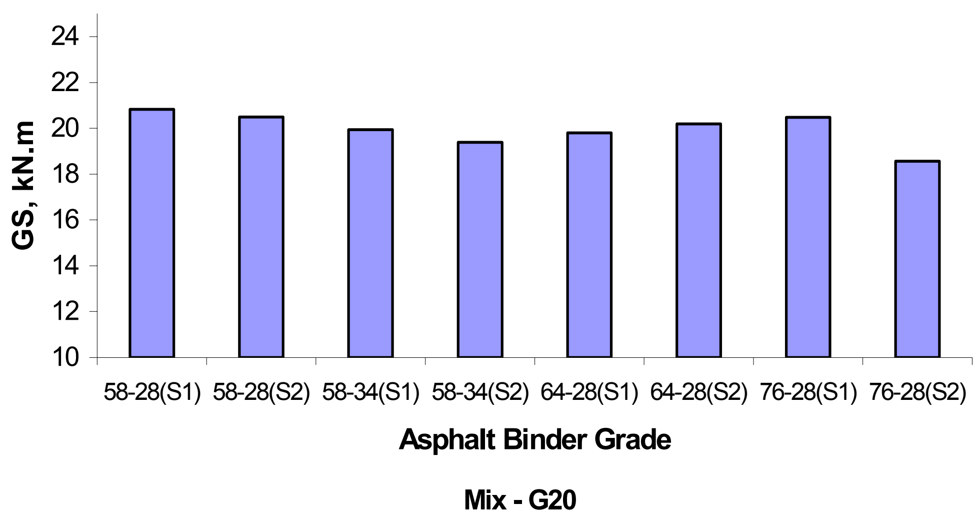

Figure 5.1 GS Sensitivity to Changes in Asphalt Binder Grade

In order to study the effect of the change of asphalt content with the same aggregate gradation, samples were prepared in the laboratory at the optimum asphalt content, optimum asphalt content plus one percent (+1%) and optimum asphalt content minus one percent (-1%). The GS results were compared against the GS for the reference mixes, as constructed in the field. It was found that the GS value captures the change in asphalt content, as shown in Figure 5.2. It was noted that an increase in asphalt content could increase or decrease the GS value, as it typically increased the deformation and decreased the shear stress developed in the mix during compaction. This finding indicates that the GS value is sensitive to asphalt content, and can be used to detect changes in asphalt content during production of HMA mixtures. Therefore, the GS value is more of an indicator of aggregate structure and asphalt content rather than binder grade. This finding is consistent with the results from Anderson, et al. (2002), Bayomy, et al. (2002) and Dessoukey, et al. (2004).

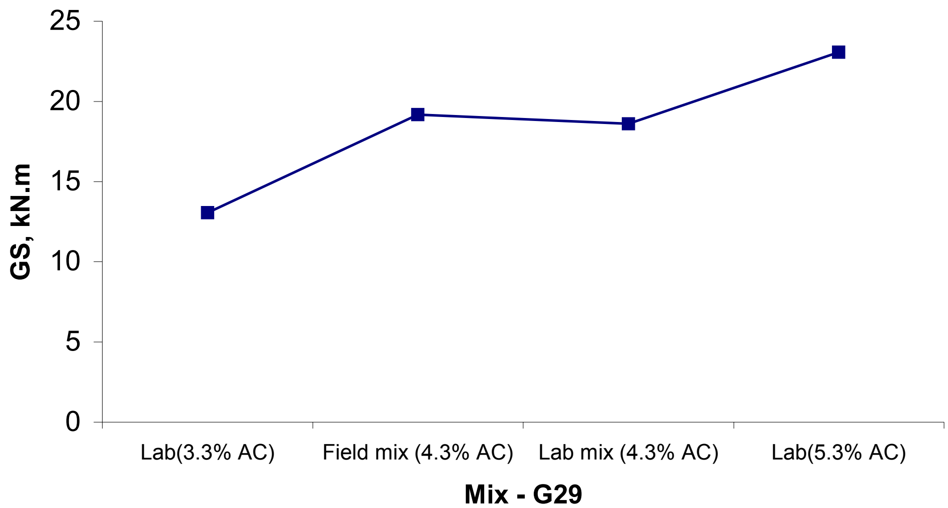

Figure 5.2 GS Sensitivity to Changes in Asphalt Binder Content

5.2.3. Comparison of GS and Hveem Stability

Since all the mixes used in this study were Hveem-designed mixes, it was necessary to determine whether the GS value could be related to the mix stability as measured by the Hveem Stability procedure. Therefore, identical batches were tested for Hveem Stability as well as for GS. Results are shown in Figure 5.3. A correlation with R-square around 0.63 was found between Hveem Stability and GS. Therefore, modeling was used to develop a relationship between GS and Hveem Stability, in order to facilitate the transition from the conventional Hveem stability to GS. The Hirotugu Akaike's Method

(AIC) in the statistical software package SAS was used to choose the best prediction model (Ott and Longnecker 2001). This model is shown in Equation 5.1.

$$GS = \alpha.HS + \beta \qquad (5.1)$$

where,

HS is the predicted Hveem Stability,

α, β are regression parameters and were found to be equal to 0.9579 and -18.988 respectively,

and $R^2 = 0.6386$.

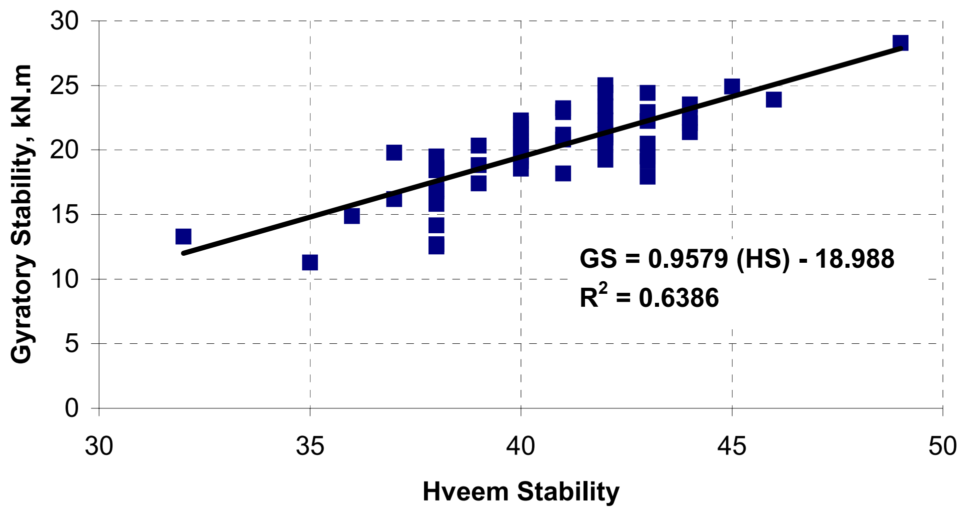

Figure 5.3 Relation between Hveem Stability and Gyratory Stability

For the tested mixes, a range of GS design threshold values were suggested as shown in Table 5.1, based on the Hveem stability limits used in the State of Idaho. The suggested GS limiting values could be different for Superpave-designed mixes.

Table 5.1 Proposed Design Values of GS for Hveem-Designed Mixes

Mix Class ITD General Specifications	Traffic Category	Hveem Stability	GS, kN.m
I	Heavy (> 10^6 ESALs)	> 37	>15
II	Medium (10^4 – 10^6 ESALs)	> 35	>12
III	Light (< 10^4 ESALs)	> 30	> 5

5.2.4. Comparison of GS with Permanent Deformation in APA

The Asphalt Pavement Analyzer (APA), which is the new generation of the Georgia Loaded-Wheel Tester, was developed to evaluate the HMA resistance to permanent deformation (Choubane, et al. 2000; Martin and Park 2003; and Bhasin, et al. 2004). The APA has the capability to test both rectangular and cylindrical specimens. Permanent deformation tendencies can be determined on three beam specimens, six cylindrical specimens, or a combination of both. The test temperature depends on the upper temperature range of the binder grade (i.e., 76 °C for PG 76-28 and PG 76-34). Sixteen of the mixtures used in this study were tested using the APA. Theses mixes were compacted to achieve 4% final air voids and to a fixed height of 150 ± 5 mm. Each mix had three duplicates.

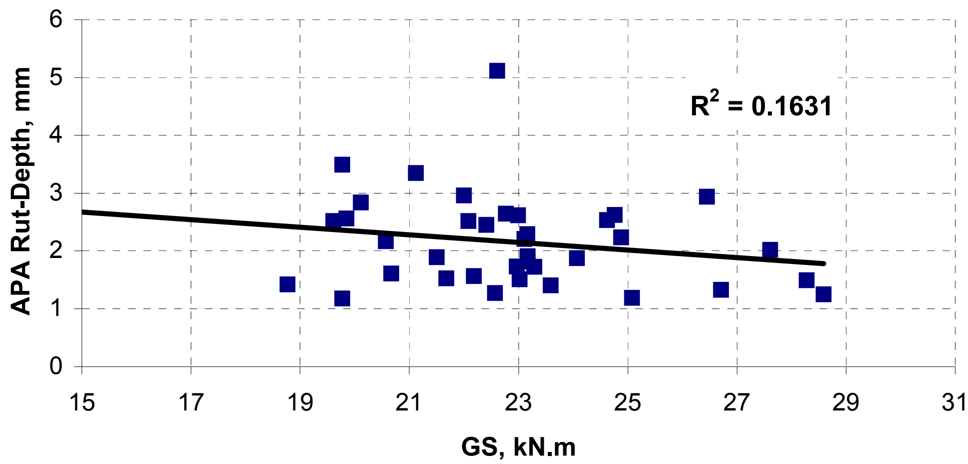

Figure 5.4 Relation Between APA Rut-Depth and GS

The GS value was compared to the APA test results as shown in Figure 5.4. The results show that there is no relationship between the APA permanent deformation and GS. This result is attributed to the fact that the APA test is conducted at different temperatures, according to the upper temperature of the PG grade, while GS is measured at the standard compaction temperature of the binder, around 149 °C. Therefore, it was decided to investigate the relationship between APA results and GS for each group of asphalt mixes with the same high temperature grade separately. Figure 5.5-a shows that a very good correlation exists between APA and GS for PG 58 – 28 and PG 58 – 34 binder grades. However, this was not the case for the PG 64 – 28 and PG 64 – 34 binders, as shown in Figure 5.5-b.

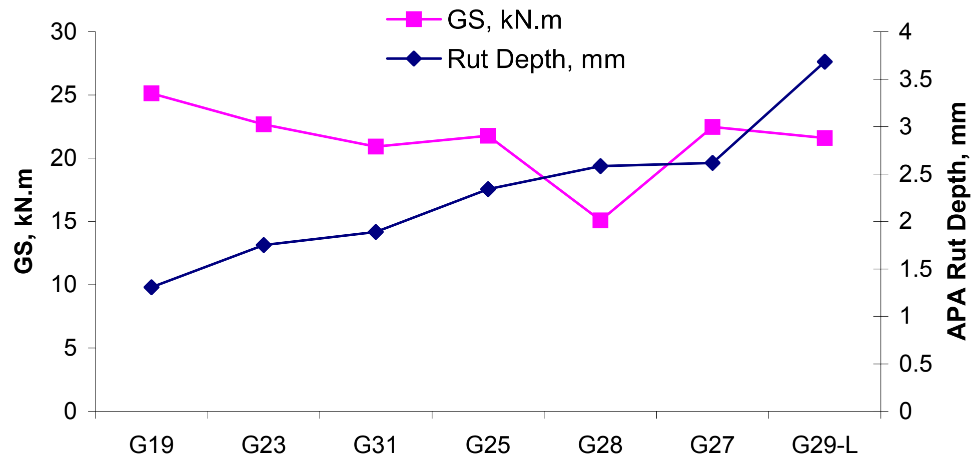

a) Mix Groups with PG 58-28 or PG 58-34

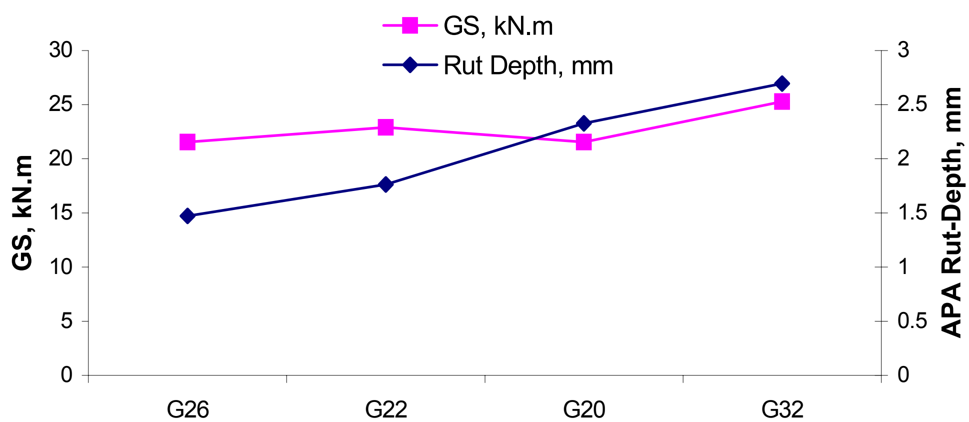

b) Mix Groups with PG 64-28 or PG 64-34

Figure 5.5 APA Test Results

5.2.5. Influence of Aggregate Shape Characteristics on GS

Previous analysis of GS development indicated that the GS value is more dependent on the interlocking mechanism of the aggregate-asphalt matrix. Therefore aggregate characteristics are expected to affect the GS value. The Aggregate Imaging System (AIMS) was used to measure three aggregate properties. These are surface texture, angularity and sphericity.

The relationship between texture data and GS is shown in Figure 5.6. There was a general trend of increase in GS with an increase in aggregate texture. This is due to the increase of the frictional resistance among aggregate particles as texture increases. However, there were no clear relationships between angularity and sphericity with GS for the range of aggregates used in these mixes. These findings are in agreement with previous studies using AIMS, which have shown that aggregate texture has the most influence on the resistance of HMA to deformation under applied forces (Fletcher, et al. 2003 and Masad, et al. 2004).

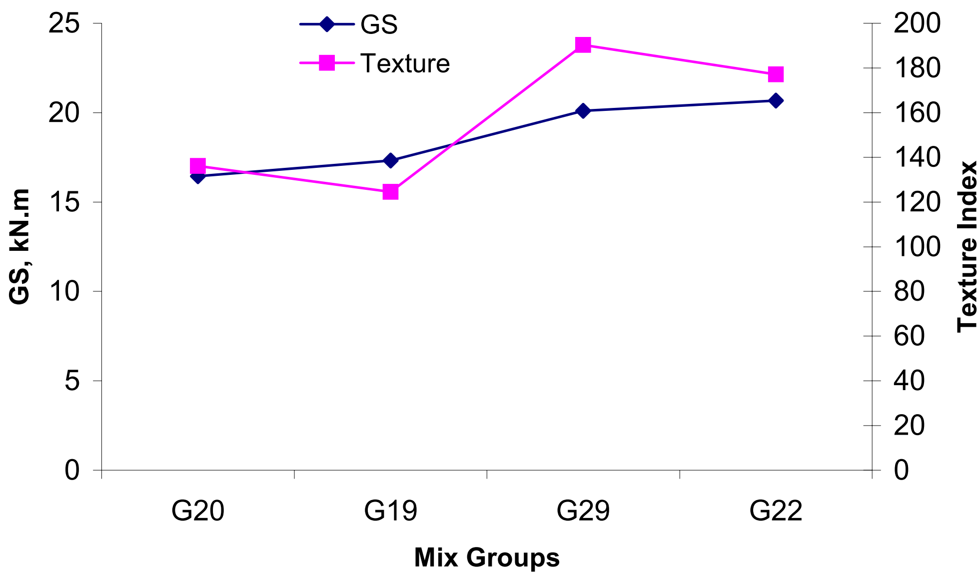

Figure 5.6 Relationship between Aggregate Texture and GS

5.2.6. Summary

Based on the results of this study, it is concluded that the Gyratory Stability (GS) could be used as a first screener to distinguish among mixes for mix design acceptance, especially to decide on the acceptance of the mix aggregate structure. The following conclusions and observations were also made:

- The GS value correlated well with the Hveem Stability of Hveem-designed mixes. Results, however, showed a wide variation in GS values for mixes that had the same Hveem Stability. This may indicate that GS is more sensitive to changes in mix design parameters than Hveem Stability. Three tiers of GS limits (5, 12 and 15) are suggested to classify HMA mixtures, based on their stability.

- Results of the APA rut testing did not correlate with the GS value of these mixes. The main reason is believed to be that the current APA testing procedure allows for testing the mix at different temperatures based on its high temperature grade; while, GS is determined at the standard compaction temperature of 149 °C. A better correlation between GS and permanent deformation in APA was obtained for mixes that had the same PG grade and were tested at the same temperature in the APA.

- Image analysis indicated that aggregate texture correlated with the GS value. There was no clear relationship between angularity and sphericity with GS, for the range of aggregates used in this study.

6. EVALUATION OF HVEEM DESIGNED HMA FRACTURE TOUGHNESS USING THE J_C PARAMETER

6.1. INTRODUCTION

The Superpave method of mix design has been used by pavement engineers for more than a decade, yet a fracture-based mix design criteria has not been developed to ensure that the designed Superpave mixes will not show cracking and fracture before the end of the design life of the mix or pavement. Superpave ensures low-rutting and low-temperature cracking of a designed mix using Performance Grade (PG) binders; however, there are no reliable design criteria and/or test methods that will ensure that the designed mix will not show cracking and fracture. There is a need for the development and evaluation of a test method and design criteria to ensure Superpave mix's resistance to fracture and cracking (Mull, et al. 2002). In this study, a fracture based parameter, J_c determined in a Semi-Circular Notched Bending Fracture (SCNBF) test is evaluated for HMA mix resistance to fracture and cracking.

The use of the fracture-based concept in asphalt mix design has been investigated for several decades. Little and Mahboub (1985) used the J_c value to compare the fracture resistance of asphalt mixes prepared with and without plasticized sulfur binder. Dongre, et al. (1989) evaluated the fracture resistance of asphalt mixes at low temperatures, using bending beam specimens. Their study showed that J_c is a promising fracture characterization parameter for asphalt mixes at low temperatures. Furthermore, their study concluded that J_c is sensitive to asphalt mix stiffness and it is a better fracture characterization parameter than the plane strain critical stress intensity factor (K_{IC}). Abdulshafi, et al. (1985) used V-shaped notched circular samples to determine J_c for different asphalt mixes and used the J_c value to predict the fatigue life of asphalt mixes. Bhurke, et al. (1997) studied polymer modified asphalt concrete using the J_c fracture resistance approach, employing three point bending beam specimens. Their study used AC-5 asphalt as a base and polymers, such as styrene-butadiene-styrene, and styrene-butadiene rubber as modifiers. They concluded that the three-point bending beam test is repeatable, and test results are sensitive to material differences due to polymer modification.

Recently, several studies were initiated to utilize the gyratory compacted samples in a three point bending test. Ven, et al. (1997), Molennar, et al. (2002), and Li, et al. (2004) adopted the semi-circular bending test set-up, using the Superpave Gyratory Compactor (SGC) samples, to determine tensile strength of asphalt mixtures, in an effort to replace the indirect tensile test. They, however, used un-notched samples and did not focus on fracture resistance parameters. In rock mechanics, Lim, et al. (1994) used a semi-circular notched specimen in a bending test to evaluate the fracture properties of natural rocks by determining the K_{IC} parameter. Mull, et al. (2002) adopted this semi-circular bending test with notched specimens to measure fracture toughness properties of asphalt mixtures. They determined J_c, to evaluate the fracture resistance of chemical crumb rubber asphalt (CMCRA) mixes. In that study, the three binders used were (i) a base binder produced from air-blown asphalt with no catalyst, (ii) the base binder modified using plain crumb rubber asphalt (CRA), and (iii) the based binder chemically modified using crumb rubber asphalt (CMCRA). Their study showed that the fracture resistance, J_c, value of the CMCRA is twice the J_c value of the CRA mix; the base mix had the lowest value of J_c. These researchers also compared their laboratory results to the micromechanical damage/fracture seen under a scanning electron microscope.

Huang, et al. (2004) used the Semi-Circular Notched Bending Fracture (SCNBF) test to study the fracture properties of various reclaimed asphalt pavement (RAP) mixes. Their analysis showed that the fracture resistance measured by the J_c increases with the increase of RAP content in the mix to a certain extent, after which, the fracture resistance decreases significantly. Mohammed, et al. (2004) used the SCNBF test geometry to study the effect of recycled polymer modified asphalt cement (RPMAC) content on the fracture resistance, the J_c. These researchers found that as the percent of RPMAC increases, the stiffness and maximum sustained load also increase, with a slight decrease in the deflection at maximum load. Their study suggests that the semi-circular fracture test used in conjunction with J_c analysis can be a useful mix design tool.

Very recently, Mull, et al. (2004) extended the concept of the SCNBF test to study fatigue crack propagation of asphalt mixes. They found that the SCNBF test geometry provides a suitable geometry for fatigue crack propagation analysis of asphalt mixes. In addition, they showed that the fatigue lifetime of CMCRA mixes are higher than that of unmodified crumb rubber mixtures. The results of the fatigue study on the crumb rubber modified mixtures have confirmed the static J_c results generated earlier by Mull, et al. (2002). Both studies found SCNBF to be a reliable test asphalt mixtures evaluation.

In addition, studies have shown that a relationship between K_{IC} and J_c exists in metals. Landes, et al. (1984) has related K_{IC} to J_c using the following equation:

$$K_{IC}^2 = \frac{J_C . E}{1-\nu^2} \tag{6.1}$$

where,

E= elastic Modulus, and

ν= Poisson Ratio.

McCabe, et al. (2005) has used a modified equation to determine an equivalent stress intensity factor defined as K_{JC} (Equation 6.2). It has been demonstrated that to determine K_{JC}, specimens can be 1/40th the size required for K_{IC} validity by ASTM Standard E 399, and still maintain sufficient control of constraint.

$$K_{JC} = \sqrt{E . J_c} \tag{6.2}$$

The aforementioned literature studies reveal that J_c can be determined by various methods and used as an indicator of the asphalt material's fracture resistance to cracking. Therefore, the present study has adopted the J_c parameter for evaluating HMA resistance to fracture and crack propagation. It can be noted that J_c is chosen over the stress intensity factor, K_{IC} in this study. The K_{IC} value represents the linear elastic energy release around a crack, where as J_c represents the non-linear elastic energy release around a crack. It is shown later that an asphalt concrete follows the nonlinear stress-strain behavior. Therefore, the adoption of J_c over K_{IC} in the study of fracture behavior of asphalt concrete is appropriate. In addition, the K_{IC} is dependent on the sample geometry, and the functional form of K_{IC} for semi-circular shape is yet unknown, to the best of this researcher's knowledge. To this end, the Semi-Circular Notched Bending Fracture (SCNBF) test is adopted for J_c evaluation in this study. The goal is to evaluate the fracture resistance parameter, $J_{c,}$ of a wide variety of field mixes used by the Idaho Transportation Department (ITD) and to identify its sensitivity to HMA properties.

6.2. FRACTURE PARAMETER, J_C

The fracture parameter, J_c, used in this study is based on the study conducted by Rice (1968). The J_c is defined as a path independent integration of strain energy density, traction, and displacement along an arbitrary contour path around the crack, as shown in Figure 6.1, and can be quantified using the following equation:

$$J_c = \int_{\Gamma} W dy - \int_{\Gamma} T \frac{\partial u}{\partial x} ds \tag{6.3}$$

where,

Γ = any path surrounding the crack tip,

x,y = rectangular coordinates normal to the crack front,

ds = increment along contour Γ,

T = stress vector acting on the contour,

u = displacement vector, and

W = the strain energy density = $\int \sigma_{ij} d\, \varepsilon_{ij}$.

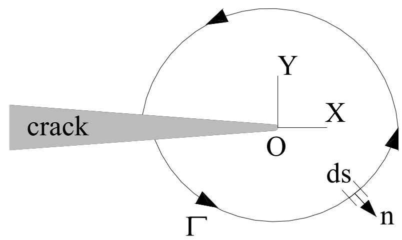

Figure 6.1 Line Contour Surrounding Crack Tip

Rice (1968) also presented an alternative and equivalent definition for J_c, based on the pseudopotential energy difference between two identically loaded bodies possessing slightly different crack lengths. A simplified form of Equation (6.1) is given below:

$$J_c = \left| \frac{\partial}{\partial a} \left(\frac{U}{b} \right) \right| \tag{6.4}$$

where,

U is the strain energy to failure, which is the area underneath the load-deformation curve up to the peak load,

b is the specimen thickness, and

a is the notch depth.

Equation (6.4) was used to calculate J_c in this study. As a preliminary step to calculating J_c, the load versus deformation diagram was plotted using laboratory data. Next, the area under the load-deformation curve, defined as the strain energy *U*, was determined and divided by the sample thickness. A total of three specimens of different notch depths were used. Next, strain energy per unit depth for all three samples were plotted as a function of notch depth. The slope of the best-fit line was determined as the critical fracture resistance parameter, the J_c, as shown in Figure 6.2.

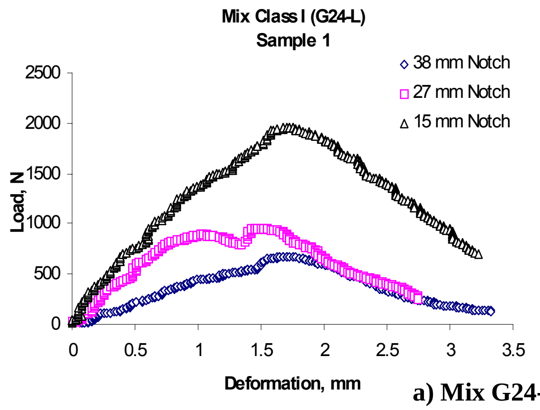

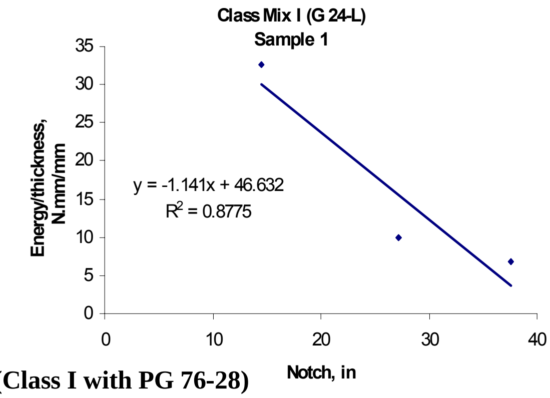

a) Mix G24-L (Class I with PG 76-28)

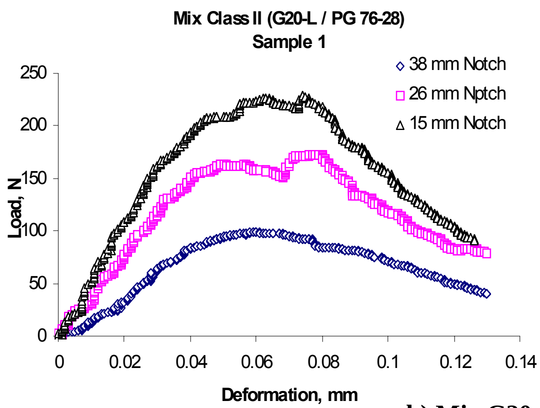

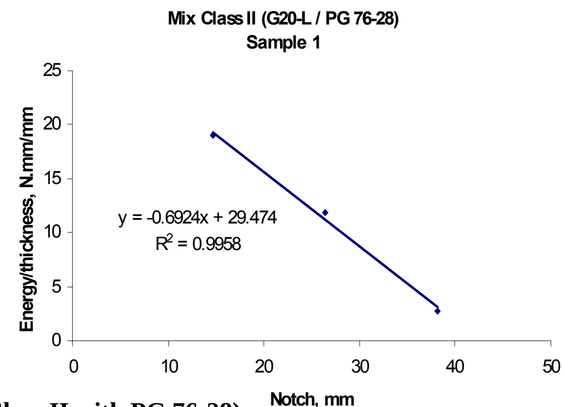

b) Mix G20-L (Class II with PG 76-28)

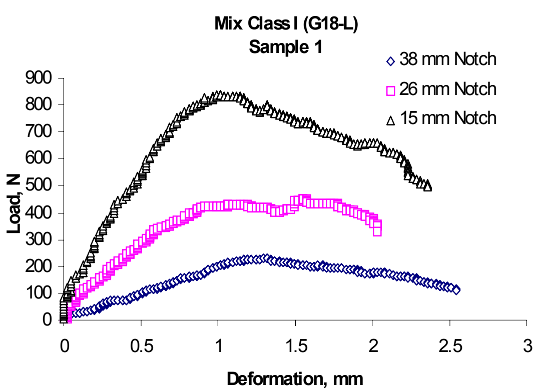

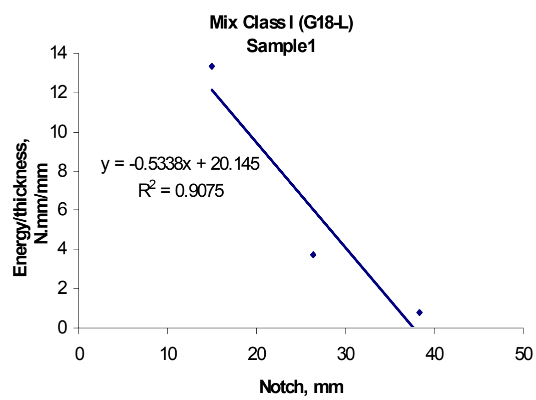

c) Mix G18-L (Class I with PG 64-34)

Figure 6.2 J_c Determination for three Different Asphalt Mixtures

6.3. PREPARATION OF SPECIMENS AND TEST SETUP

The HMA samples were compacted using a Superpave Gyratory Compactor (SGC) to achieve final air voids of 4±1%. Each sample was sliced into 4-quarter specimens. These quarter specimens were tested to determine J_c. One of the quarters was left un-notched to determine the stiffness, which was used in the development of the Finite Element Analysis (FEA) model. The other three quarters were notched to various notch depths. Notches were in the range from 12.5 mm (½ in) to 38 mm (1 ½ in) in depth and about 2 mm in width, as shown in Figure 6.2. Three replicates were prepared for each mix. All specimens had 150 mm diameter and 110±5 mm height, which is the standard size of a Superpave Gyratory compacted specimen.

Figure 6.3 illustrates the test configuration of the Semi-Circular Notched Bending Fracture (SCNBF) test. In the fracture bending test, the spacing between the two roller supports is 122 mm. A ramp load with a constant vertical deformation rate of 0.5 mm/minute was applied until fracture occurred. The test was conducted at a room temperature of approximately 25±1°C.

Figure 6.3 Semi-Circular Notched Specimens Sliced from a Standard Gyratory Compacted HMA Sample

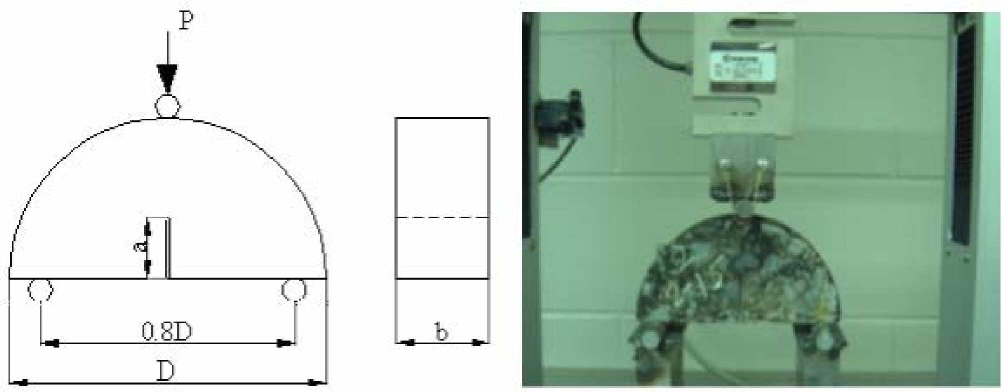

Figure 6.4 Semi-Circular Notched Bending Fracture Test Setup

6.4. ANALYSIS OF RESULTS

6.4.1. J_c Calculations

The value of J_c was determined for all tested mixtures given in the Appendices, in accordance with the concepts presented previously. For each sample, the applied load versus the vertical deformation was plotted. The strain energy U, which is equal to the area underneath the load-deformation curve up to the peak load, was determined. After determining the strain energy, the ratio of the strain energy to the specimen thickness, U/b, for each specimen was plotted against the notch depth, a. The value of J_c was obtained from the slope of the U/b versus a best straight line fit. As indicated earlier, at least three data points are needed to develop such a line fit, and therefore, three specimens with different notch depth were tested for the J_c calculation. For each notch depth, three replicate specimens were used to evaluate test repeatability.

The laboratory produced mixes in Figure 6.2 and 6.5 were designated as G24-L (Class I, PG 76-28), G20-L (Class II, PG 76-28) and G18-L (Class I, PG 64-34). The difference between the first two mix classes is that one mix is finer than the other (courser grade aggregate). The difference between the first mix and the third mix class is in PG grade. The test results are shown in Figure 6.2 and 6.4. It can be seen from Figure 6.4 that the fracture resistance parameter J_c for the G24-L mix is higher than that of the G18-L mix.

Comparing G24-L and G20-L, it is seen that the J_c for the courser grade is lower than that for the finer grade mix with the identical PG.

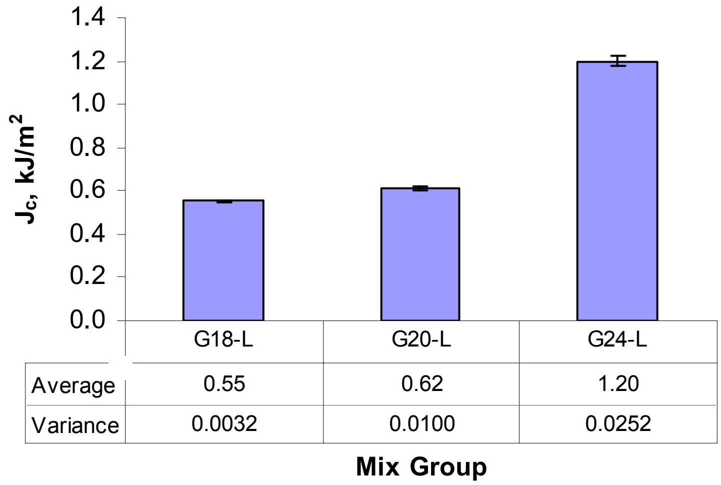

Figure 6.5 J_c Determination for three Different Asphalt Mixtures

These comparisons show that J_c is affected by the change in mixture composition, both in terms of aggregate gradation and asphalt type. Therefore, it may be useful to find the relationships between HMA properties and J_c. The values of J_c for the mixtures studied herein range from 0.53 to1.2 kJ/m^2, which is within the range of J_c values reported previously in other studies (Mull, et al. 2002), as shown in Figure 6.6.

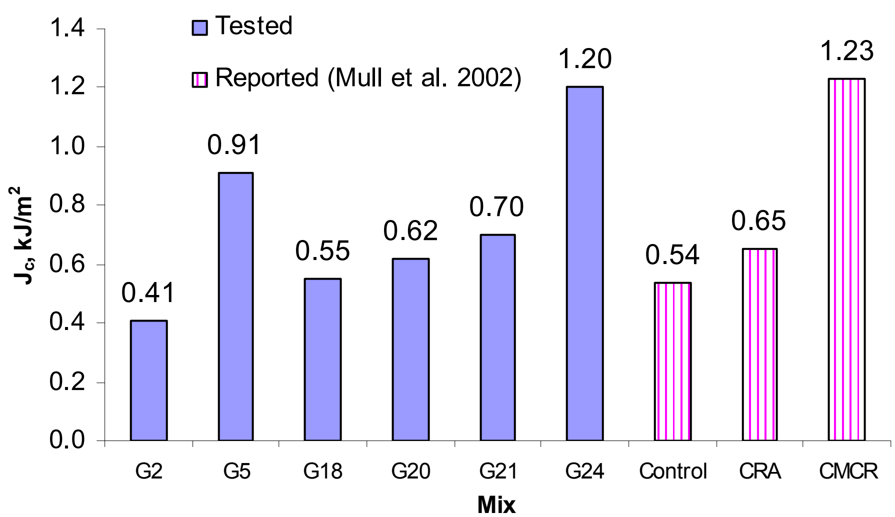

Figure 6.6 Comparison of J_c between ITD Mixes and Reported Mixes

6.4.2. Finite Element Analysis

To calculate the elastic modulus, an approximation was made by assuming that the asphalt mixture was a homogeneous and isotropic material. Finite Element Analysis (FEA) software, ALGOR version 15.0, was used in this study to calculate the elastic modulus *E* of the asphalt mixtures. In FEA, a 3-D idealization model with quadratic elements was used. Quadratic elements are more suitable than the tetrahedral elements in defining the geometrically isotropic characteristics. Also, the linear variation of stress-strain over the entire area of a quadratic element makes the quadratic elements more appropriate for studying bending characteristics. The boundary conditions for the FE model were set to restrain the specimen vertically at 0.1 and 0.9 the diameter, with one side restrained horizontally to avoid movement of the whole model. The load was statically increased. A few changes were made, especially at the loading and support points. For example, the number of the loading and restrained nodes was increased to avoid local failure, especially by compressive stresses.

The simplest way to characterize the behavior of an asphalt mix under a given load is to consider it as a homogeneous half-space material. A half-space has an infinitely large area and an infinite depth with a top plane on which the loads are applied. Commonly, the stresses, strains and deflections are calculated using the Burmister (1943) theory, which is based on elastic half-space. Further, the HMA is assumed to be isotropic, linearly elastic with an elastic modulus, weightless, and with uniform and clean surfaces (Huang 2004). Running the simulation in ALGOR, as shown in Figure 6.7, we observed that the maximum tensile stress occurs in the bottom of the specimen as expected. Employing Equation (6.3) with the value of $\delta_{z,}$ as measured from the experiments, the value for the elastic modulus *E* of the mixes listed in the Appendices were back calculated.

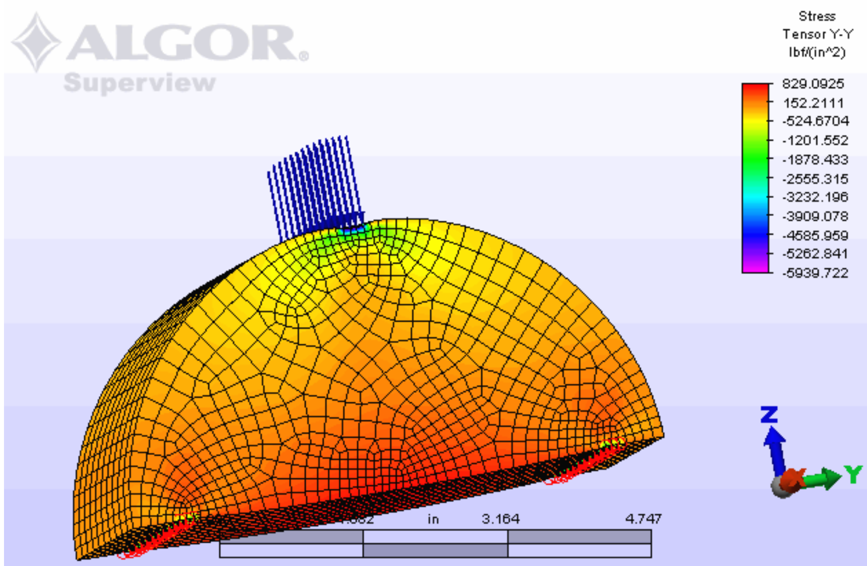

Figure 6.7 Contour of Tensile Stress from the FE Model

The research team adopted Finite Element Method (FEM) due to the lack of fracture tests and parameters at their disposal to evaluate the J_c parameter. The research team acknowledges that FEA is not accurate in describing the behavior of HMA, due to the basic assumptions in FEA: that HMA is isotropic, linearly elastic with an elastic modulus, weightless, has uniform and clean surfaces, and that no separation of elements may occur (no fracture). The calculated E values were used to evaluate J_c.

6.4.3. Effect of Elastic Modulus on J_c

There is no closed-form solution for determining the tensile stress and deformation of a Semi-Circular Notched Specimen loaded in a three-point bending setup as in the configuration described here. Therefore, Finite Element Analysis (FEA), as well as statistical analysis, is employed to develop Equations (6.5) and (6.6) for determining the tensile stresses at the bottom of a sample, and vertical deformation of an un-cracked semi-circular specimen. These stress and deformation values are used to calculate elastic modulus:

$$\sigma_t = \frac{4.888F}{WD} \qquad (6.5)$$

$$\delta_z = \frac{2.26F}{WE} \tag{6.6}$$

where,

σ_t = Tensile stress at the bottom of the sample,

δ_z= Deformation in the vertical direction,

F= Applied force,

W= Width of the specimen,

D= Diameter of the sample, and

E= Elastic modulus.

The aforementioned approach was demonstrated by Ven de Ven, et al. (1997). In the present study, the un-notched specimen (un-cracked semi-circle) shows linear elastic – plastic and viscoelastic response. Nevertheless, the first portion of the curve appears to be linear where the elastic modulus can be obtained (see Figure 6.2).

The relationship between the elastic modulus (E) and fracture resistance (J_c) for all the mixtures under consideration is shown in Figure 6.8. The results show that an increase in the E value is associated with high toughness. This is because an increase in the stiffness, or E, will lead to an increase in the strain energy U required to fracture the sample. Further examination of the data in Figure 6.8 reveals that, for the three classes of the ITD mixtures, Class III (lowest stability) has lower stiffness and lower J_c when compared to Class I (highest stability). Some of the Class I mixtures, such as G24-L with PG76-28, possess the highest J_c and the highest stiffness. Class II mixtures, however, had higher values of J_c than that of Class III with some of the mixes in Class II overlapping with Class I. Overall, it was observed that J_c and E results reflect that Hveem-designed mixes with higher stabilities (as indicated by the mix class) may also have higher stiffness and higher resistance to fracture as measured by the J_c parameter.

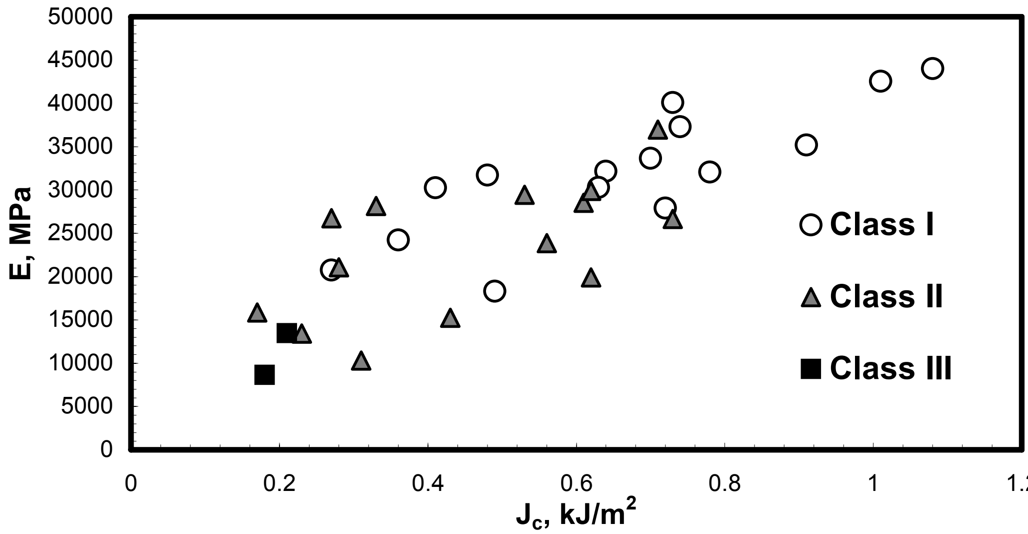

Figure 6.8 Relationships of J_c and the Calculated Elastic Modulus

Using the estimated E from the developed FEA model and the J_c for the tested mixes, K_{JC} was calculated using Equation (6.2) and compared to J_c as shown in Figure 6.9. Results have shown that K_{JC} followed the same trend as J_c for the tested mixes. In addition, Dongre, et al. (1989) has reported a range of 3.62 – 5.34 MPa.m$^{1/2}$ for K_{IC} at 25°C testing temperature for tested asphalt mixes. K_{JC} of the tested mixes in this study has a range of 1.42 – 7.43 MPa.m$^{1/2}$ at the same temperature (Figure 6.10).

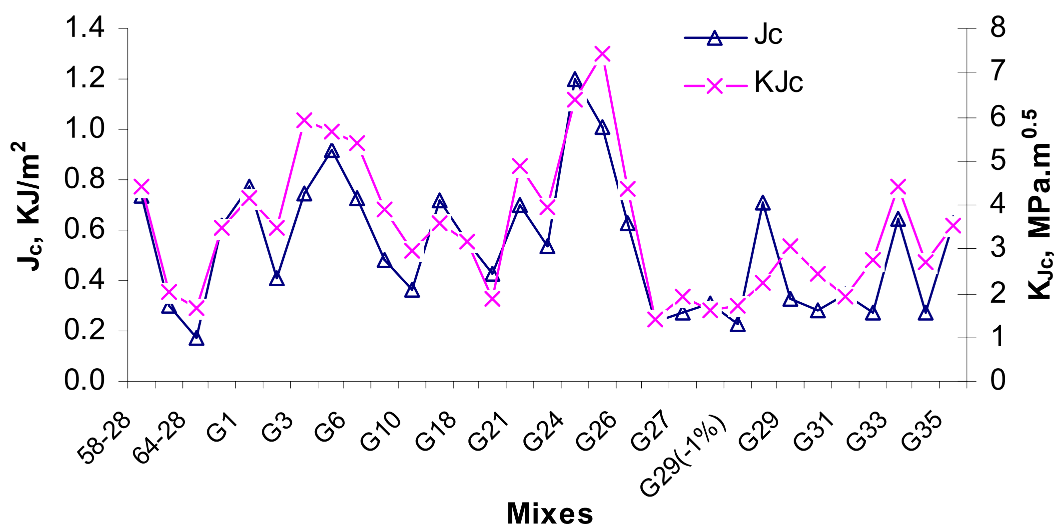

Figure 6.9 K_{JC} and J_C Results

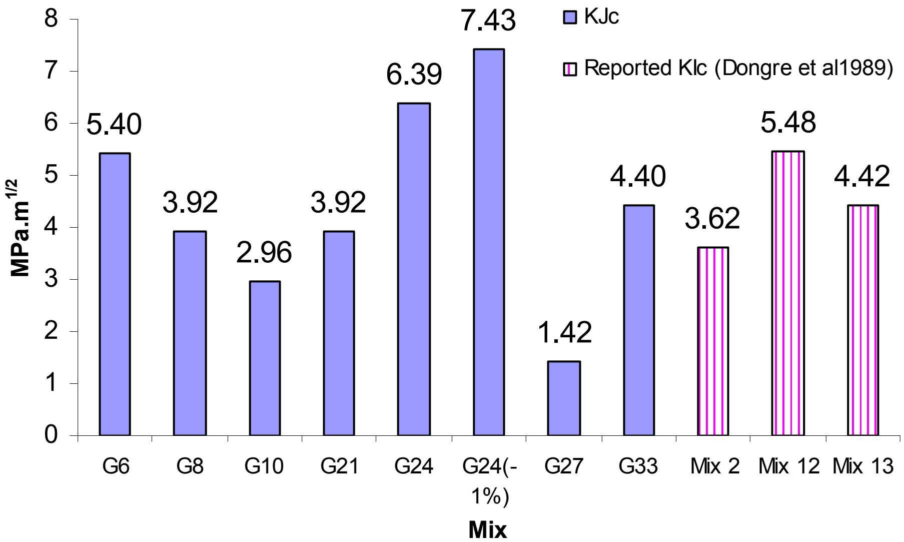

Figure 6.10 K_{JC} and Reported K_{IC}

6.4.4. Effect of Aggregate Characteristics on J_c

The analysis of J_c as it varies with mix class may reflect changes in aggregate gradation, but does not reflect its variation in aggregate shape and texture properties. Therefore, an investigation of the effect of aggregate surface characteristics was conducted. The Aggregate Imaging System (AIMS) developed by Masad (2003) was used to determine aggregate shape and surface properties. The AIMS at Texas A&M University testing laboratory was used to measure three aggregate properties as recommended by Masad, et al. (2004). These included surface texture, angularity, and sphericity. Texture is analyzed using the wavelet transform, which captures the changes of texture on gray scale images. The wavelet transform gives a higher texture index for particles with rougher surfaces. Aggregate angularity is measured using the gradient method. In this method, the changes in the gradients on the boundary of a two-dimensional projection of a particle are calculated. The angularity index, calculated using the gradient method, increases with an increase in aggregate angularity. Shape is quantified using the sphericity index, which is equal to one for particles that have equal dimensions, and decreases as particles become more flat and elongated (Masad 2003 and Fletcher, et al 2003).

The relation between J_c and the aggregate characteristics (texture, sphericity, and aggregate shape or L/S ratio) measured by AIMS was investigated. Here, L is the length and S is shortest dimension of an aggregate. Initial findings showed that:

- The J_c increased for mixes that contained aggregates with rough surface texture. This is due to the fact that rougher aggregate surfaces have higher bond strength between the aggregates and the binder, thus they display a higher fracture resistance (Figure 6.11-a).

- The J_c increased for mixes that have more angular aggregates. The angular aggregates resisted crack propagation and made the failure path longer, which resulted in higher fracture toughness. (Figure 6.11-b).

- Aggregate flatness and elongation, as indicated by an L/S ratio of > 3 and > 5, has been shown to have an adverse effect on mix performance. Results show that J_c decreases for mixes that have a higher percentage of aggregates with L/S > 3 and > 5. This indicates that a mix with a higher percentage of flat and elongated aggregates tends to be weak and more easily fractured than a mix with a lower percentage (Figure 6.11-c) of flat and elongated particles.

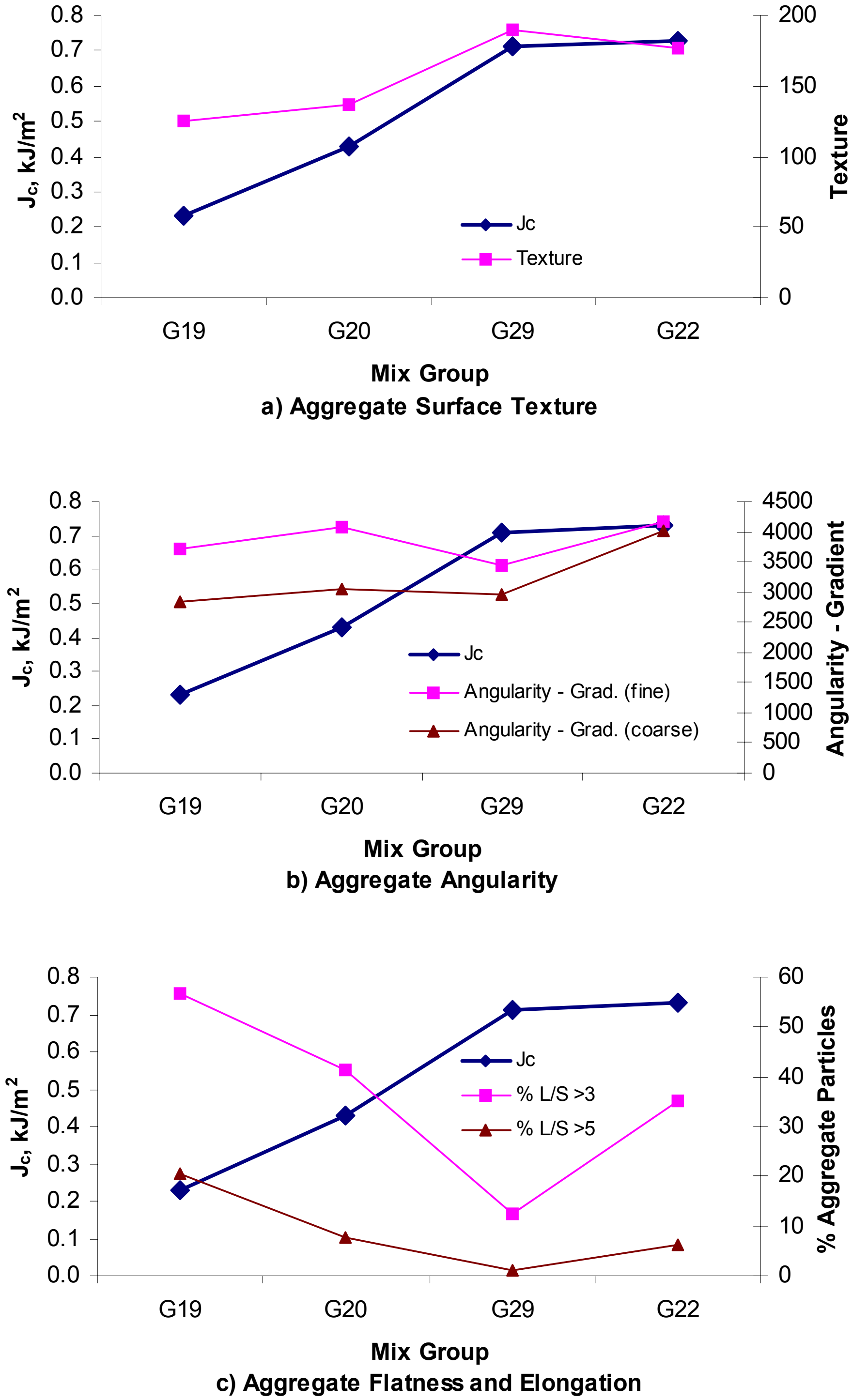

Figure 6.11 Variation of J_c with Aggregate Shape and Texture Characteristics

6.5. EFFECTS OF ASPHALT CONTENT AND BINDER GRADE

Figure 6.12 shows the J_c values of mixes with identical aggregate gradation but different asphalt binder contents. The value of J_c was found to be sensitive to the variation in the asphalt binder content. As the percentage of asphalt content increases, the value of J_c increases. As expected, the J_c for the field mix is very close to that prepared in the laboratory with the same asphalt binder content. The increase in the binder content increases the cohesion behavior of the mixture, which has resulted in an increase in the fracture resistance (J_c) potential of an HMA mix.

The effect of binder grade on the J_c was also studied, based on four mixtures from Class II shown with their results in Figure 6.13. No trend in the data can be observed from Figure 6.13 in this study. It is possible that the dependency of J_c on asphalt binder grade is complex.

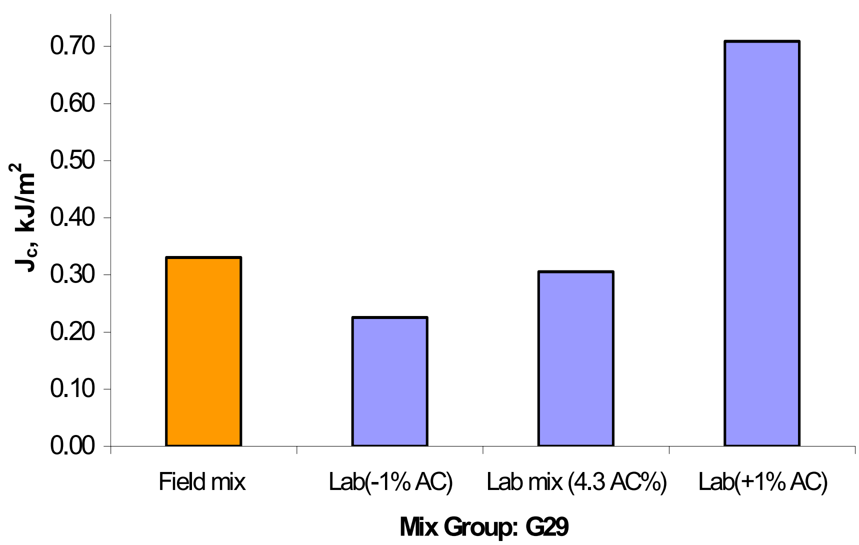

Figure 6.12 Variation of J_c with Asphalt Binder Content

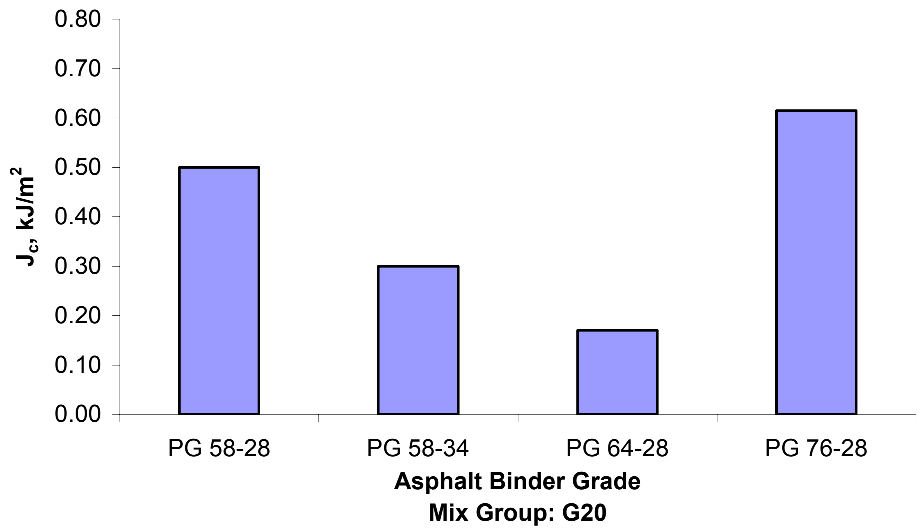

Figure 6.13 Sensitivity of J_c to Asphalt Binder Grade

6.6. SUMMARY

As a summary based on the results presented, the following observations are made:

- The J_c parameter measured by the semi-circular notched bending fracture (SCBNF) test can represent HMA resistance to fracture. The SCBNF test is simple and quick to perform, and can be implemented at the mix design stage of HMA design.

- Finite Element Analysis was used to model the SCBNF test configuration. FEA results were used to calculate the mixture elastic modulus. The elastic modulus was correlated to the J_c. It is shown that J_c increases with the increase in modulus values of HMA. It is postulated that Hveem mixes with higher stabilities have higher stiffness and therefore, higher resistance to fracture, as measured by the J_c parameter.

- Results have shown that K_{JC}, which is equivalent to K_{IC}, follows the same trend as J_c for the tested mixes and fall in the range of reported K_{IC}.

- The J_c parameter was found to be sensitive to changes in the mix aggregate gradations and to the aggregate shape and surface texture properties, as measured by the Aggregate Imaging System (AIMS). Mixes with finer aggregate gradations showed higher resistance to fracture compared to the mixes with coarser aggregate gradations. Mixes with rougher aggregate texture and more angular particles showed higher J_c values. Mixes that had high percentages of flattened and elongated aggregates showed lower J_c values.

- The J_c parameter was found to be sensitive to variations in the asphalt binder content. In this study, as the binder content increased, the value of J_c increased.

- In this study, no clear trend was found to demonstrate J_c sensitivity to variations in binder grades.

- Overall, this study concludes that J_c, determined in a SCNBF test, can be used to assess an HMA mixture's propensity to fracture during the design stage.

7. EVALUATION OF IDAHO SUPERPAVE MIXES

7.1. INTRODUCTION

The research outcomes of the Strategic Highway Research Program (SHRP) included state-of-the-art methods to design the Hot-Mix Asphalt (HMA) based on performance. However, and for practical implementation of SHRP products, the main design criterion in the current Superpave system is based only on volumetric analysis. There is a need to develop simple, practical and reliable methods and procedures that can be incorporated into the design criteria of Superpave. Research efforts since the release of Superpave in 1992 have continued to address this issue. A few test procedures and new performance indicators have been developed.

Under the NCHRP Project 9-19 a simple performance test (SPT) setup was developed that included Dynamic Modulus, Flow Number and Flow Time tests. Recent Studies (Bhasin, et al.; Tandon, et al.; Zborowski, et al. 2004; and Bahia, et al. 2005) have concluded that SPT can be used to indicate the performance of HMA. However, mix performance evaluation methods such as SPT that were developed under the SHRP plans were found to be highly sophisticated and time consuming for the mix design stage.
As a final stage of this study, the research team investigated the utilization of Gyratory Stability (GS) and the Fracture Toughness Parameter (J_c) as simple and practical test methods that can be used in conjunction with the current Superpave mix design procedure. Hence, mix performance can be assessed and incorporated into the design criteria during the mix design stage.

7.2. EXPERIMENT MEASUREMENT AND ANALYSIS

7.2.1. Selected Mixes

ITD has recently begun the implementation of Superpave mix design. Three trial projects were underway when this study was completed. Two different mixes were procured from two projects. These two mixes have different aggregate types and gradation (Figure 7.1.)

Figure 7.1 Tested Superpave Mixes

To achieve the goals and objectives of the final stage of this study, an experimental mix matrix was prepared to evaluate these mixes and the effect of binder content and grade on the performance, as shown in Table 7.1.

Table 7.1 Idaho Superpave Mixes Matrix

Mix	PG	AC%				
		-1.0%	-0.5%	Optimum	+0.5%	+1%
1	64-34		√	5.5%	√	√
2	64-22			√		
	64-28	√	√	5.9%	√	√
	64-34			√		

7.2.2. Sample Preparation

For the purpose of investigating the performance of these mixes, their raw materials were provided by ITD. All specimens were mixed and compacted under controlled lab conditions. Specimens used to determine the Gyratory Stability and J_c were compacted using the Servopac Gyratory Compactor to a number of gyrations to produce specimens with 4% air voids. For the optimum asphalt content for both mixes, the number of gyration coincided as expected with their set N-design.

Specimens used in the Dynamic Modulus and Flow Number tests were compacted to achieve seven inch height specimens with a total of 9% air voids. Then the specimens were cored and sawed to obtain specimens with a four inch diameter, six inch height and 7% air voids.

7.2.3. Gyratory Stability (GS) and Asphalt Pavement Analyzer (APA) Test

See Chapter 5 for test setup and test procedures.

7.2.4. Fracture Toughness (J_c)

See Chapter 6 for test setup and test procedures.

7.2.5. Dynamic Modulus Test

The Dynamic Modulus (|E*|) is defined as the absolute value of the Complex Modulus (E*), which is the stress-to-strain relationship for a linear viscoelastic material. Mathematically, the Dynamic Modulus is equal to the maximum stress (σ_o) divided by the maximum recoverable strain (ε_o) as in shown in Equation 7.1.

$$|E^*| = \frac{\sigma_o}{\varepsilon_o} \tag{7.1}$$

The Dynamic modulus Test (AASHTO TP 62-03) consists of applying a uniaxial sinusoidal (haversine) compressive stress to an unconfined HMA cylindrical test specimen as shown in Figure 7.2 and measuring the corresponding strain using two to three LVDTs mounted on the middle of the specimen.

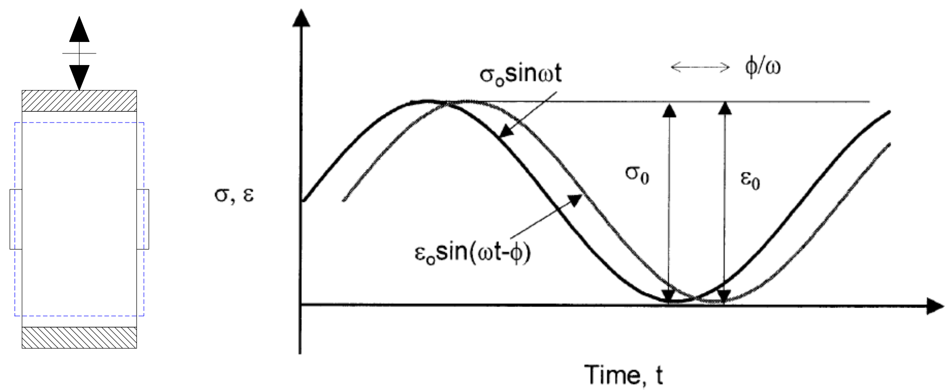

Figure 7.2 Haversine Loading for the E* Test (after Witczak 2002)

The Dynamic Modulus Test protocol AASHTO TP 62-03 indicates that the test shall be conducted under a series of temperatures (14° F, 40 ° F, 70 ° F, 100 ° F and 130 ° F) and loading frequencies (0.1 Hz, 0.5 Hz, 1 Hz, 5 Hz, 10 Hz and 25 Hz) at each temperature. The (E*/sin δ) parameter at a loading frequency of 5 Hz at temperatures of 100 ° F and 130° F was used as a permanent deformation (rutting) indicator and where δ represented the time lag between the application of load and the material response (Figure 7.2). In addition, the (E*.sin δ) parameter at a loading frequency of 5 Hz at temperatures of 40 ° F and 70° F was used as a fracture resistance indicator for the tested mixes. Both parameters and conditions are recommended by Witczak, et al. (2002).

7.2.6. Flow Number Test

The Flow Number (F_N) is defined as the number of load repetitions at which shear deformation, under constant volume, starts (Figure 7.3). Witczak, et al. (2002) concluded in their study that this fundamental engineering property of HMA can also be used as a performance indicator for permanent deformation (rutting). The Flow Number test is conducted using a loading cycle of 1.0 second in duration, which consists of a 0.1 second haversine load, followed by a 0.9 second rest at a testing temperature of 130° F. This test utilized the same specimens used for the Dynamic Modulus Test. Both tests (the Dynamic Modulus and Flow Number) were conducted at Washington State University labs.

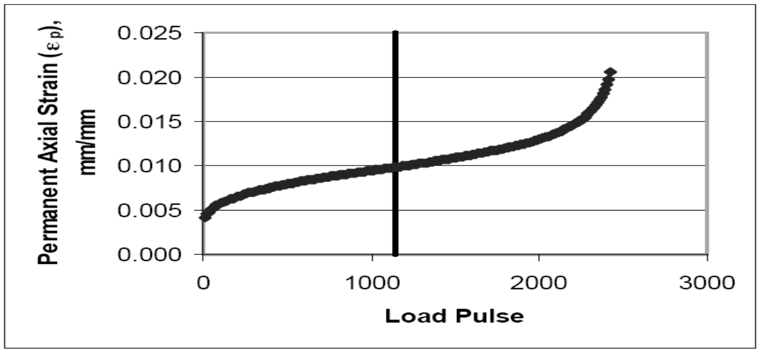

a. Permanent Axial Strain in Flow Number Test.

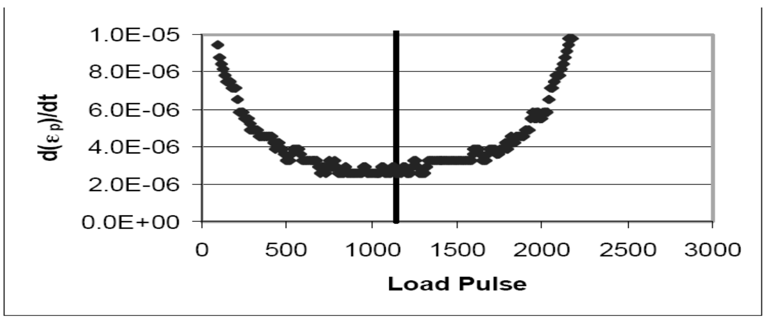

b. Rate of Change of Permanent Axial Strain.

Figure 7.3 Typical Repeated Load Test Response and Flow Number (after Banaquist 2003)

7.3. ANALYSIS OF RESULTS

7.3.1. Gyratory Stability

The GS values were calculated for both mixes with different asphalt contents, and as per Superpave Mix Design, these mixes were expected to perform best at the optimum asphalt content, at which the air voids of the compacted specimen at N-design is four percent. As shown in Figure 7.4 both mixes yielded the highest GS, as expected, at optimum asphalt content. In addition, when comparing the two mixes' GS values, Mix 2 yielded higher GS values, which leads us to the conclusion that Mix 2 may perform better than Mix 1.

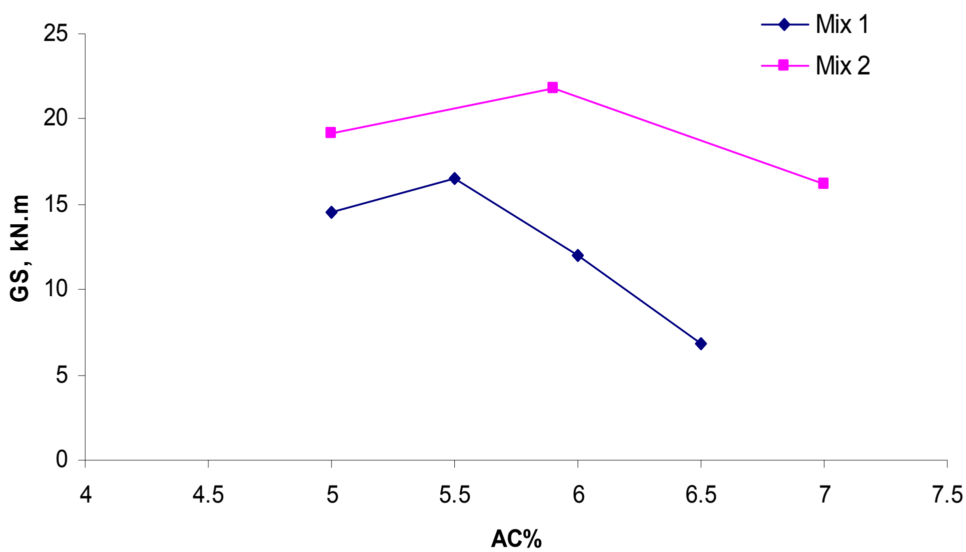

Figure 7.4 Superpave Mix GS Results for Different Asphalt Contents

The GS sensitivity to binder type (PG grade) was evaluated for Mix 2 (Figure 7.5). As expected, the results showed that GS is not very sensitive to the changes in binder grade. These findings matched the results for Hveem-designed mixes (Chapter 5). This can be explained by the fact that at compacting temperatures, asphalt binder is in a liquid state and the difference in grade does not influence the performance of the mix.

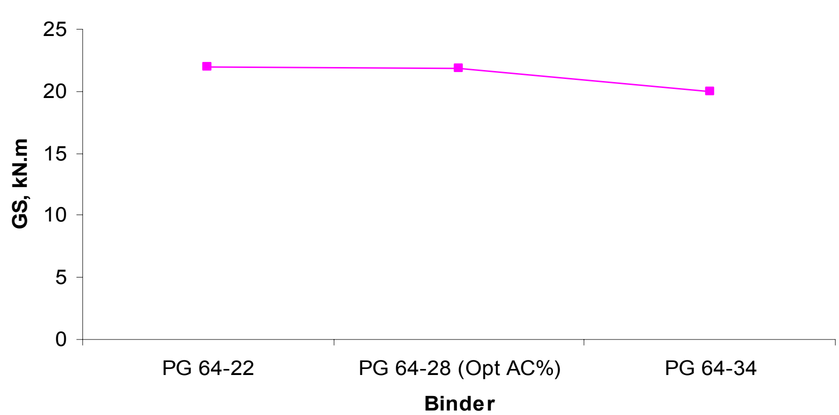

Figure 7.5 Sensitivity of GS to Different PGs (Mix 2)

Then GS results were compared to the APA test results. Figure 7.6 shows that a very good correlation between GS and permanent deformation resulted from APA ($R^2 = 0.58$). These results vary from the results for the Hveem mixes (Chapter 5). The correlation is attributed to the fact that the APA test is conducted at different temperatures, according to the upper temperature of the PG grade; and since both mixes have the same upper temperature of the PG grade (64 °C) a correlation should exist between the two parameters. This relation shows that the higher the GS, the lower the permanent deformation predicted by APA will be.

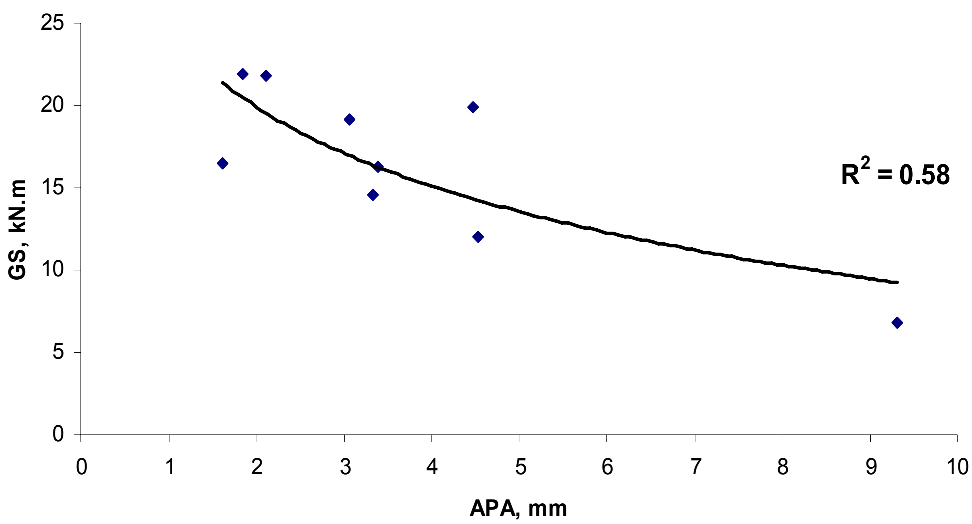

Figure 7.6 Relationship of GS versus APA Test

As suggested by Witczak, et al. (2002) E*/sin δ at the 130 °F or at the 100° F parameter should be used as a rutting indicator for asphalt mixes, because the higher the value of this parameter at a given temperature, the better resistance to rutting the mix exhibits. The GS was compared to E*/sin δ at both temperatures. Figure 7.7 shows that a very good relationship exists between GS and E*/sin δ at 130° F with an R^2 equal to 0.76; and also between GS and E*/sin δ at 100° F with an R^2 equal to 0.65.

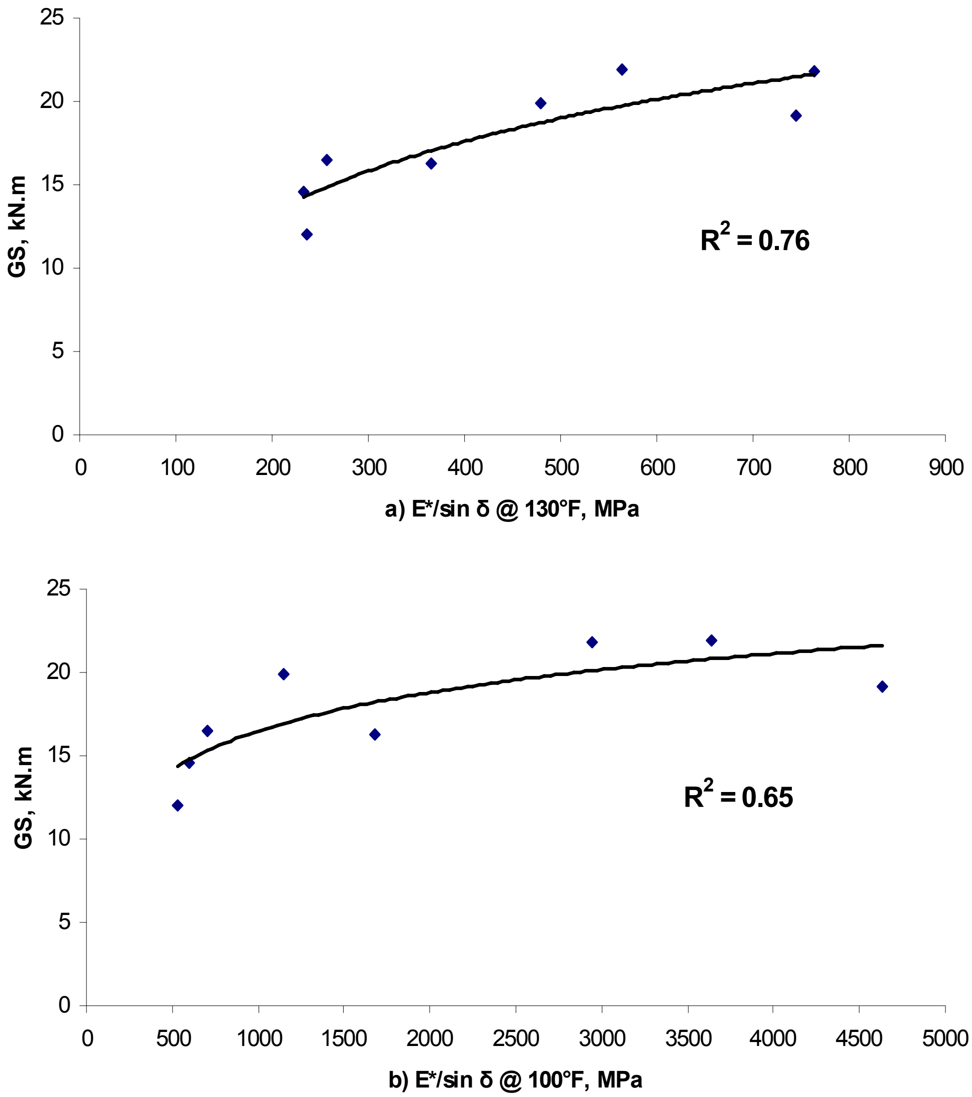

Figure 7.7 Relationship of GS versus E*/sin δ

Finally, GS was compared to the Flow Number (F_N) Test results. Similar to E*/sin δ, it is believed that the higher the F_N is, the better performing the asphalt mix will be. Although it has been observed that the results of this test vary much within the same mix, the results show a good correlation between GS and F_N with an R^2 equal to 0.49 (Figure 7.8).

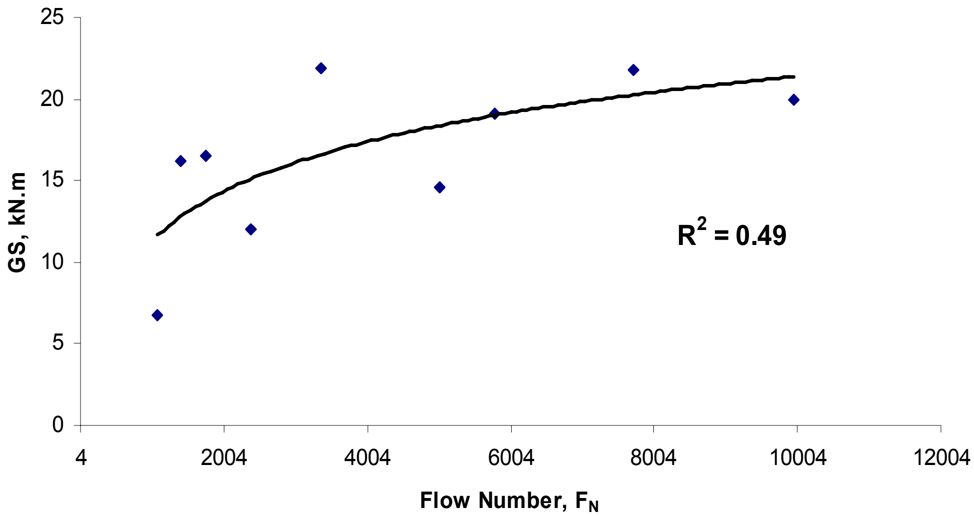

Figure 7.8 Relationship of GS versus F_N at 130°F

7.3.2. Fracture Toughness (J_c)

Figure 7.9 shows the variation of J_c values for both mixes due to different asphalt binder contents. As was observed with Hveem mixes, the value of J_c was found to be sensitive to the variation in the asphalt binder content. J_c for Mix 1 decreased with the increase of binder content, with a maximum value at the lowest asphalt content. Unlike Mix 1, a maximum J_c value for Mix 2 was observed at the optimum asphalt content.

The effect of binder grade on J_c was also studied as shown in Figure 7.10. Although it was expected that the J_c results for PG 64-34 should be the highest, it was shown that the highest J_c values were obtained for PG 64-28. This might be explained by the fact that PG 64-34 is a modified asphalt binder, which may affect its ability to resist fracture at room temperature. This may also explain why Mix 2 (PG 64-28) had a higher J_c than Mix 1 (PG 64-34). Further, no trend in the results can be observed. It is possible that the dependency of J_c on asphalt content and binder grade is more complex than anticipated.

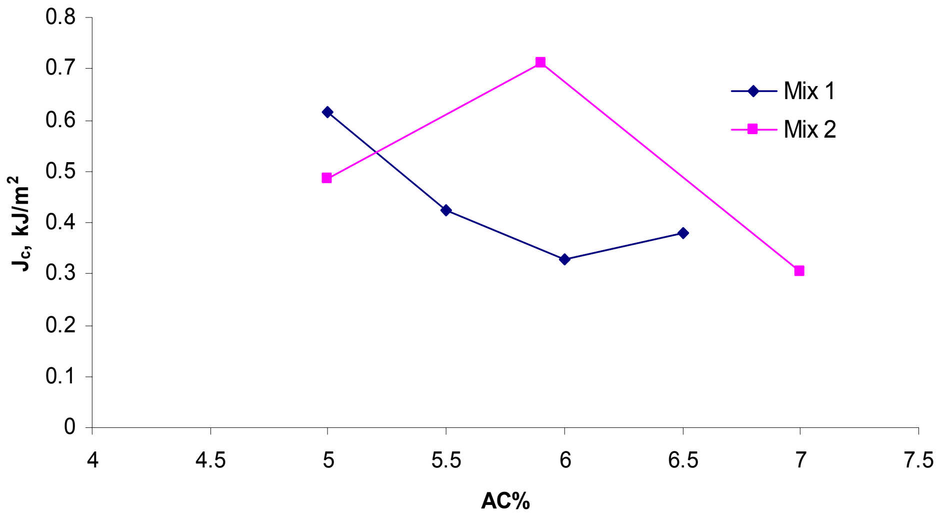

Figure 7.9 Superpave Mixes J_c Results at Different Asphalt Contents

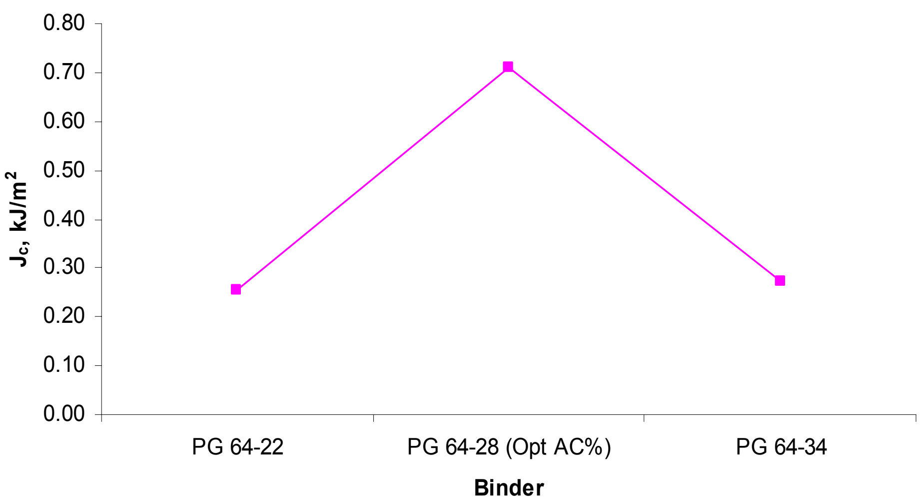

Figure 7.10 Sensitivity of J_c to Different PGs (Mix 2)

It was observed that when comparing J_c and E*.sin δ at the 70 °F or at the 40° F parameter for both mixes, there was no visible trend; but it was found that within each mix E*.sin δ and J_c follow the same trend. Overall, when comparing J_c and E*.sin δ for both mixes at optimum asphalt content (Figure 7.11), Mix 2 has yielded higher values than Mix 1. Therefore, it may be concluded that Mix 2 will perform better than Mix 1 with regards to fatigue cracking.

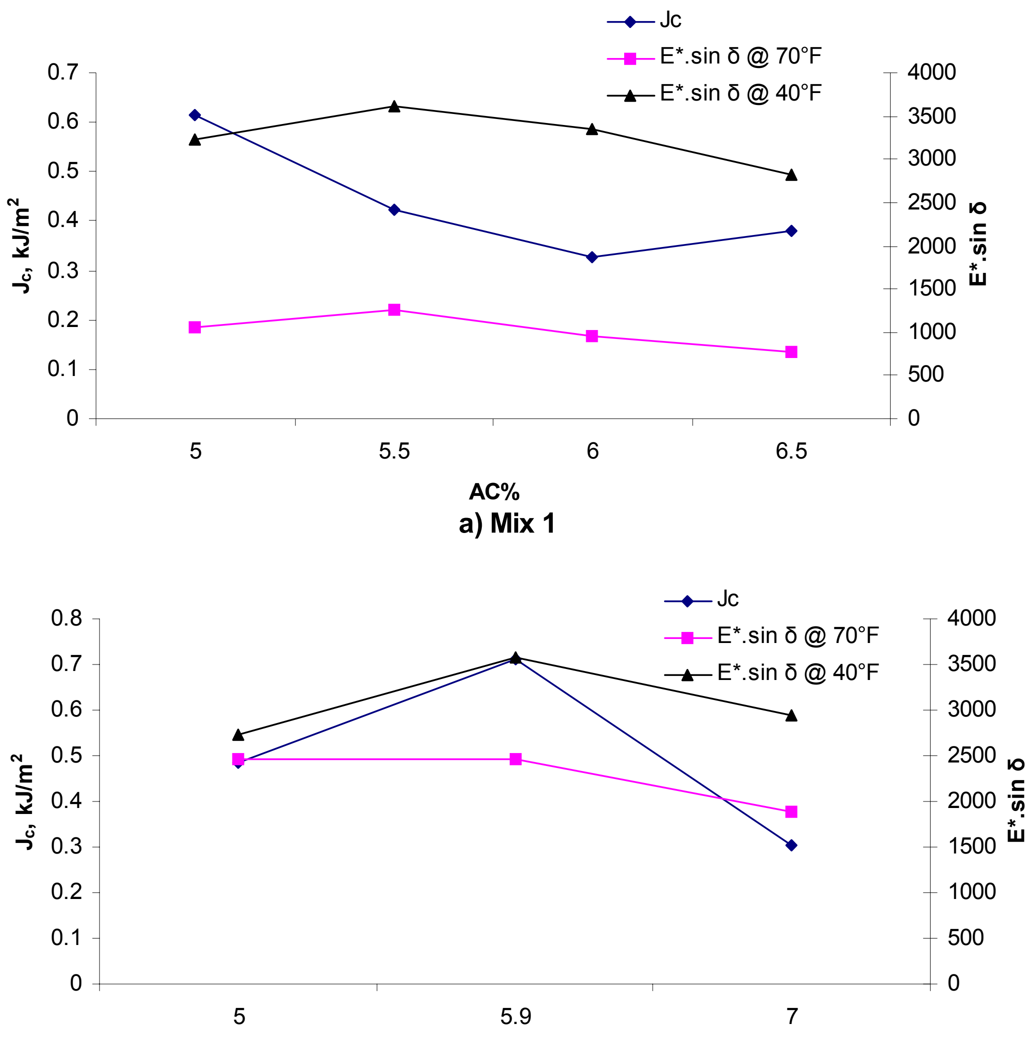

a) Mix 1

b) Mix 2

Figure 7.11 J_c versus E*.sin δ Results

7.4. SUMMARY

Based on the results, the GS and J_c measurements can be used as a screening tool for different Superpave mixes at the design stage. Further, it was found that using these parameters, Mix 2 will perform better than Mix 1 under the same loading conditions. Based on the results presented, the following observations are made:

- GS was found to be sensitive to asphalt content but not to asphalt binder grade. This is attributed to the compacting temperatures at which GS is determined.

- GS which was determined at optimum asphalt content was the highest for both Mixes.

- GS correlated very well with the APA test results with a reported R2 equal to 0.58. It was observed that the higher the GS values, the lower the permanent deformation the mix will endure, as determined by APA.

- E*/sin δ at both temperatures 130° F and 100° F correlated with the GS with an R2 equal to 0.76 and 0.65 respectively. In addition, GS correlated well with the Flow Number test results with a reported R2 equal to 0.49.

- E*/sin δ at both 130° F and 100° F correlated with the GS with an R2 equal 0.76 and 0.65 respectively.

- The J_c parameter was found to be sensitive to the variation in the asphalt binder content. It was found that there is no clear relationship between the optimum asphalt content and J_c.

- There was no clear trend between J_c and E*.sin δ at both 70° F and 40° F when both mixes are compared. But within each mix, both parameters followed the same trends.

8. GYRATORY STABILITY SOFTWARE

8.1. INTRODUCTION

As has been discussed early in the report, the Contact Energy Index (CEI) is calculated from the sample compaction data to the final number of Gyrations (N-final), where the Gyratory Stability is calculated to the N-Design. Thus, the GS is a special case of the CEI and shall always be smaller. In most design cases, the designer will rely on the GS value since the mix design shall be based on N-Design.

To facilitate the calculation of the Contact Energy Index (CEI) and the Gyratory Stability (GS), a Visual Basic.Net software was developed (referred to as G-STAB) that can be integrated with the gyratory compactor. In addition, a Microsoft Excel file with built-in macros was developed to calculate both CEI and GS. Both, the Visual Basic software (G-STAB) and the Excel file allow the user to import the compaction data directly from the gyratory compactor data files. They also allow the user to enter compaction data manually.

G-STAB and the Excel file are not proprietary and can be modified easily to include agency specific procedures and design specifications. The current versions of G-STAB and the Excel file can be used with the Servopac and Pine AFG1 compactors. In addition the Excel file can import the change of height data from a Troxler Model 4140 compacter's output file. In addition, they can be used with any other model with the use of a load sensor device such as the PDA. In this case, however, the user would have to enter the force data and change of height to the program or the Excel file manually. The software is provided on the project CD (Appendix C).

8.2. INPUT DATA

To determine CEI and GS for a given sample, essential input data is required. This data can be found in the Job Mix Formula, compaction data, and air voids calculations for the compacted sample. The required data includes:

1. Mix data:
   a. Maximum Theoretical Specific Gravity (G_{mm}).
   b. Final Bulk Specific Gravity (G_{mb}).
   c. Final Weight of compacted sample (dry weight).

2. Compactor data:
   a. Vertical Stress (default value is 600 kPa).
   b. Gyration Angle (default value is 1.25°).
   c. Mold Diameter (150 or 100 mm).
   d. Output file for either Servopac or Pine compactor. For other compactors change of height and vertical forces versus number of gyrations data is required.
   e. N-design is only required to determine GS.

8.3. INSTRCUTIONS FOR USING THE EXCEL FILE

Basically this Excel file contains all the tools and options found in any Excel file. The Excel file was developed to be user friendly and to facilitate the calculation of CEI and GS on the spot. It can be modified to suit any specifications required by the user. General view of the Input sheet is shown in Figure 8.1. The sheet is divided into two main parts. Part one is the Results Table, which is located at the top of the sheet. The second part includes the Input Tables: Table A is for the specimen and compactor input data, and Table B is for the compaction input data.

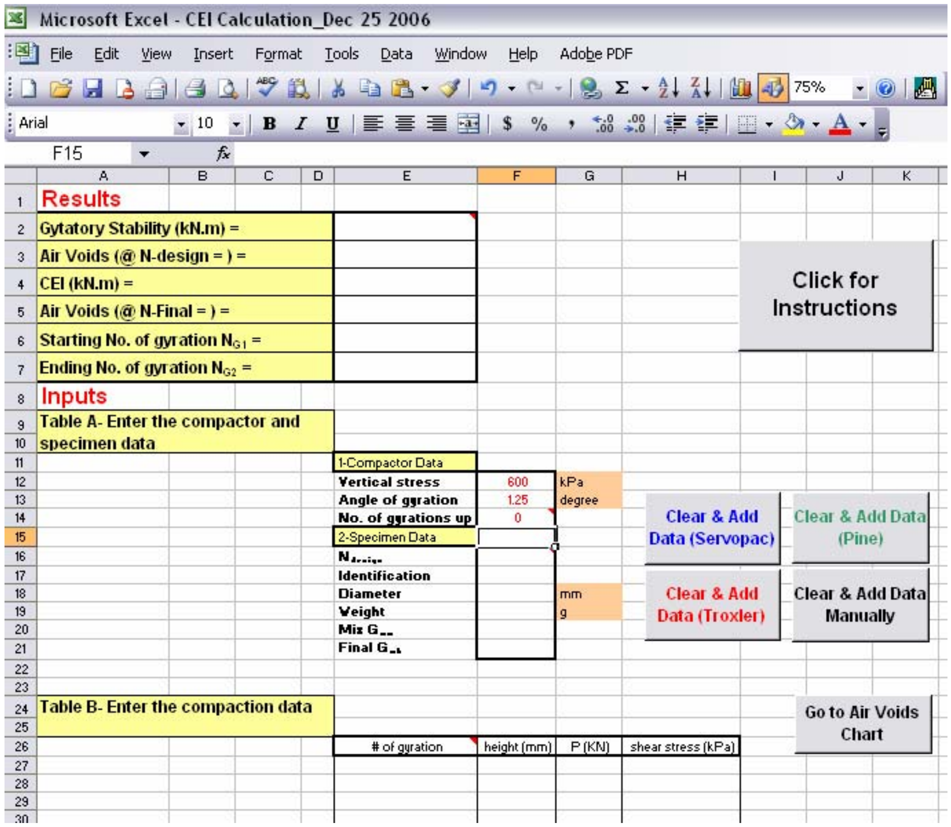

Figure 8.1 General View of the GS/CEI Calculation Excel Sheet

To determine the CEI/GS values for a specimen using the Excel file, one follows these instructions:

1. To open, save, or close the Excel file, use the same procedure as with any Microsoft Excel file. To open, save or close it use the **File** pull down Menu.
2. When opening this file a Security Warning window will appear (Figure 8.2). Press on the **Enable Macros** button. If the **Disable Macros** button is pressed the file will not function as intended.

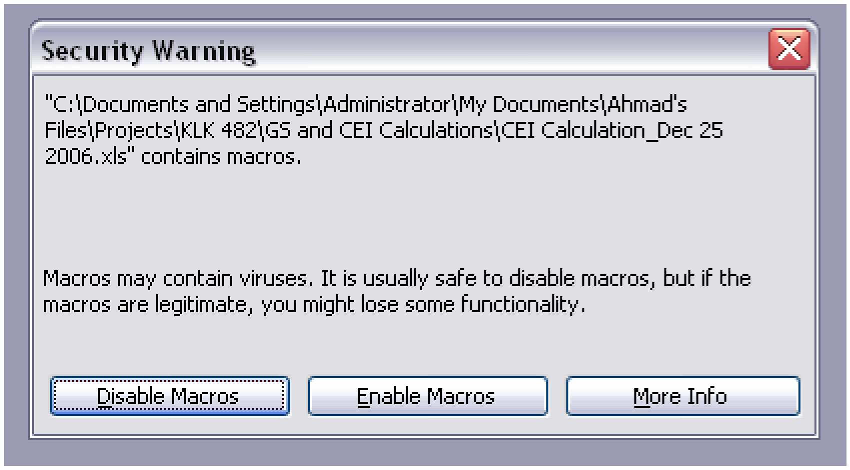

Figure 8.2 Macros Enabling Window

3. The Excel file has three sheets: Instructions, Inputs, and Air Voids Graph Sheets. To navigate between the three, use the buttons located on the sheet (Figure 8.1).
4. In order to input data, note that the Input Sheet is setup for inputting the compaction data (Table B) before the compactor and mix data (Table A).
5. For Manual Inputs of Compaction Data (typically used if you are using an external device to measure force, such as PDA):
    a. Click on **Clear** button. This will clear all input data except for defaults
    b. Enter sample data in Table A.
    c. Do not change default values given for the compactor data (cells with red font).
    d. Enter pr Specimen data, complete the cells as shown. Pay attention to the units.
    e. Enter the compaction data in Table B. Input the change in height in **Column F**. Input either the vertical force in **Column G** or the shear stress in **Column H** for all number of gyrations.
6. To input files from Gyratory Compactors, observe that the Excel file is developed for three types of compactors: Servopac, Pine, Model AFG1 (Baby pine), and Troxler.
    a. Click on the appropriate button for the Gyratory compactor.
    b. This will open a text import wizard. Open the appropriate Gyratory file. Select "**Delimited**" and click **Next** (Figure 8.3). From the delimiters,

choose "**Tab**" and "**Space**" for all compactors (Figure 8.4 a). For Servopac compactor choose "**Tab**", "**Space**" and "**Other:,**" type "=" in the text box beside "**Other:**" (Figure 8.4 b). Then click **Finish**. The data will be filled automatically in Table B of the Input sheet.

Figure 8.3 Text Import Wizard (Step 1 of 3)

7. Enter sample data in Table A. Do not change default values given for the compactor data.
8. To enter specimen and compactor data, complete the cells as shown. Pay attention to the units.

a) Pine and Troxler Compactors

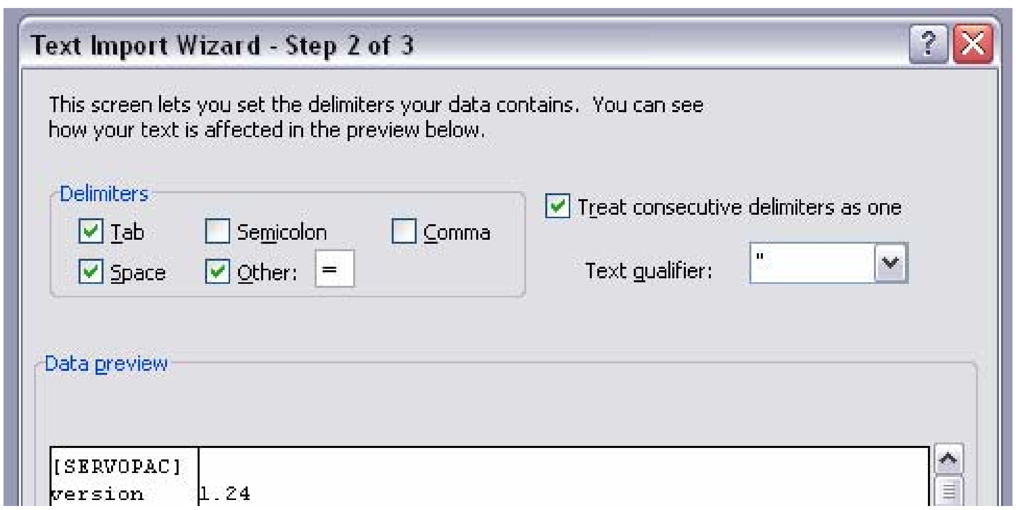

b) Servopac Compactor

Figure 8.4 Text Import Wizard (Step 1 of 3)

9. Once the data input is complete, the calculated GS and CEI will show in the RESULTS Table at the top of the sheet, along with the air voids at N-design and N-final and the calculated N_{G1} and N_{G2} (that were used in the calculation of the GS/CEI value). If the N-design is not specified the GS and air voids will not be

calculated. To view the air voids curve click on **Go to Air Voids Chart** button (Figure 8.1).

8.4. INSTRUCTIONS FOR USING THE G-STAB SOFTWARE

G-STAB was developed using Visual Basic.Net framework. It can be run under any Microsoft Windows environment. G-STAB consists of four main windows: Intro, Project Information, HMA Specimen Data, and Gyratory Compactor Details.

It varies from the Excel file by the input sequence. It is designed to guide the user through the software with ease. The software will not allow the user to skip a step. Each step must be completed before going to the next. To determine the CEI/GS values for a specimen follow these instructions:

1. To run the G-STAB double click on the G-STAB.exe file. The Intro windows will appear as shown in Figure 8.5. Press **Next** button to continue or **Exit** button to exit.

Figure 8.5 Intro Window for G-STAB Software

2. The Project Information window will appear (Figure 8.6). Project Information (i.e, Project Title, ID, Section ID, Location, and Date) can be completed. Notice

the red square beside the **HMA Data** and **Compactor Data** buttons. This indicates that the inputs for both section is not complete. In addition, the **Compactor Data** button is not active. It will only be activated when the specimen input data is completed.

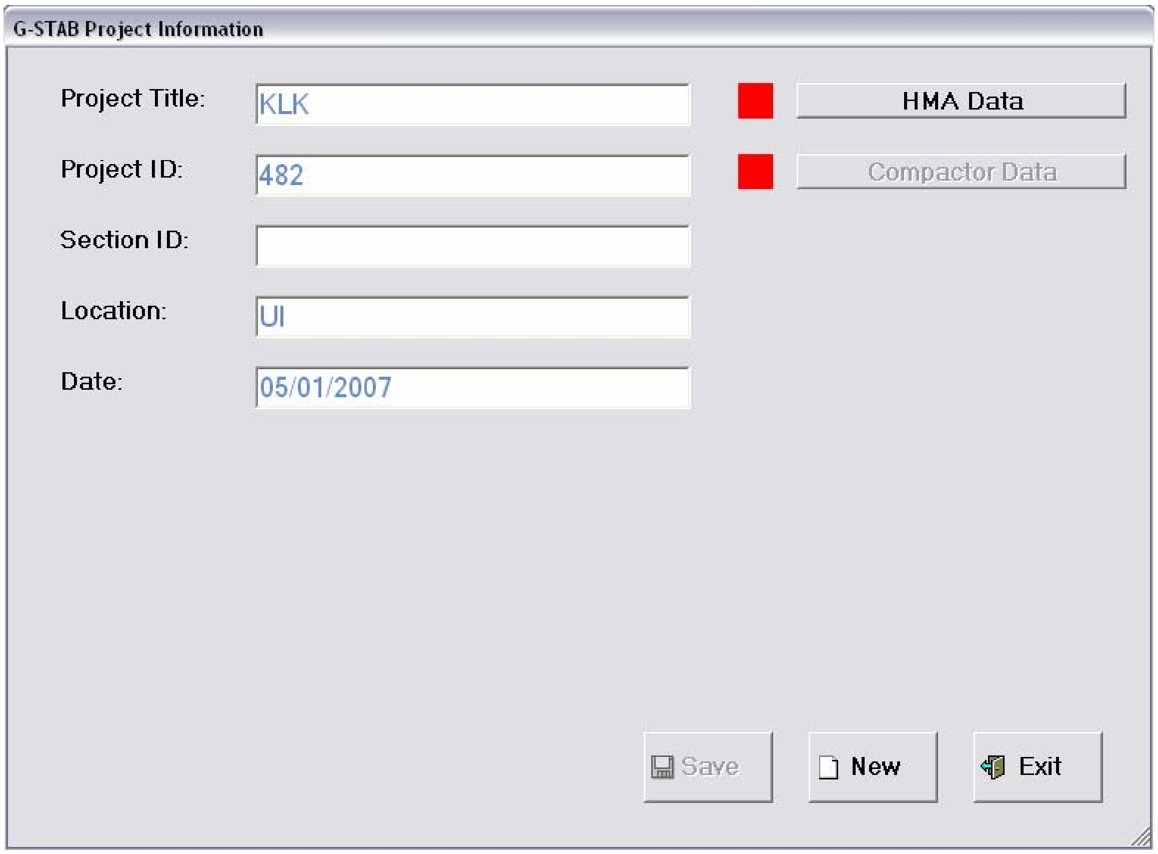

Figure 8.6 Project Information Window for G-STAB Software

3. Press the **HMA Data** button to open the HMA Specimen Data window (Figure 8.7). Enter the required data in the designated boxes. When completed press the **Next** button. Note that if the data is not complete, the software will prompt the user to input the missing data. The HMA Specimen window will close and the Project Information window will be reactivated. The red square beside the **HMA Data** button will turn green indicating that specimen input data is completed and the **Compactor Data** button is activated (Figure 8.8).

4. Press the **Compactor Data** button to open the Gyratory Compactor Details window (Figure 8.9). This window consists of two parts: the first is for general information about the compaction data; the second part is for the gyratory compactor data.

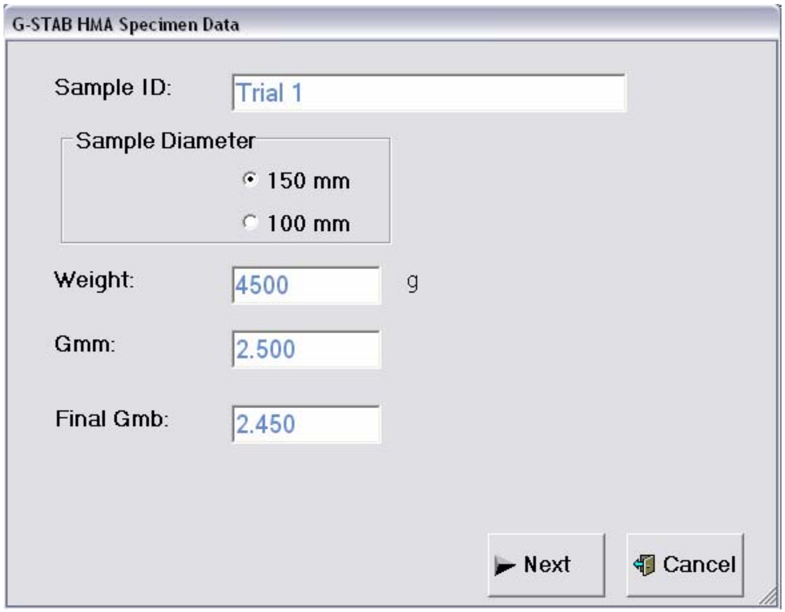

Figure 8.7 HMA Specimen Data Window for G-STAB Software

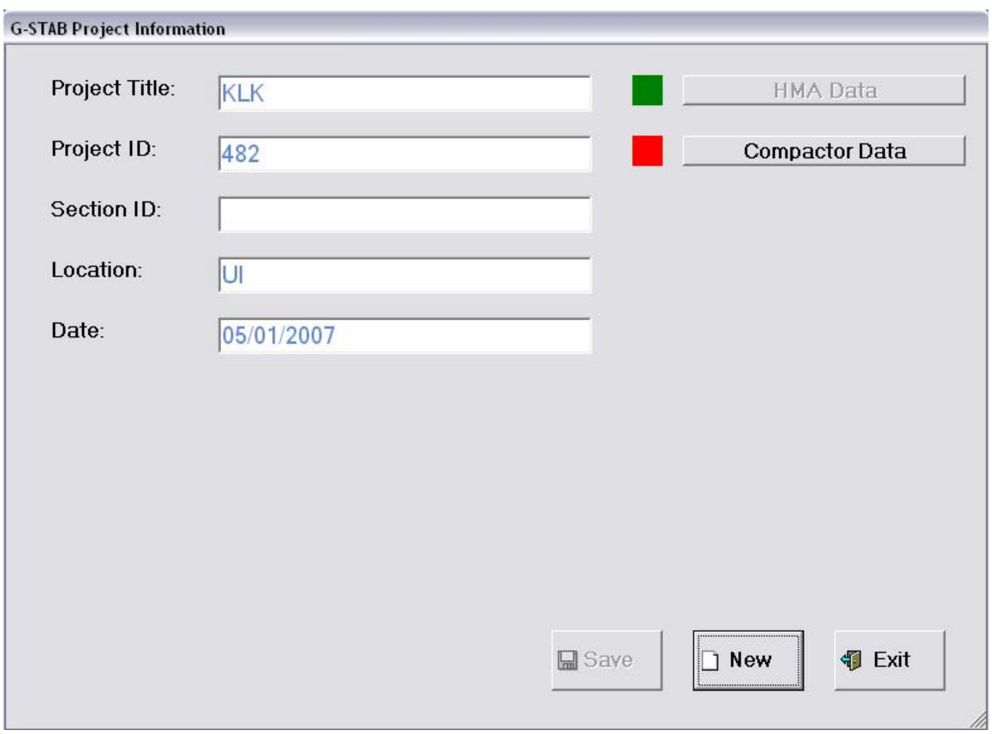

Figure 8.8 Project Information Window when Specimen Data is completed

5. If the height of the load measuring device is included in the height measurement while compaction, check the box beside "**Height of PDA Included.**" A box will appear where one can input the height of the load cell (Figure 8.9). It's essential to subtract the height of the loading cell in order to calculate the actual air voids.

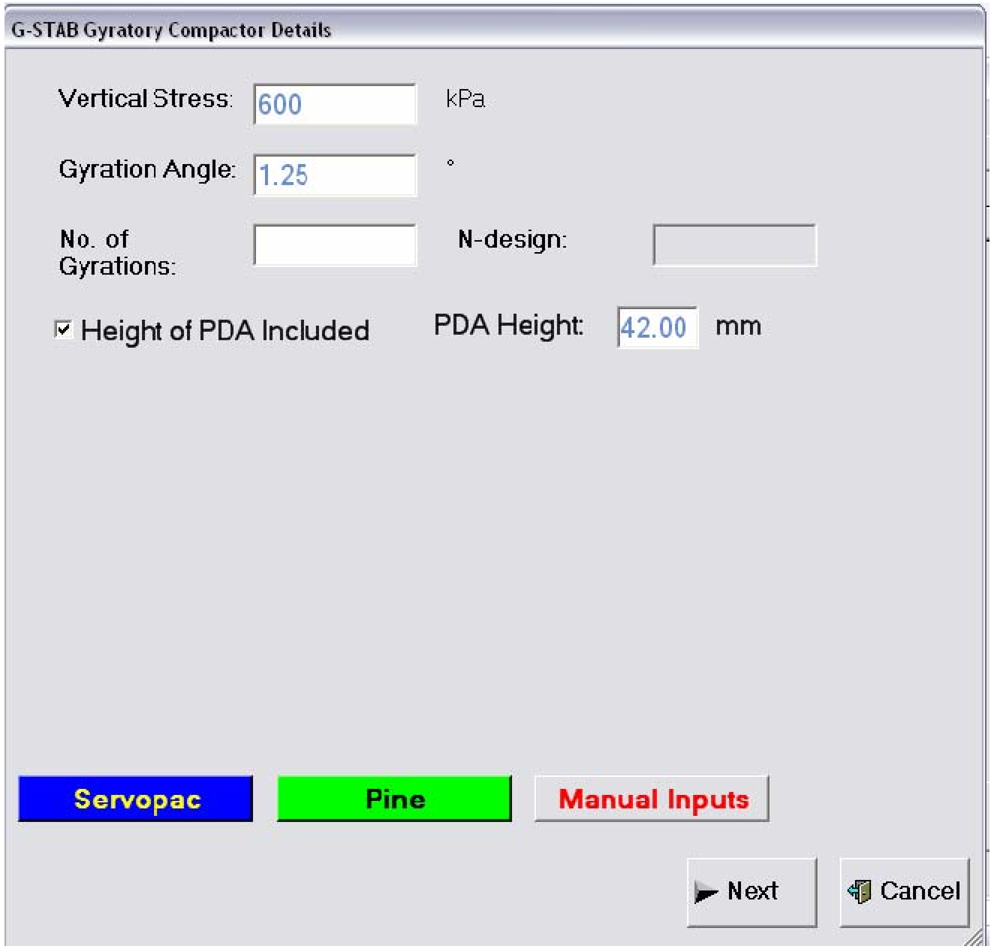

Figure 8.9 Gyratory Compactor Data Inputs Window for G-STAB Software

6. For Manual Inputs of Compaction Data (typically used if you are using an external device to measure force, such as PDA), click on the **Manual Inputs** button. The software will prompt the user to choose the type of loading: Shear Stress or Vertical Force (Figure 8.10).
   a. If "**Shear Stress**" is selected, two input boxes will appear. Input the height and the shear stress versus the number of gyrations shown in the adjacent box. Press **Add Entry** after each entry. The entered values will be shown in the text box (Figure 8.10 a). The same process should be followed until

all values are entered. To edit any entry, press the **Find Entry** button, and the software will prompt the user to input the number of gyrations for this entry. The entry can be edited by re-entering the correct value. Then press the **Edit Entry** button.

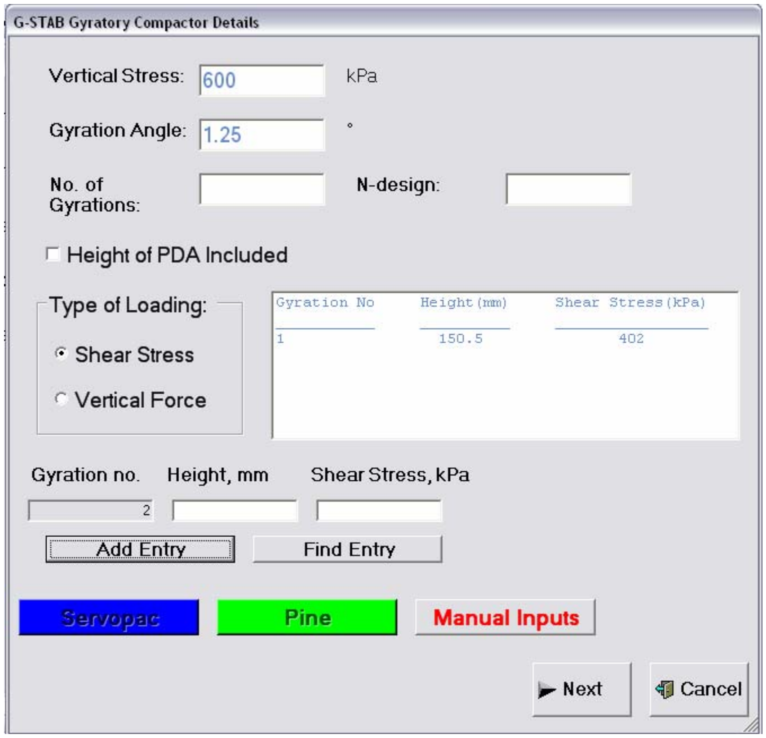

a) Shear Stress Inputs

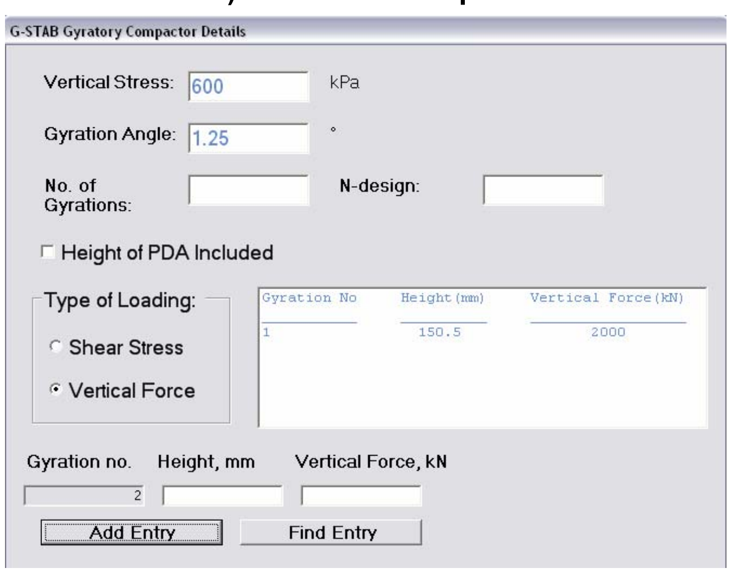

b) Vertical Forces Inputs

Figure 8.10 Manual Inputs of Compaction Data

b. If "**Vertical Force**" is selected, two input boxes will appear. Input the height and the vertical force versus the number of gyrations shown in the adjacent box. Press **Add Entry**. The entered values will be shown in the text box (Figure 8.10 b). The same process should be followed until all values are entered. To edit any entry, press the **Find Entry** button, and the software will prompt the user to input the number of gyration for this entry. The entry can be edited by re-entering the correct value. Then press the **Edit Entry** button.

7. For a manual inputs check, the total number of gyration should be entered in the designated box as shown in Figure 8.10.

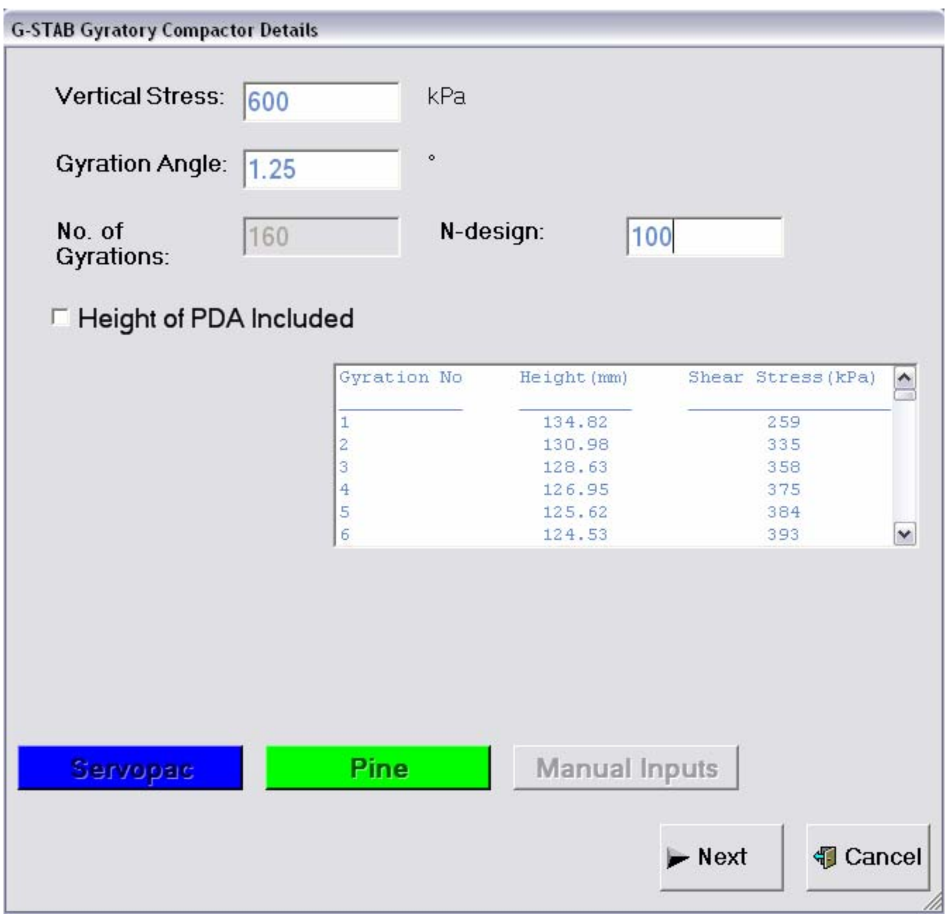

Figure 8.11 Importing Compaction Data form a Gyratory Output File

8. Importing Files from the Gyratory Compactor output file: G-STAB has been developed for two types of compactors: Servopac and Pine Model AFG1. Click on the appropriate button for the Gyratory compactor. The software will prompt the user to choose the gyratory output file. When the data import is complete a message will appear confirming the completion. In addition the imported data and the total number of gyrations will be displayed as shown in Figure 8.11.
9. To determine GS, N-design should be entered in the designated box. To only determine CEI, "0" must be entered in the N-design designated box.
10. When all data entries are completed press the **Next** button. Note that if the input data is not complete, the software will prompt the user to input the missing data. The Gyratory Compactor Details window will close and the Project Information window will be reactivated. The red square beside the **Compactor Data** button will turn green, indicating that specimen input data is completed and the button is activated (Figure 8.11). In addition, the **Run Analysis** button will appear.

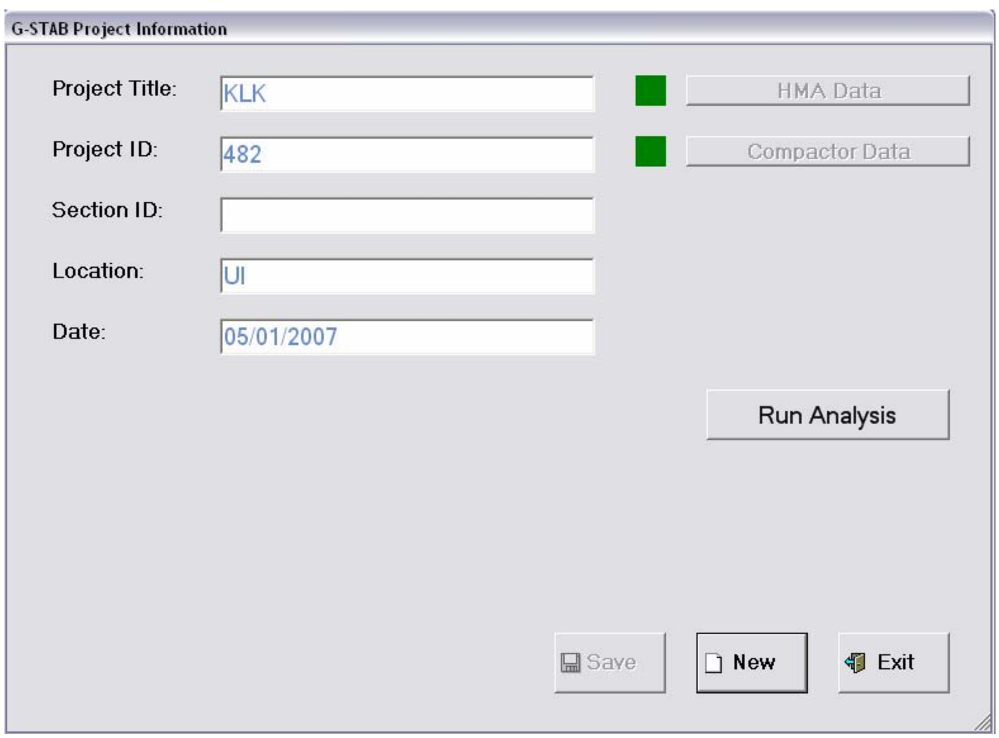

Figure 8.12 Project Information Window when All Data Entries are completed

11. Press the **Run Analysis** button. The software will calculate CEI/GS and a message will appear when the calculations are complete. The calculated CEI/GS values will be displayed as in Figure 8.12.

Figure 8.13 Project Information Window when the Analysis is Completed

12. For documentation, the calculation can be saved as a text file with a "*.cei" file extension. This file will include all data inputs and air voids at each number of gyrations. This file can be accessed for viewing or printing by any word document program such as Notepad that is available in all Microsoft Windows environments. To save, press the **Save** button (Figure 8.12), and the software will prompt the user to choose a file name and location.
13. To start a new analysis, press the **New** button. If the previous analysis is not saved, the software will only prompt the user to save the analysis once.
14. When finish, press the **Exit** button. If the previous analysis is not saved, the software will only prompt the user to save the analysis once.

8.5. EXAMPLE

To demonstrate the procedure for CEI/GS calculations using both G-STAB and Excel file and the variations between the two, one example is used.

8.5.1. Inputs

A trial HMA sample was mixed and compacted using the Pine compactor in the laboratory as per Superpave specifications. The data required to determine CEI and GS for this mix is listed in Table 8.1.

Table 8.1 Required Data for CEI/GS Calculations

Mix Data	Maximum Theoretical Specific Gravity (G_{mm})	2.436
	Final Bulk Specific Gravity (G_{mb})	2.363
	Final Weight of compacted sample (dry weight)	4500 g
Compactor Data	Vertical Stress	600 kPa
	Gyration Angle	1.25°
	Mold Diameter	150 mm
	N-design	100
	Pine Gyratory Output File	G48P1.dat

8.5.2. Using the Excel File

Using the data in Table 8.1, the above instructions were followed for determining the CEI and GS values for this trial mix. The resulting GS and CEI values, as shown in Figure 8.14, are equal to15.61 kN.m and 18.56 kN.m, respectively. In addition, the air voids at N-design were determined to be 3.7%, and 3.0% at N-final. The air void curve was plotted as shown in Figure 8.15.

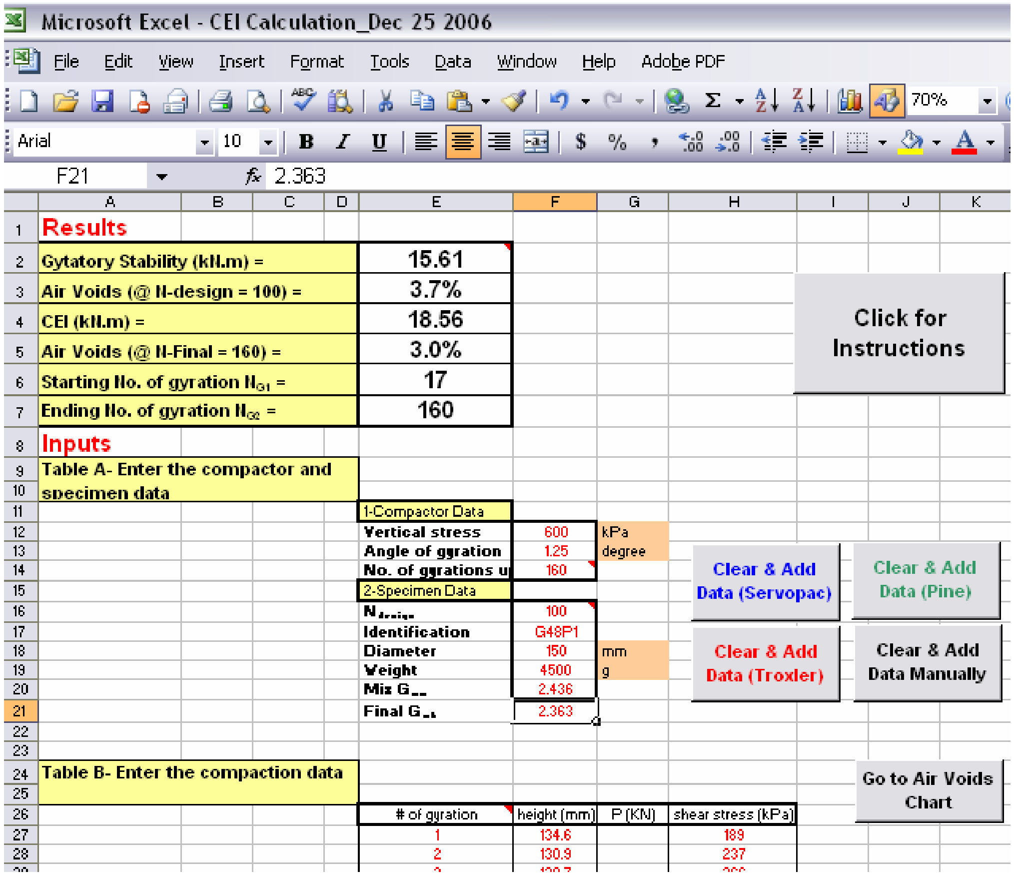

Figure 8.14 CEI and GS Calculation Results for the Trial Mix Using the Excel File

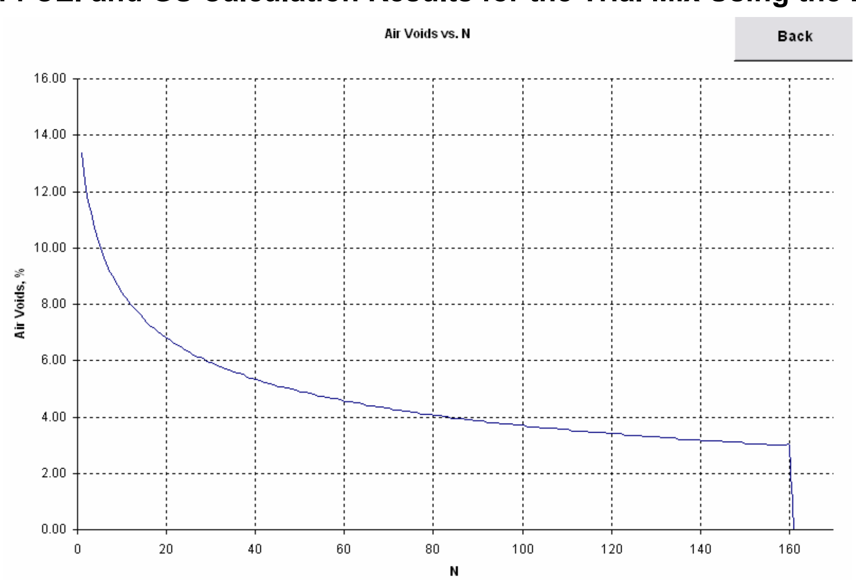

Figure 8.15 Air Voids Curve for the Trial Mix

8.5.3. Using the G-STAB Software

The instructions were also followed for determining the CEI and GS values using G-STAB for the same trial mix and utilizing the data in Table 8.1. The resulting GS and CEI values, as shown in Figure 8.16, are equal to15.59 kN.m and 18.54 kN.m, respectively. In addition, all input data, calculation results, and change of height, air voids, and Shear Stress versus gyration numbers can be saved as a text file as shown in Figure 8.17.

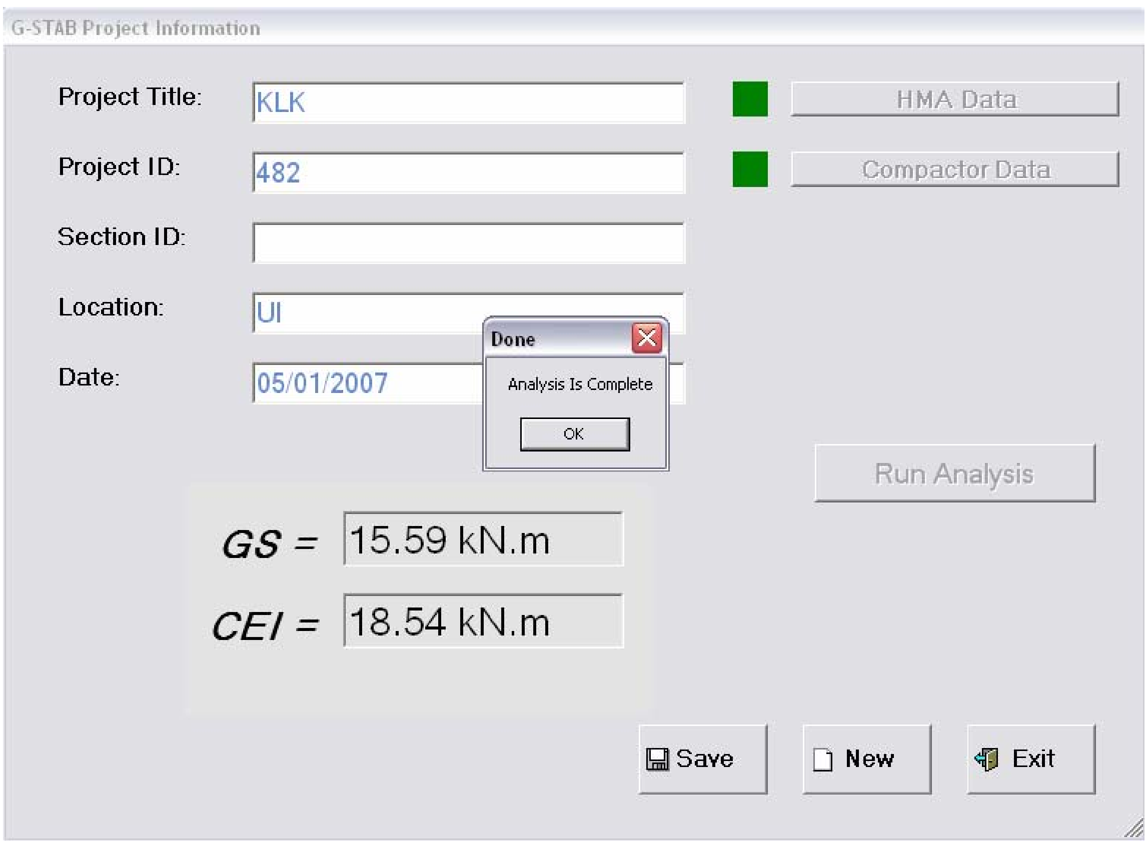

Figure 8.16 CEI and GS Calculation Results for the Trial Mix Using G-STAB

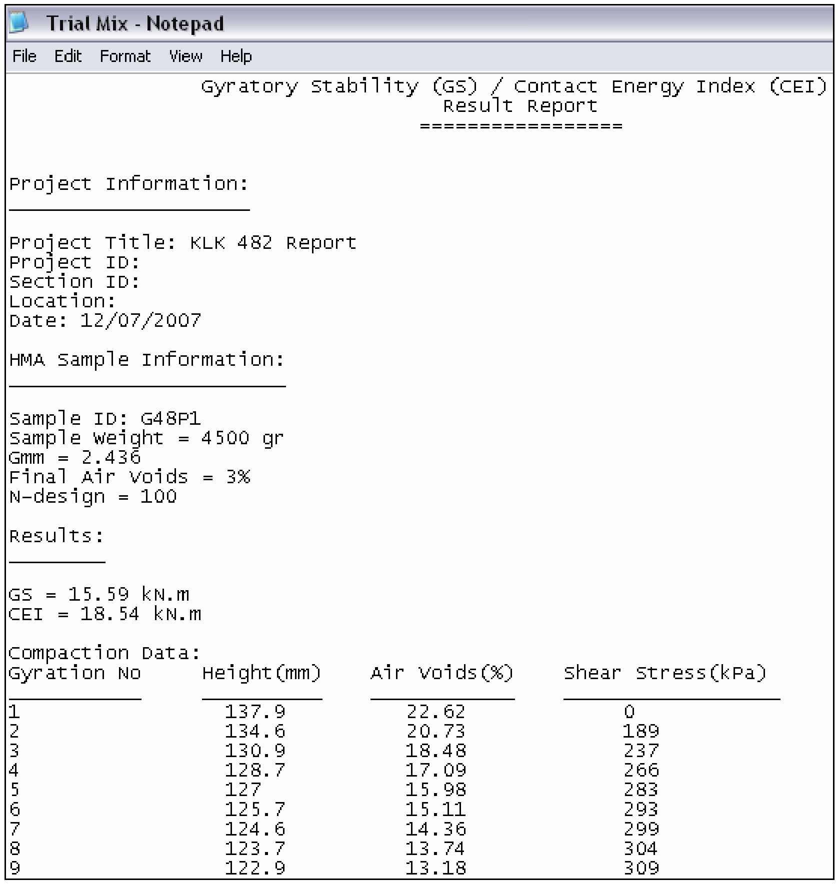

Trial Mix - Notepad

File Edit Format View Help

Gyratory Stability (GS) / Contact Energy Index (CEI)
Result Report
=================

Project Information:

Project Title: KLK 482 Report
Project ID:
Section ID:
Location:
Date: 12/07/2007

HMA Sample Information:

Sample ID: G48P1
Sample Weight = 4500 gr
Gmm = 2.436
Final Air Voids = 3%
N-design = 100

Results:

GS = 15.59 kN.m
CEI = 18.54 kN.m

Compaction Data:

Gyration No	Height(mm)	Air Voids(%)	Shear Stress(kPa)
1	137.9	22.62	0
2	134.6	20.73	189
3	130.9	18.48	237
4	128.7	17.09	266
5	127	15.98	283
6	125.7	15.11	293
7	124.6	14.36	299
8	123.7	13.74	304
9	122.9	13.18	309

Figure 8.17 Page 1 of G-STAB Output File

There is a minor difference between the results of G-STAB and that of the Excel file. This is believed to be due to the different process for rounding numbers in each framework.

9. SUMMARY AND CONCLUSIONS

9.1. SUMMARY

This research addressed the development of new testing methods that can be augmented with the Superpave asphalt mix design system. Superpave was developed under the Strategic Highway Research Program (SHRP). The research outcomes of SHRP included state-of-the-art methods to design Hot-Mix Asphalt (HMA) based on performance.

However, and for practical implementation of SHRP products, the design criterion in the current Superpave system is based only on volumetric analysis. There has been a need to develop simple, practical and reliable methods and procedures to be incorporated in the design criteria of Superpave. Research efforts since the release of Superpave in 1992 have continued to address this issue. A few test procedures and new performance indicators have been developed.

The main goal of this study was to evaluate the potential of using the gyratory compaction forces and deformation to measure the aggregate structure stability in hot-mix asphalt (HMA) during the mix design process. This method is intended as a screening tool to identify aggregate structures that have low resistance to applied forces prior to conducting further performance testing. The measured compaction shear forces and deformation of a wide spectrum of hot-mix asphalt (HMA) mixtures were used to calculate a stability index referred to as the Gyratory Stability (GS). Further, this study addressed the development and evaluation of the critical strain energy release rate J_c, as an indicator of HMA resistance to fracture. J_c was determined from load-deformation data of a simple three-point bending fracture test using notched semi-circular specimens. The test specimens were prepared from standard Superpave Gyratory compacted HMA samples.

In the first stage of this study, using forty-seven Hveem-designed mixes in Idaho, the GS values of these mixes were compared to their Hveem Stability (HS) values. In addition, the aggregate used in these mixes was evaluated using the Aggregate Imaging System (AIMS), and the texture results were compared to the GS values. To evaluate the effect of the HMA material properties on the variation of J_c, thirty-four mixes of the forty-seven Hveem-designed mixes were used in the analysis. All mixes were designed and constructed in accordance to the Hveem design method. Experimental results indicated that CEI/GS and J_c are sensitive to mix design components including the asphalt binder content and the aggregate structure.

In the second stage of this study, two Superpave-designed mixes were tested, to investigate if the GS and J_c measurements could be used as screening tools at the mix design stage to assess the mix performance, before implementing sophisticated and time-consuming performance tests. Further, a Visual Basic software program and an Excel file were developed to facilitate the calculation of GS and CEI.

9.2. CONCLUSIONS

Based upon the test results and data analysis presented in this research, the following conclusions and observations are made:

9.2.1. Hveem-Designed Mixes

- The GS correlated well with the Hveem Stability of Hveem-designed mixes. Results, however, showed wide variation in GS values for mixes that had the same Hveem Stability. This may indicate that GS is more sensitive to changes in mix design parameters than Hveem Stability. A three tier GS limits of 5, 12 and 15 are suggested to classify HMA mixtures based on their stability.

- Results of the APA rut testing did not correlate with the GS of these mixes. It is believed that the main reason is that the current APA testing procedure allows testing the mix at different temperatures based on its high temperature grade, while the GS is determined at the standard compaction temperature of 149 °C. A better correlation between GS and permanent deformation in APA was obtained for mixes that have the same PG grade and tested at the same temperature in the APA.

- Image analysis indicated that aggregate texture correlated with the GS. There was no clear relationship between angularity and sphericity with GS for the range of aggregates used in this study.

- The J_c measured by the semi-circular notched bending fracture (SCBNF) test can represent HMA resistance to fracture. The SCBNF test is simple and quick to perform, and can be implemented at the mix design stage of HMA design.

- Finite Element Analysis was used to model the SCBNF test configuration. FEA results were used to calculate the mixture elastic modulus. The elastic modulus was correlated to the J_c. Results indicate that J_c increases with the increase in modulus values of HMA. It is postulated that Hveem mixes with higher stabilities have higher stiffness, and therefore exhibit a higher resistance to fracture as measured by the J_c parameter.

- Results have shown that K_{JC},which is equivalent to $K_{IC,}$ followed the same trend as J_c for the tested mixes and the results fell into the range of reported K_{IC}.

- The J_c parameter was found to be sensitive to changes in the mix aggregate gradations and to the aggregate shape and surface texture properties as measured by the Aggregate Imaging System (AIMS). Mix with finer aggregate gradations showed higher resistance to fracture compared to the mix with coarser aggregate gradations. Mixes with rougher aggregate texture and more angular particles showed higher J_c values. Mixes that had high percentages of flattened and elongated aggregates showed lower J_c values.

- The J_c parameter was found to be sensitive to variation in the asphalt binder content. Results showed that as the binder content increased the value of J_c increased. However, no clear trend was found that relates J_c to different binder grades.

- Overall, this study concludes that J_c determined in a SCNBF test can be used to assess a HMA mixture's propensity to fracture during the design stage.

9.2.2. Superpave-Designed Mixes

- Based on the two mixes evaluated by means of GS and Jc, it was found that Mix 2 performs better than Mix 1 under the same loading conditions.

- GS was found to be sensitive to asphalt content but not to asphalt binder grade. This is attributed to the compacting temperatures at which GS is determined.

- GS determined at optimum asphalt content was the highest for both mixes.

- GS correlated well with the APA test results with a reported R^2 equal to 0.58. It was observed that the higher the GS values the lower the permanent deformation the mix will endure, as determined by APA.

- The rutting parameter (E*/sin φ) at both 130 °F and 100 °F correlated with the GS, with an R^2 equal to 0.76 and 0.65, respectively. In addition, GS correlated well with the Flow Number results with a reported R^2 equal to 0.49.

- The J_c was found to be sensitive to the variation in the asphalt binder content. It was found that there is no clear relationship between the optimum asphalt content and J_c.

- There was no clear trend between J_c and the fatigue indicator (E*.sin φ) at both 70° F and 40 °F when both mixes are compared. But within each mix, both parameters followed the same trends.

REFERENCES

AASHTO Designation TP 62-03. (2004). “Standard Method of Test For Determining Dynamic Modulus of Hot-Mix Asphalt Concrete Mixtures.” American Association of State Highway and Transportation Officials.

Abdulshafi, A. and K. Majidzadeh. (1985). “J-Integral and Cyclic Plasticity Approach to Fatigue and Fracture of Asphalt Mixtures.” Transportation Research Record 1034, Transportation Research Board, National Research Council, Washington, D.C.

Abu Abdo, A. (2005). “Development of Performance Parameters for the Design of Hot-Mix Asphalt.” Master Thesis, University of Idaho, Moscow, Idaho.

ALGOR, FEMPRO Version 13.24-WIN 28-OCT-2002. ALGOR, Inc., Pittsburgh, PA.

Anderson, R., P. Tuner, R. Peterson, and R. Mallick. (2002). “Relationship of Superpave Gyratory Compaction Properties to HMA Rutting Behavior.” NCHRP Report 478, TRB, Washington, D.C.

Australian Standards – AS/NZS 2891.2.2. (1995). “Methods of Sampling and Testing Asphalt, Method 2.2 Sample Preparation - Compaction of Asphalt Test Specimens Using a Gyratory Compactor.”

Bahia, H., T. Friemel, P. Peterson, J. Russell, and B. Poehnelt. (2003). “Optimization of Contractibility and Resistance to Traffic: A New Design Approach for HMA Using the Superpave Compactor.” Journal of Association of Asphalt Paving Technologists, Vol. 72.

Bahia, H., E. Masad, A. Stackston, S. Dessouky, and F. Bayomy. (2003). “Simplistic Mixture Design Using the SGC and the DSR.” Proceedings of the Association of Asphalt Paving Technologists, Vol. 72, pp 196-225.

Bayomy, F., E. Masad, and S. Dessouky. (2002). “Development and Performance Prediction of Idaho Superpave Mixes.” Interim Report ITD-NIATT Project KLK464, National Institute for Advanced Transportation Technology, University of Idaho, Moscow, Idaho.

Bhasin, A., J.W. Button, and A. Chowdhury. (2004). “Evaluation of Simple Performance tests on Hot-Mix Mixtures from The South Central United States.” Transportation Research Record 1891, TRB, Washington, D.C.

Bhurke, A., E. Shin and L. Drzal. (1997)."Fracture Morphology and Fracture Toughness Measurement of Polymer Modified Asphalt Concrete." 76th annual meeting of the Transportation Research Board, Paper No. 970942.

Binaquist, R.F., D.W. Christensen, and W. Stump. (2003). “Simple Performance Tester for Superpave Mix Design: First-Article Development and Evaluation.” NCHRP Report 513, TRB, Washington, D.C.

Butcher, M. (1998.) “Determining Gyratory Compaction Characteristic Using Servopac Gyratory Compactor.” Transportation Research Record 1630, TRB, Washington, D.C.

Choubane, B., G. Page, and J. Musselman. (2000). “Suitability of Asphalt Pavement Analyzer for Predicting Pavement Rutting.” Transportation Research Record 1723, TRB, Washington, D.C.

Cominsky, J., G. Huber, T. Kennedy, and R. Anderson. (1994). “The Superpave Mix Design Manual for New Construction and Overlays.” SHRP Report A-407, Strategic Highway Research Program, Washington, D.C.

Dessouky, S., E. Masad, and F. Bayomy. (2004). “Prediction of Hot Mix Asphalt Stability Using the Superpave Gyratory Compactor,” Journal of Materials in Civil Engineering, Vol. 16, No. 6.

DeSombre, R., B. Chadbourn, D.E. Newcomb, and V. Voller. (1998.) “Parameters to Define the Laboratory Compaction Temperature Range of Hot-Mix Asphalt.” Journal of Association of Asphalt Paving Technologists, Vol. 67.

Dongre, R., M.G. Sharma, and D.A. Anderson. (1989). “Development of Fracture Criterion for Asphalt Mixes at Low Temperatures.” Transportation Research Record 1228, TRB, National Research Council, Washington, D.C.

Faheem, A.F., H.U. Bahia, and H. Ajideh. (2005). “Estimating Results of a Proposed Simple Performance Test for Hot-Mix Asphalt from Superpave Gyratory Compactor Results.” Transportation Research Record 1929, TRB, Washington, D.C.

Fletcher, T., C. Chandan, E. Masad, K. Sivakumar. (2003). “Aggregate Imaging System (AIMS) for Characterizing the Shape of Fine and Coarse Aggregates.” Transportation Research Record 1832, Transportation Research Board, National Research Council, Washington D.C.

Guler, M., H. Bahia, P. Bosscher, and M. Plesha. (2000). “Device for Measuring Shear Resistance for Hot Mix Asphalt in Gyratory Compactor.” Transportation Research Record 1723, TRB, Washington, D.C.

Huang, B., W. Kingery, Z. Zhang, and G. Zuo. (2004). “Laboratory Study of Fatigue Characteristics of HMA Surface Mixtures Containing Rap.” Presented at 83rd Annual Meeting of the Transportation Research Board, Washington, D.C.

Huang, Y.H. (2004). *Pavement Analysis and Design*. Pearson Prentice Hall, Second Edition, New Jersey.

Idaho Department of Transportation. “Standard Specifications for Highway Construction.” Boise, Idaho.

Kumar A., and W. Goetz. (1974). “The Gyratory Testing Machine as a Design Tool and Instrument for Bituminous Mixture Evaluation.” Asphalt Paving Technology, Vol. 43.

Landes, J., and D. McCabe. (1984). “Effect of Section Size on Transition Temperature Behavior of Structural Steel.” ASTM STP 833.ASTM International, West Conshohocken, PA.

Li, X., and M. Marasteanu. (2004). “Evaluation of Low Temperature Fracture Resistance of Asphalt Mixture Using the Semi Circular Bend Test.” Journal of the Association of Asphalt Paving Technologists, Vol. 73.

Lim, I.L., I.W. Johnston, S.K. Choi, and J.N. Boland. (1994). “Fracture Testing of a Soft Rock with Semi-Circular Specimens Under Three-point Bending. Part 1-Mode I.” International Journal of Rock Mechanics and Mining Science, Vol. 31, No. 3.

Little, N. and K. Mahboub. (1985). “Engineering Properties of First Generation Plasticized Sulfur Binders and Low Temperature Fracture Evaluation of Plasticized Sulfur Paving Mixtures.” Transportation Research Record 1034, TRB, National Research Council, Washington, D.C.

Mallick, R. (1999). “Use of Superpave Gyratory Compactor to Characterize Hot Mix Asphalt.” Transportation Research Record 1681, TRB, Washington, D.C.

Martin, A. and D. Park. (2003). “Use of the Asphalt Pavement Analyzer and Repeated Simple Shear Test at Constant Height to Augment Superpave Volumetric Mix Design.” Journal of Transportation Engineering, Vol. 129, No. 5.

Masad, E. (2003). “The Development of A Computer Controlled Image Analysis System for Measuring Aggregate Shape Properties.” NCHRP-IDEA Project 77 Final Report, Transportation Research Board, Washington, D.C.

Masad, E., D. Little, and R. Sukhwani. (2004). “Sensitivity of HMA Performance to Aggregate Shape Measured Using Conventional and Image Analysis Methods.” International Journal of Road Materials and Pavement Design. Vol. 5, No. 4.

McCabe, D., J. Merkle, and K. Walin. (2005). “An Introduction to the Development and Use of the Master Curve Method.” ASTM MNL52, ASTM International, West Conshohocken, PA.

McRea, J.L. (1962). “Gyratory Compaction Method for Determining Density Requirements for Subgrade and Base of Flexible Pavements.” Miscellaneous Paper No. 4-494, U.S. Army Engineering Waterways Experiment Station, Corps of Engineering, Vicksburg, MS.

McRea, J.L. (1965). “Gyratory Testing Machine Technical Manual.” Engineering Developments Company Inc., Vicksburg, MS.

Mohammad, L.N., Z. Wu, and M. A. Mull. (2004). “Characterization of Fracture and Fatigue Resistance on Recycled Polymer-Modified Asphalt Pavements.” 5th RILEM International Conference on Cracking in Pavements. Limoges, France.

Molennar, A., A. Scarpas, X. Liu, and G. Erkens. (2002). “Semi Circular Test; Simple but Useful?” Journal of the Association of Asphalt Paving Technologists, Vol. 71.

Mull, M., K. Stuart, and A. Yehia. (2002). "Fracture Resistance Characterization of Chemically Modified Crumb Rubber Asphalt Pavement." Journal of Materials Science, Vol. 37.

Mull, M. A., A. Othman, and L. Mohammad. (2004). "Fatigue Crack Propagation Analysis of Chemically Modified Crumb Rubber Asphalt Mixtures." Journal of Elastomers and Plastics. Vol 37.

Ott, R.L. and M. Longnecker. (2001). *An Introduction to Statistical Methods and Data Analysis.* Fifth Edition. Duxbury, Pacific Grove, CA.

"Pressure Distribution Analyzer (PDA)." Test Quip Inc., http://www.testquip.com, Minneapolis, Mn.

Rand, D. (1997). "Comparative Analysis of Superpave Gyratory Compactors and TxDOT Gyratory Compactors." Master Thesis, University of Texas, Austin, TX.

Rice, J.R. (1968). "A Path Independent Integral and the Approximate Analysis of Strain Concentration by Notches and Cracks." Journal of Applied Mechanics, Vol. 35.

Ruth, B., X. Shen, and L. Wang. (1991). "Gyratory Evaluation of Aggregate Blends to Determine their Effects on Shear Resistance and Sensitivity to Asphalt Content." American Society for Testing and Materials, 1147.

Segerlind, L.J. (1984). *Applied Finite Element Analysis*. John Wiley and Sons Inc., Second Edition, New York, NY.

Sigurjonsson, S., B. Ruth. (1990). "Use of Gyratory Testing Machine to Evaluate Shear Resistance of Asphalt Paving Mixture." Transportation Research Record 1259, TRB, Washington, D.C.

Stackston, A., J. Bushek, and H. Bahia. (2002). "Effect of Fine Aggregates Angularity (FAA) on Compaction and Shearing Resistance of Asphalt Mixtures." Presented at TRB 81st Annual Meeting, Washington, D.C.

Tandon, V., B.S. Kambham, R., Bonaquist and M. Solaimanian. (2004). "Results of Integrating Simple Performance Tests and Environmental Conditioning System." Transportation Research Record 1891, TRB, Washington, D.C.

Van de Ven, M., A. de Fortier Smit, and R. Krans. (1997). "Possibilities of a Semi-Circular Bending Test." Proceedings of the Eighth International Conference on Asphalt Pavements, Vol. II, Seattle, WA.

Witczak, M., K. Kaloush, T. Pellinen, M. Al-Basyouny, and H. Von Quintus. (2002). "Simple Performance Test for Superpave Mix Design." NCHRP Report 465, TRB, Washington, D.C.

Zborowski, A., A. Sotil, K.E. Kaloush, and G.B. Way. (2002). "Material Characteristics of Asphalt Material." TRB 83rd Annual meeting CD-ROM, Washington, D.C.

APPENDICES

Appendix A:

Mix Design Details and Job Mix Formula (JMF) for All Mixes. This is provided in PDF on the attached CD

Appendix B:

Gyratory Stability and Gyratory Compaction Data Files. Provided on the attached CD.

Appendix C:

CEI and GS Software. Provided on the attached CD.